Turbulence and dissipation in magnetized space plasmas

Fouad Sahraoui
Laboratoire de Physique des Plasmas

LPP, CNRS-Ecole Polytechnique-UPMC-Observatoire de Paris, France

Collaborators: L. Hadid, S. Huang, S. Banerjee, N. Andrés, S. Galtier, K. Kiyani, G. Belmont, M. Goldstein, L. Rezeau and many others

Outline

1. Part I: Turbulence in space plasmas (solar wind and planetary magnetosheaths): Introduction, space instrumentation, data analysis techniques
2. Part II: MHD Turbulence
3. Part III: Kinetic turbulence

Part I: Turbulence in space plasmas

1. Plasmas in the Universe
2. Space plasmas: Sun, Solar wind, Planetary magnetospheres
3. Why do we need to study plasma turbulence ?
4. In-situ space instrumentation and related measurements
5. Multispacecraft data analysis techniques (e.g., the k-filtering)

Turbulence in the Univers

Turbulence is ubiquitous in the Univers –It covers all scales, from quantum to cosmological ones!

Observed heating and particle acceleration (i.e. jets) in astrophysical objects are caused by turbulence dissipation

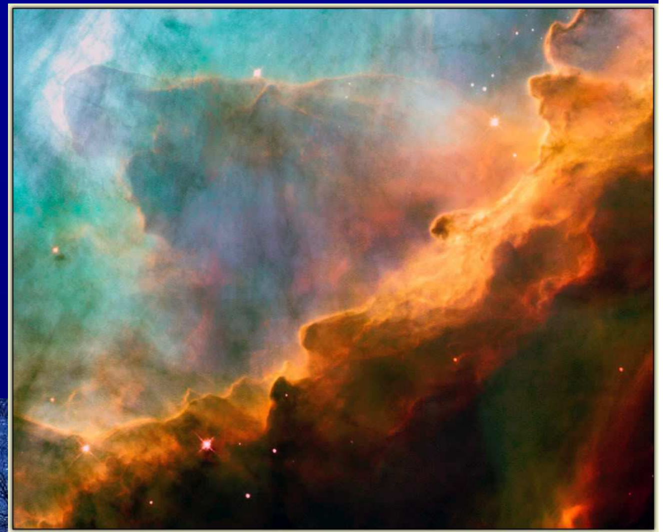

Turbulence in galaxies & nebulas

Solar corona heating

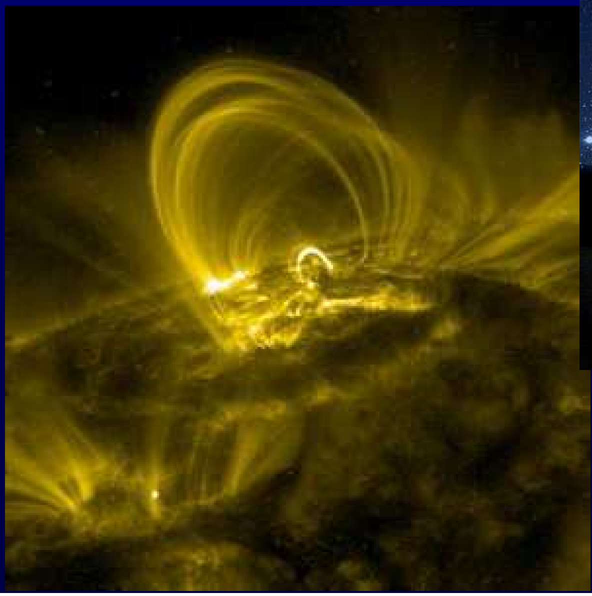

Accretion disks of black holes

[Hawley & Balbus, 2002 (simulations)]

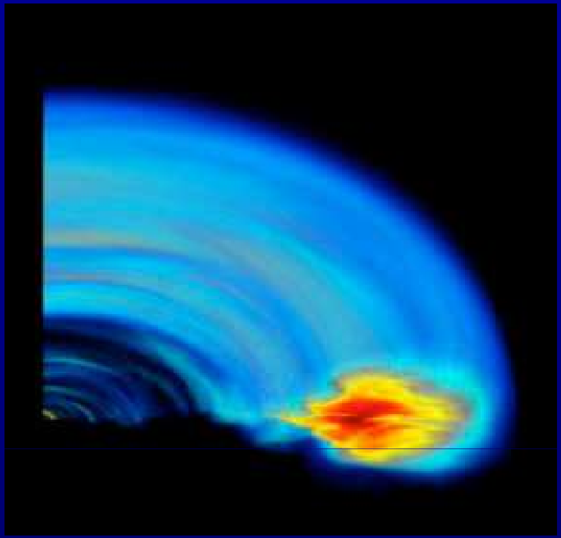

Articst's view: NASA/JPL-Caltech

Matter spirals into the black hole, converting huge gravitational potential energy into heat:

- Magnetorotational Instability (MRI) drives turbulence [Balbus, 1992]
- Turbulence cascades nonlinearly to small scales
- Kinetic mechanisms damp turbulence and lead to plasma heating

Emitted radiations (e.g. X-rays) are function of the plasma heating

The Sun

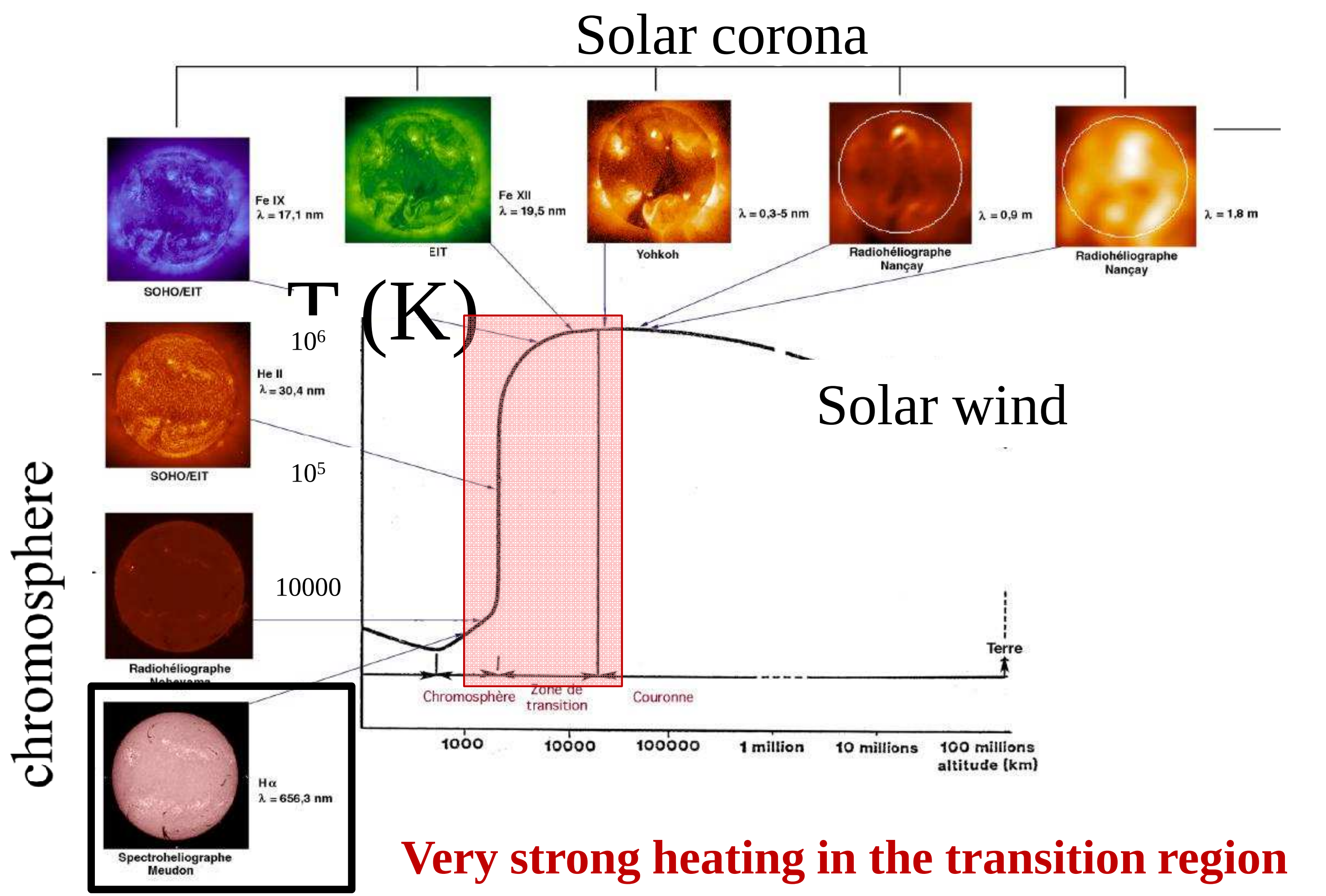

Very strong heating in the transition region

visible

The solar wind

The solar wind plasma is generally:

- Fully ionized (H^+, e^-)
- Non -relativistic (V_A<<c), V~350-800 km/s
- *Collisionless*

[Richardson & Paularena, 1995]

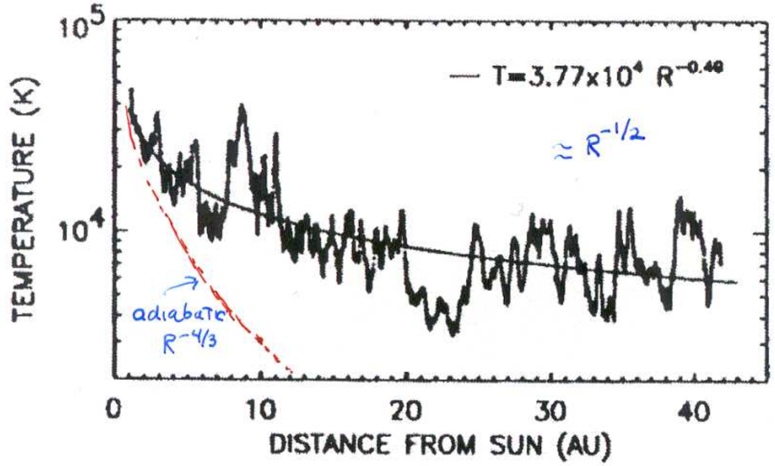

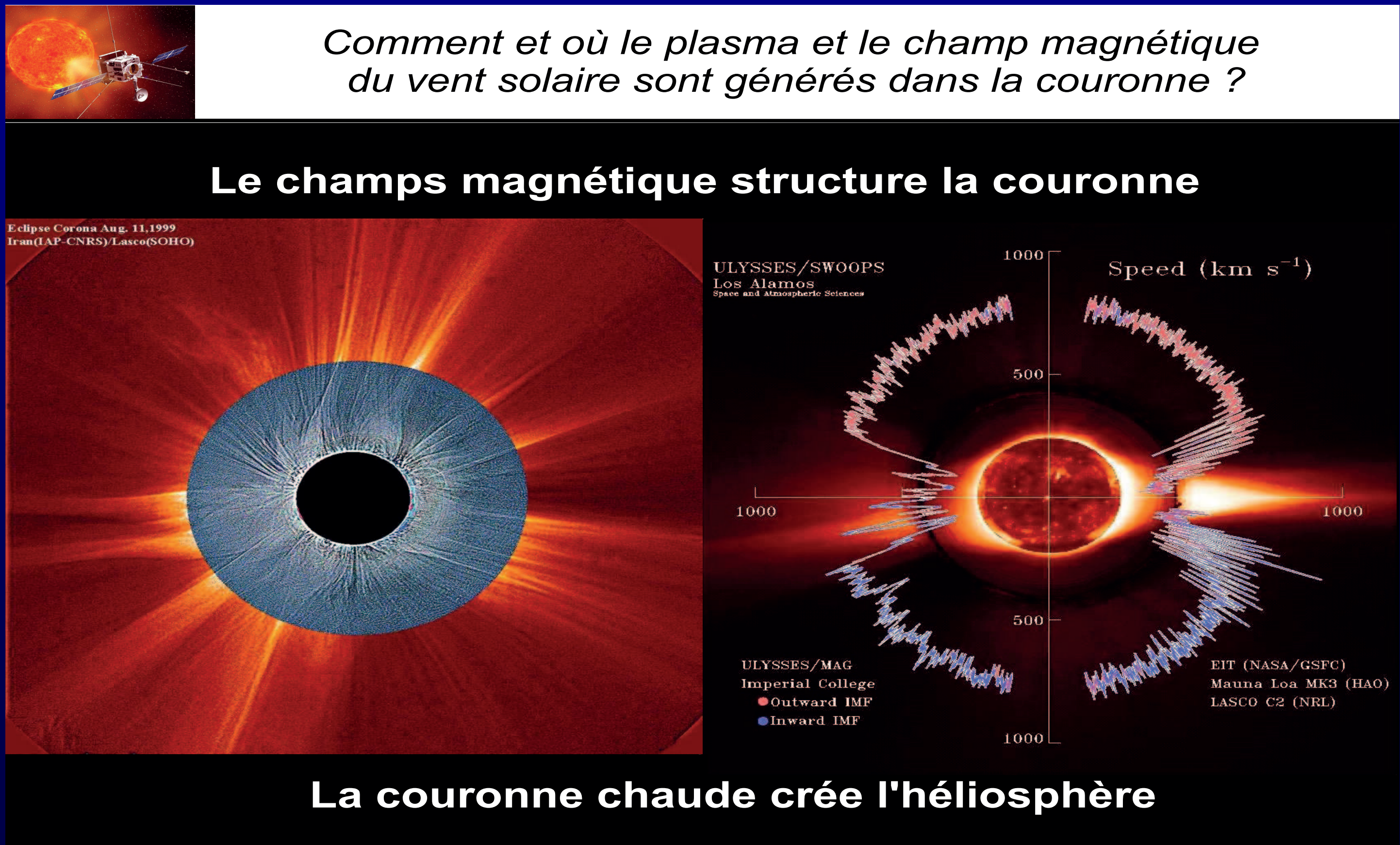

Sun-Earth coupling

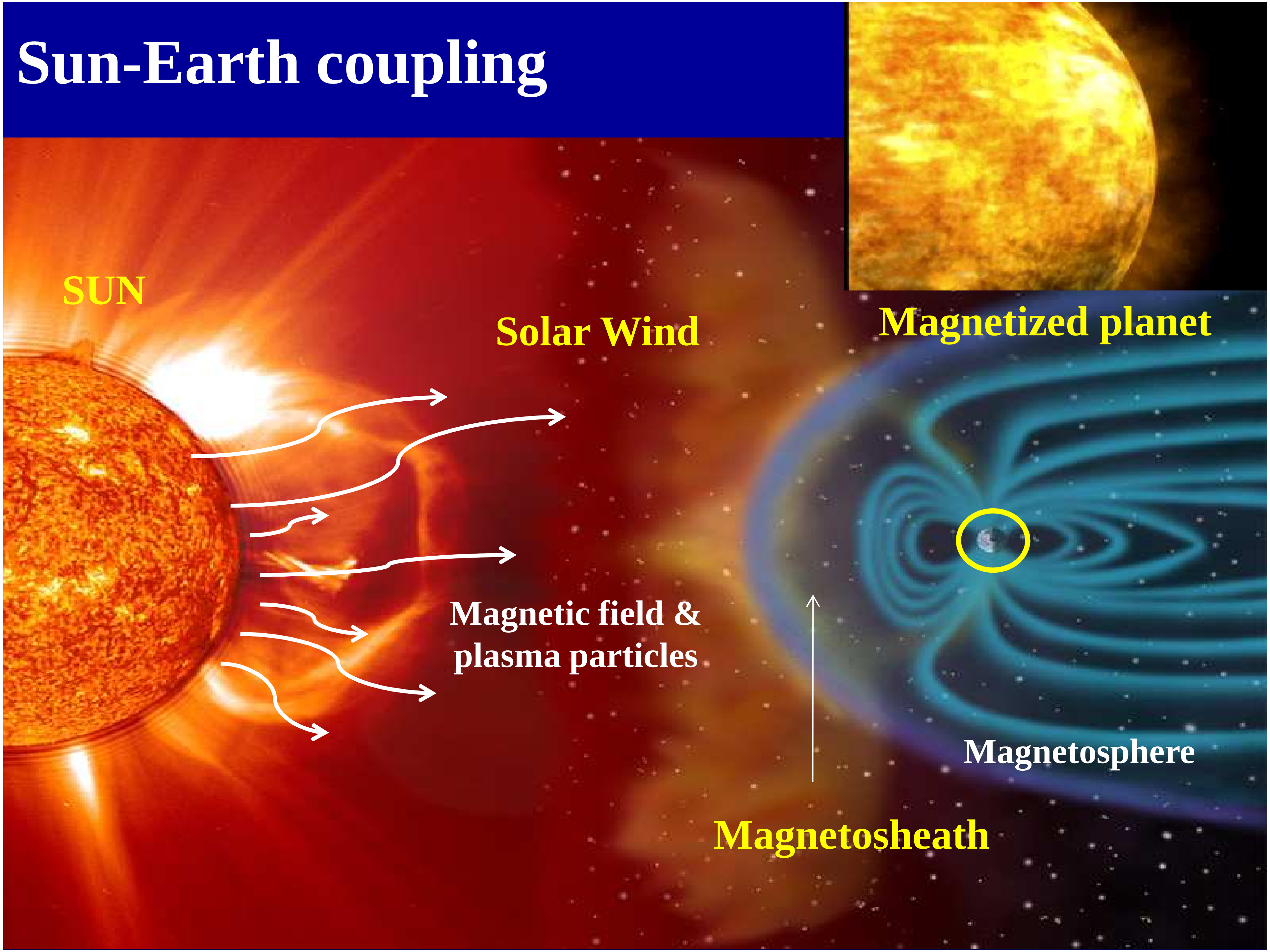

Planetary magnetospheres

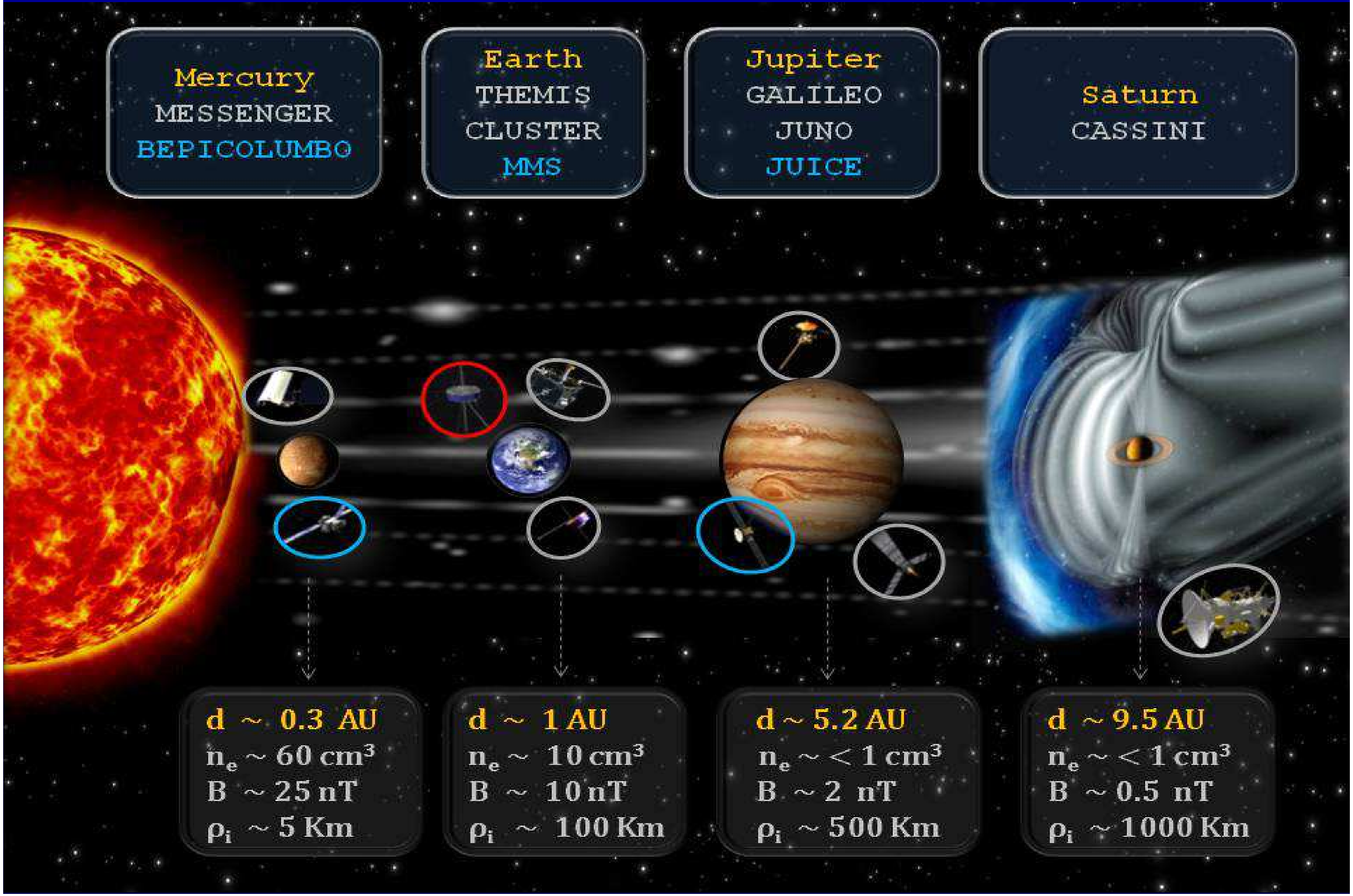

Turbulence in fusion devices

Turbulence is the main obstacle to plasma confinement

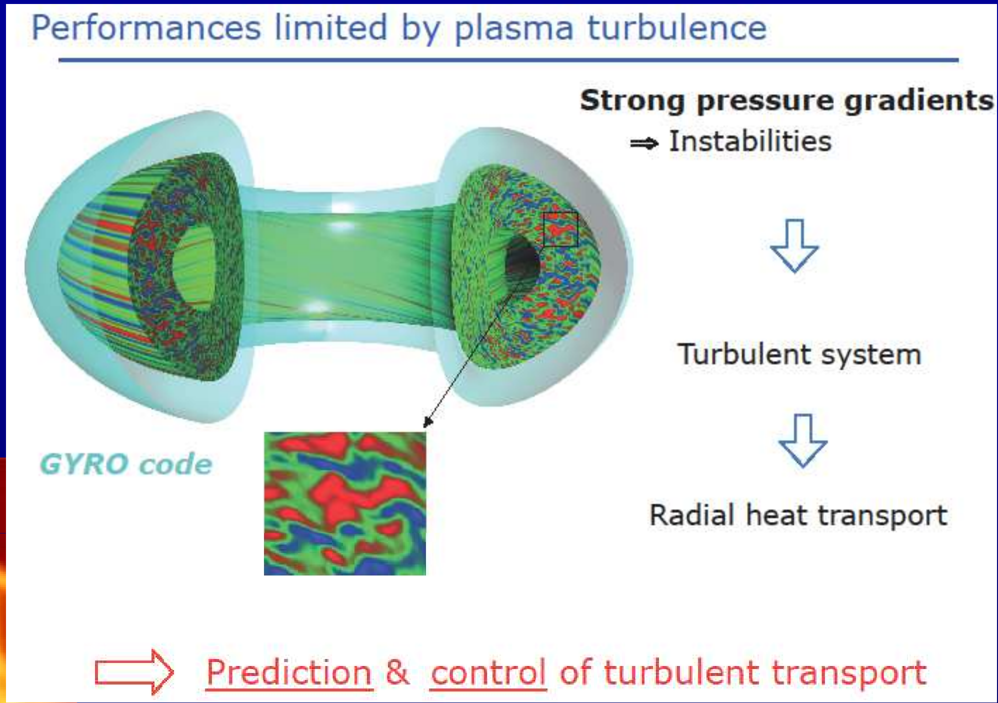

A better understanding of turbulent transport → A better control → A longer confinement

Any common physics ?

$N \sim 10^6$ cm^{-3}

$T_i \sim 10^{12}$ K

$B \sim 10^6$ nT

M100 galaxy 10^{23} *m*

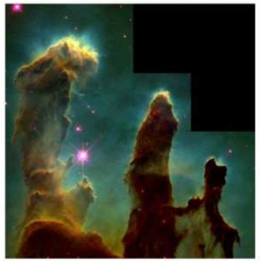

Eagle nebula 10^{18} *m*

Performances limited by plasma turbulence

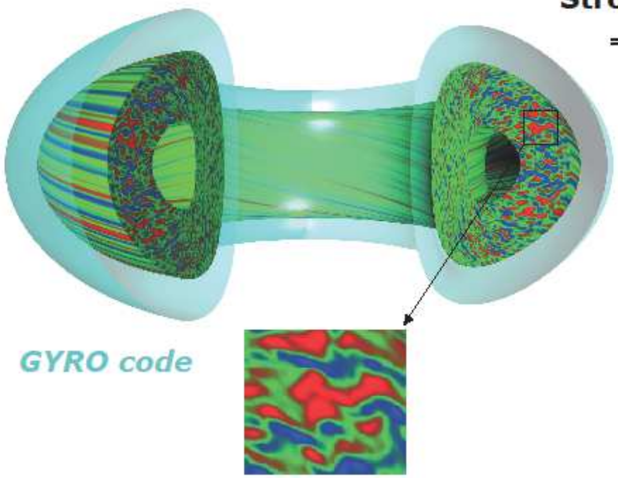

Strong pressure gradients
⇒ Instabilities

⇩

Turbulent system

⇩

Radial heat transport

GYRO code

⇨ Prediction & control of turbulent transport

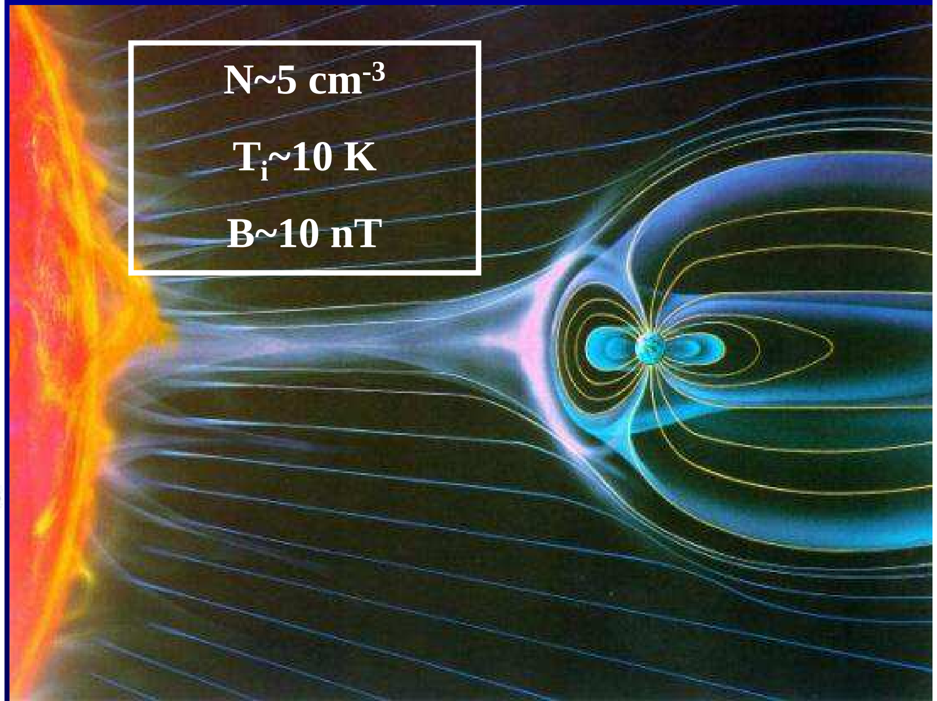

$N \sim 5$ cm^{-3}

$T_i \sim 10$ K

$B \sim 10$ nT

Near-Earth space plasmas

[Scheckochihin et al., ApJ, 2009]

$$\beta = \frac{\text{Pression thermique}}{\text{Pression magnétique}} \approx 0.4\frac{NT}{B^2}$$

Representative Parameters for Astrophysical Plasmas

Parameter	Solar wind at 1 AU[a]	Warm ionized ISM[b]	Accretion flow near Sgr A*[c]	Galaxy clusters (cores)[d]
$n_e = n_i$, cm^{-3}	30	0.5	10^6	6×10^{-2}
T_e, K	$\sim T_i$[e]	8000	10^{11}	3×10^7
T_i, K	5×10^5	8000	$\sim 10^{12}$[f]	?[e]
B, G	10^{-4}	10^{-6}	30	7×10^{-6}
β_i	5	14	4	130
v_{thi}, km s^{-1}	90	10	10^5	700
v_A, km s^{-1}	40	3	7×10^4	60
U, km s^{-1}[f]	~ 10	~ 10	$\sim 10^4$	$\sim 10^2$
L, km[f]	$\sim 10^5$	$\sim 10^{15}$	$\sim 10^8$	$\sim 10^{17}$
$(m_i/m_e)^{1/2}\lambda_{\text{mfpi}}$, km	10^{10}	2×10^8	4×10^{10}	4×10^{16}
λ_{mfpi}, km[g]	3×10^8	6×10^6	10^9	10^{15}
ρ_i, km	90	1000	0.4	10^4
ρ_e, km	2	30	0.003	200

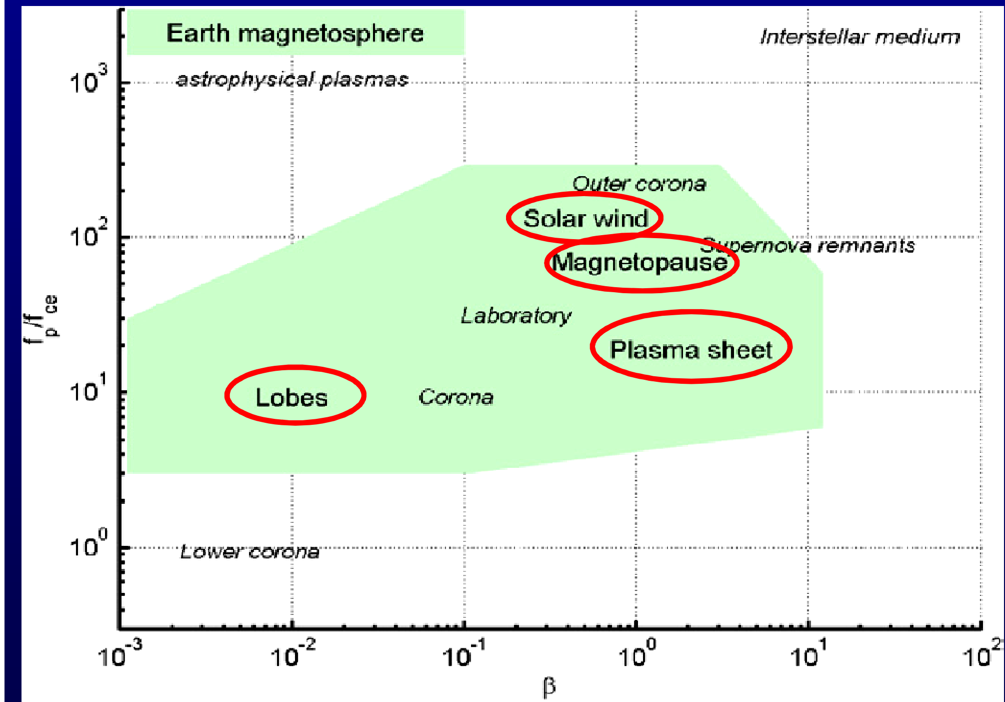

[Vaivads et al., Plasma Phys. Contr. Fus., 2009]

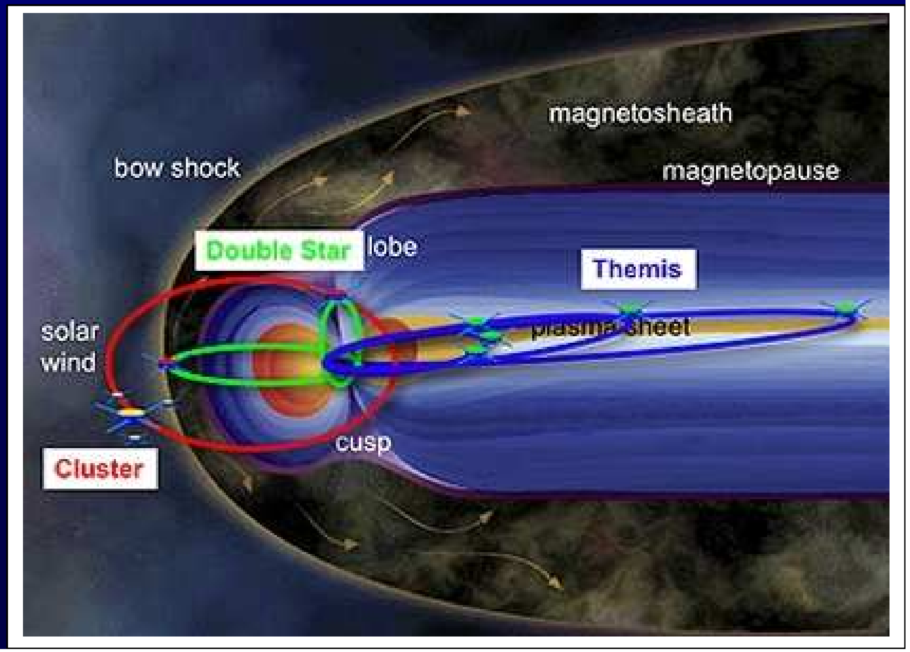

Remote sensing (distant plasmas)

Bernard Lyot, the inventor of coronograph (*photo Observatoire de Paris*)

Bernard Lyot Telescope at Observatoire du Pic du Midi (*photo P. Petit*)

In-situ measurements (space plasmas)

Plasmas →A coupled system of equations

$$\begin{cases} \nabla\times\mathbf{E} = -\partial_t \mathbf{B} \\ \nabla\times\mathbf{B} = \dfrac{1}{c^2}\partial_t\mathbf{E} + \mu_0\mathbf{j} \\ \nabla.\mathbf{E} = \dfrac{\rho}{\varepsilon_0} \\ \nabla.\mathbf{B} = 0 \end{cases}$$

$$\begin{cases} \partial_t n_e + \nabla.(n_e\mathbf{u}_e) = 0 \\ n_e m_e \partial_t \mathbf{u}_e + n_e\mathbf{u}_e\nabla.(\mathbf{u}_e) + \nabla p_e = -n_e e\left(\mathbf{E} + \mathbf{u}_e\times\mathbf{B}\right) \\ \partial_t n_i + \nabla.(n_i\mathbf{u}_i) = 0 \\ n_i m_i \partial_t \mathbf{u}_i + n_i\mathbf{u}_i\nabla.(\mathbf{u}_i) + \nabla p_i = n_i e\left(\mathbf{E} + \mathbf{u}_i\times\mathbf{B}\right) \end{cases}$$

$$\mathbf{j} = n_i e\mathbf{u}_i - n_e e\mathbf{u}_e$$
$$\rho = n_i e - n_e e$$

Ideally , a space plasma physicist would like to measure:

- **B & E:** 3 components over a broad range of frequencies [DC, MHz]
- $N_{i,e}$, $V_{i,e}$, $T_{i,e}$: in 3D at all energies (eV, MeV) and with high resolutions

In-situ measurements

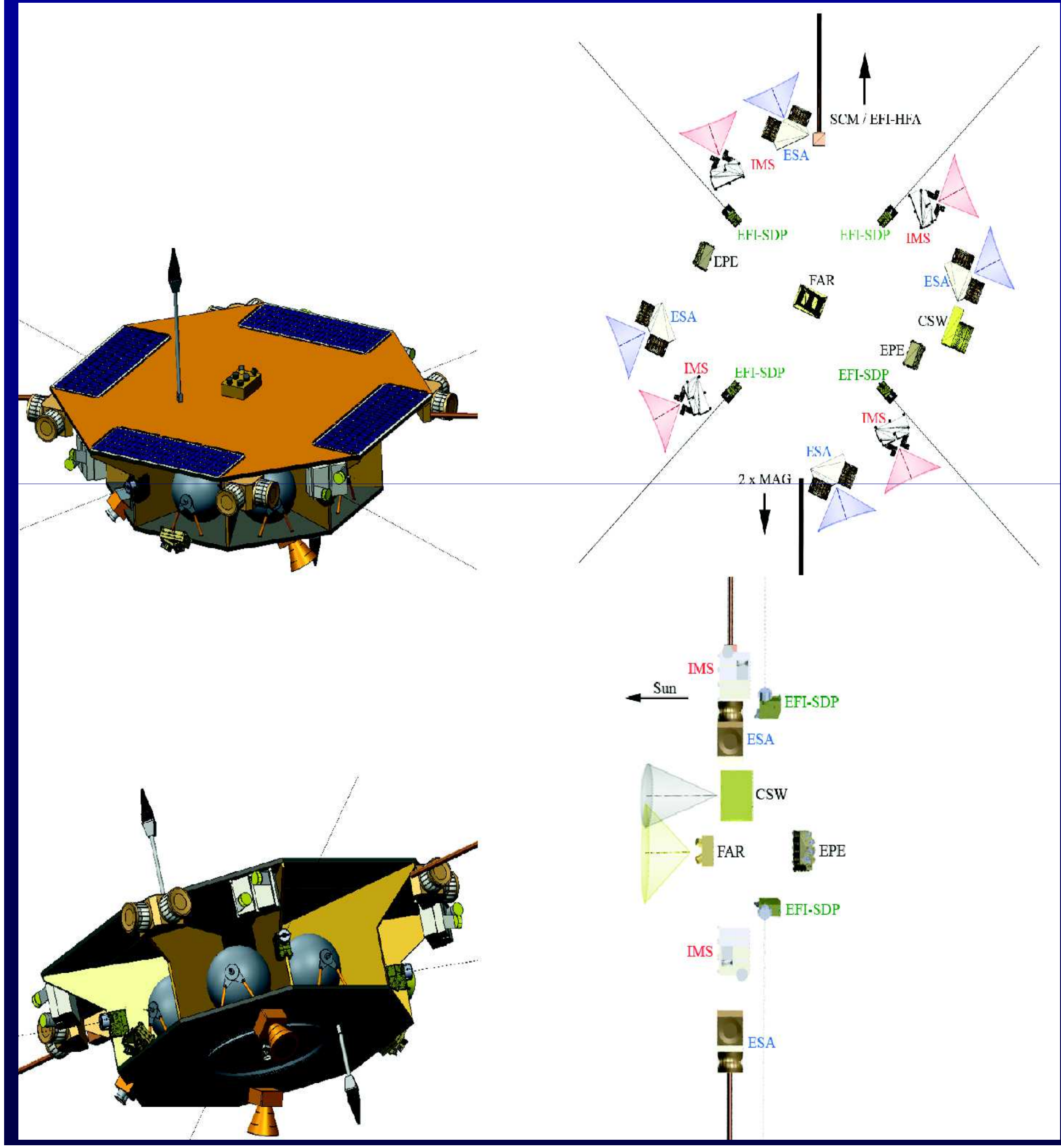

THOR spacecraft: 10 instruments (currently under phase A study at ESA)

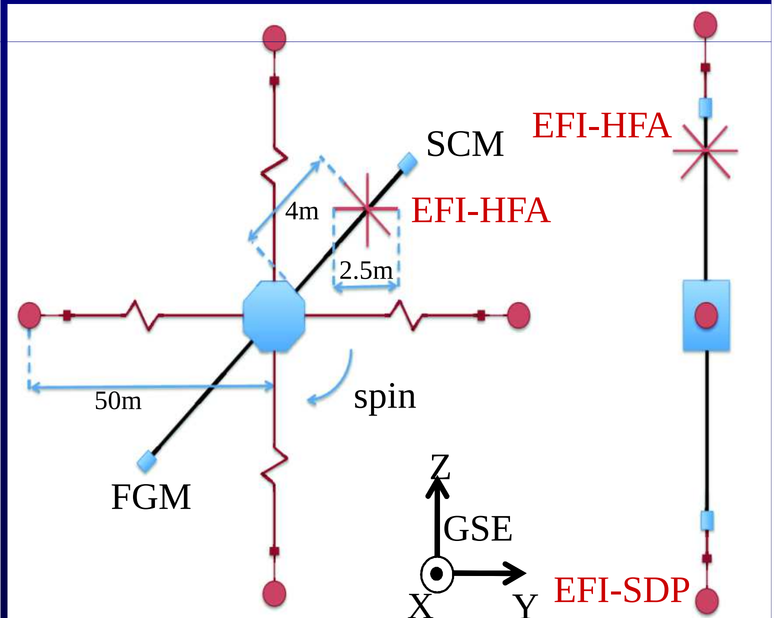

Instruments overview: fields (1)

Fluxgate magnetometer: B measurements in [DC, 1Hz]

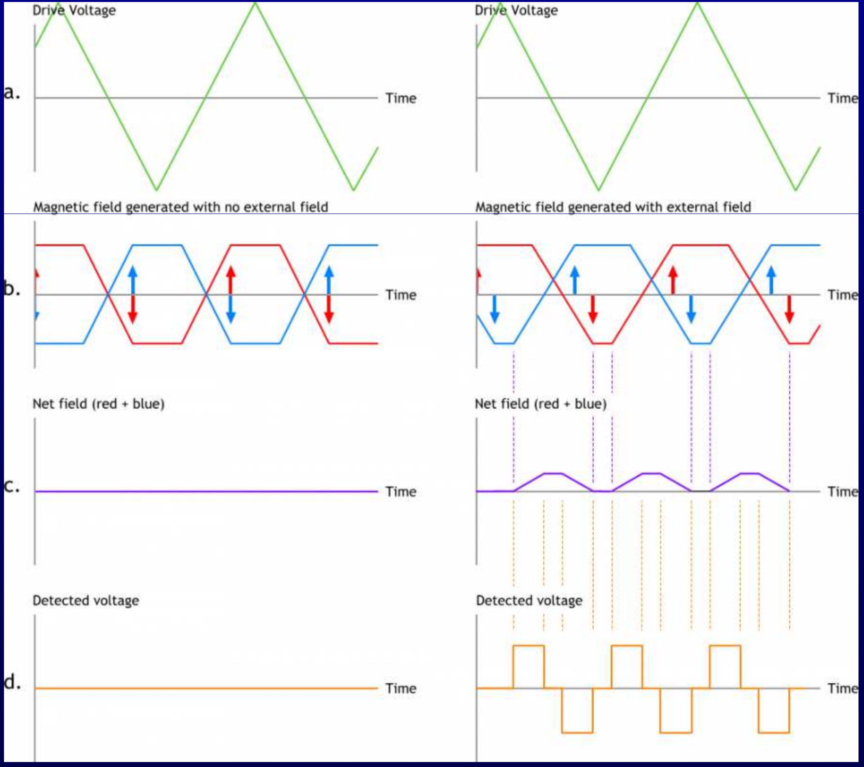

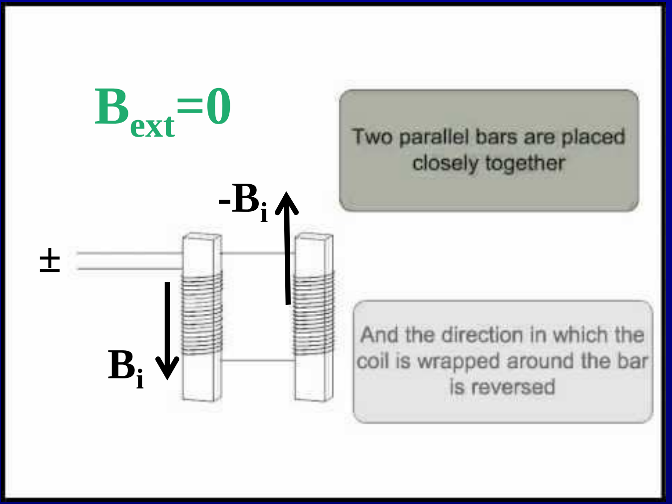

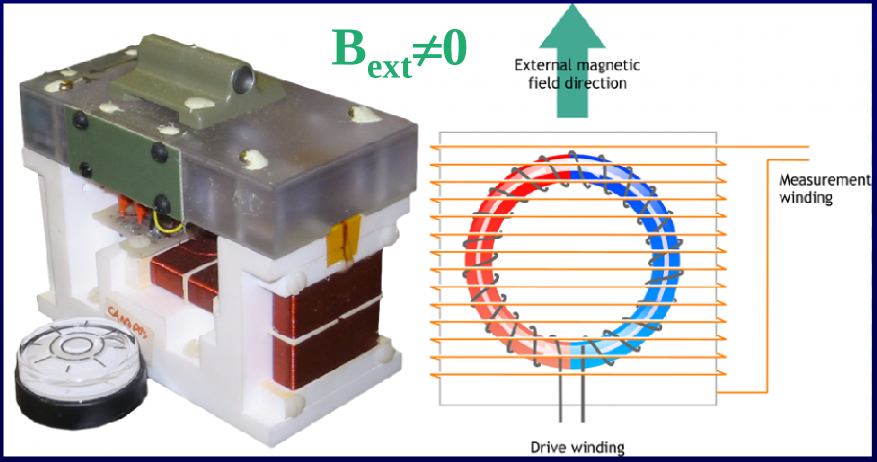

Instruments overview: fields (2)

Search-coil magnetometer (SCM): [0.1Hz, ~1MHz]

Lenz's law (induced voltage): $V_C = -N\dfrac{d\Phi}{dt} = -j2\pi f\, N\, S\, \mu_{\text{eff}}\, B\cos\theta$

μ_{eff} *effective permeability of the core*

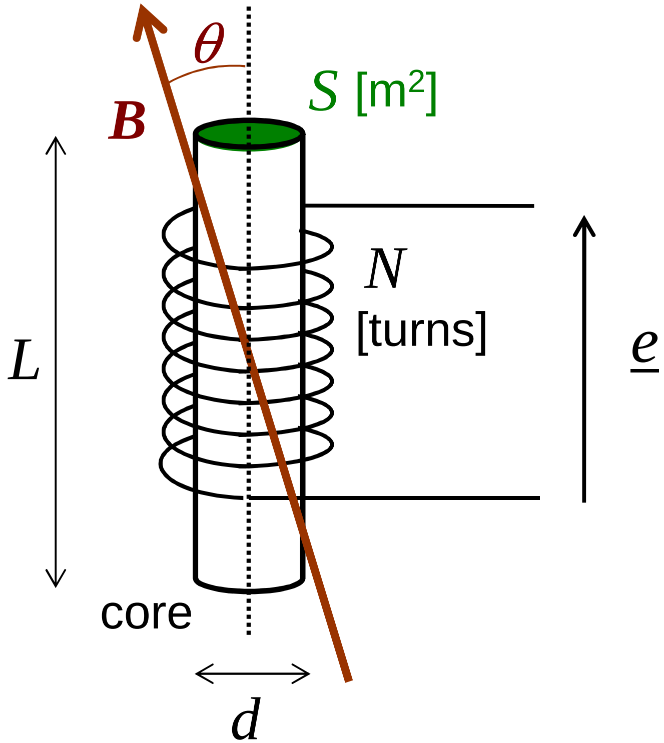

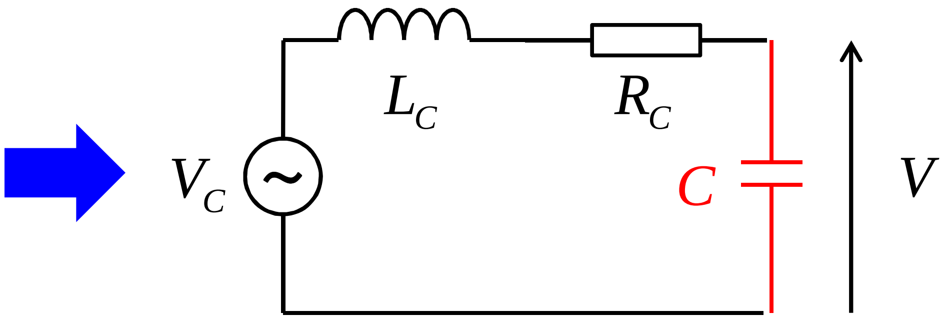

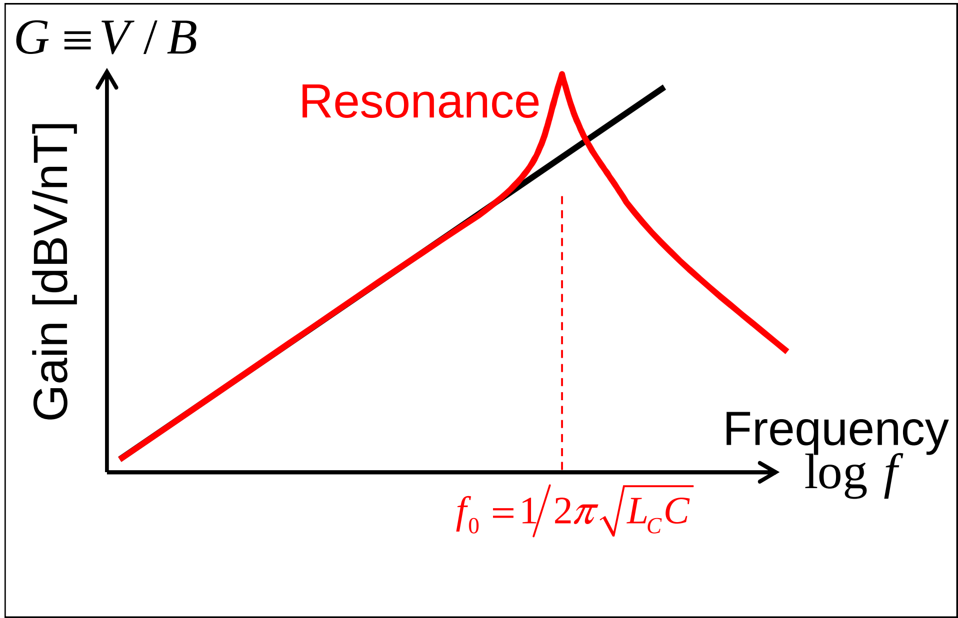

A feedback ractionis needed to obtain a flat response function

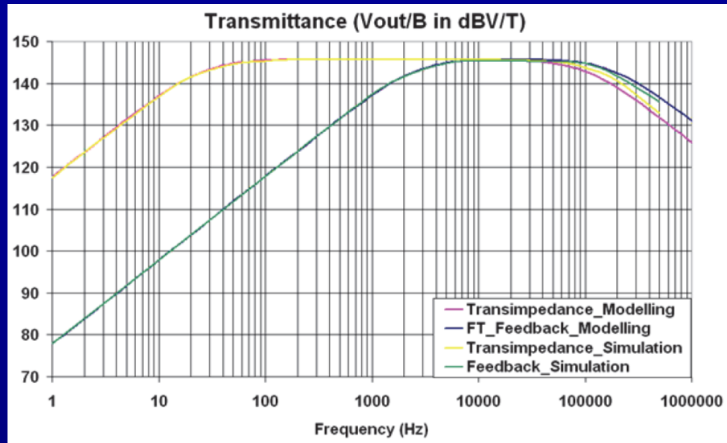

Dual band SCM:
LF [1Hz, 4kHz]
HF [1kHz, 1MHz]

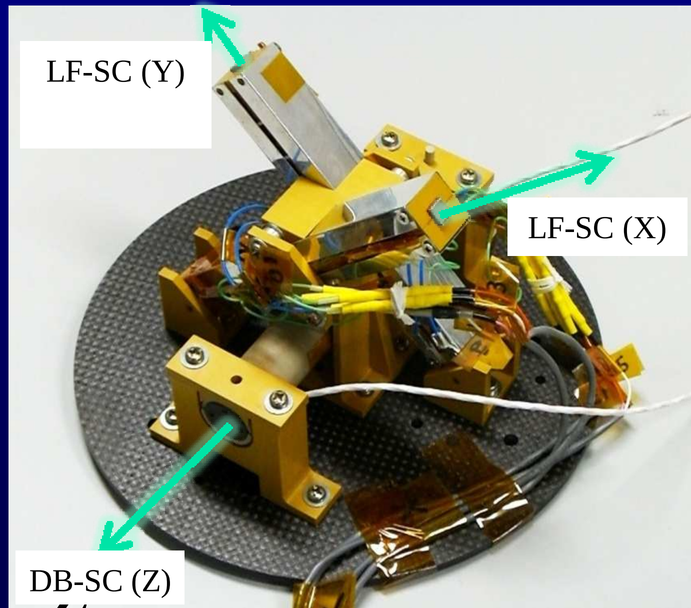

Solar Orbiter/SCM (LPC2E)

BepiColombo/SCM (LPP-Univ. Kanasawa, JP)

Instruments overview: fields (3)

Electric field: [DC, 1MHz]

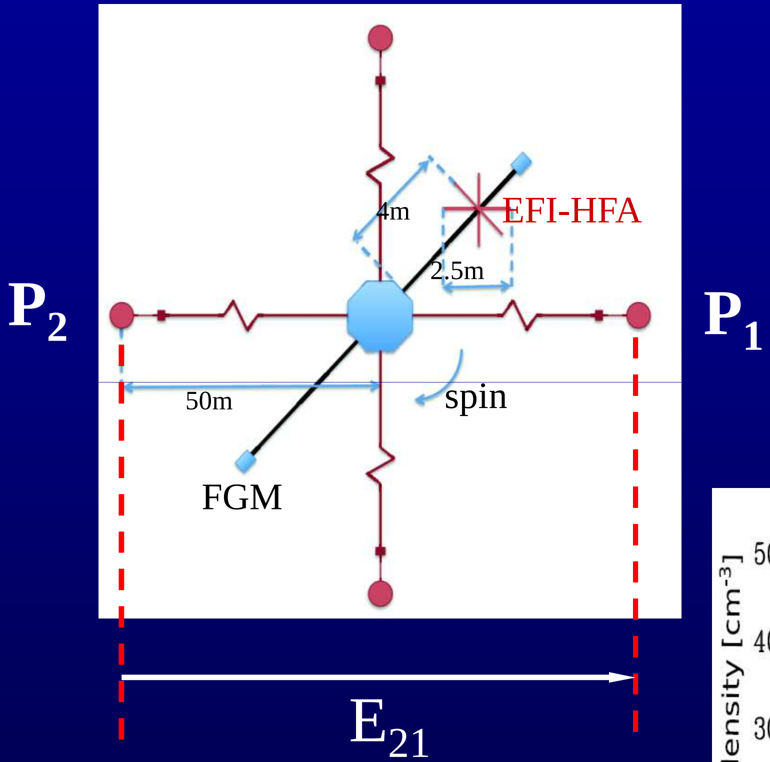

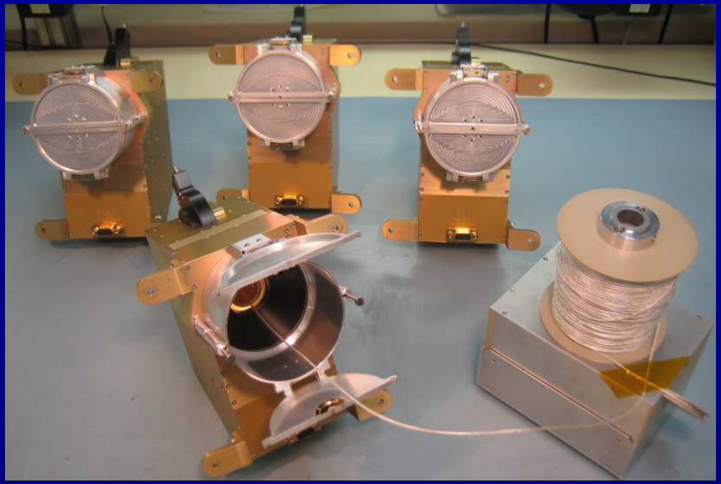

RBSP/EFW (from the THOR proposal)

Spacecraft potential V_{sc}
→ electron density n_e

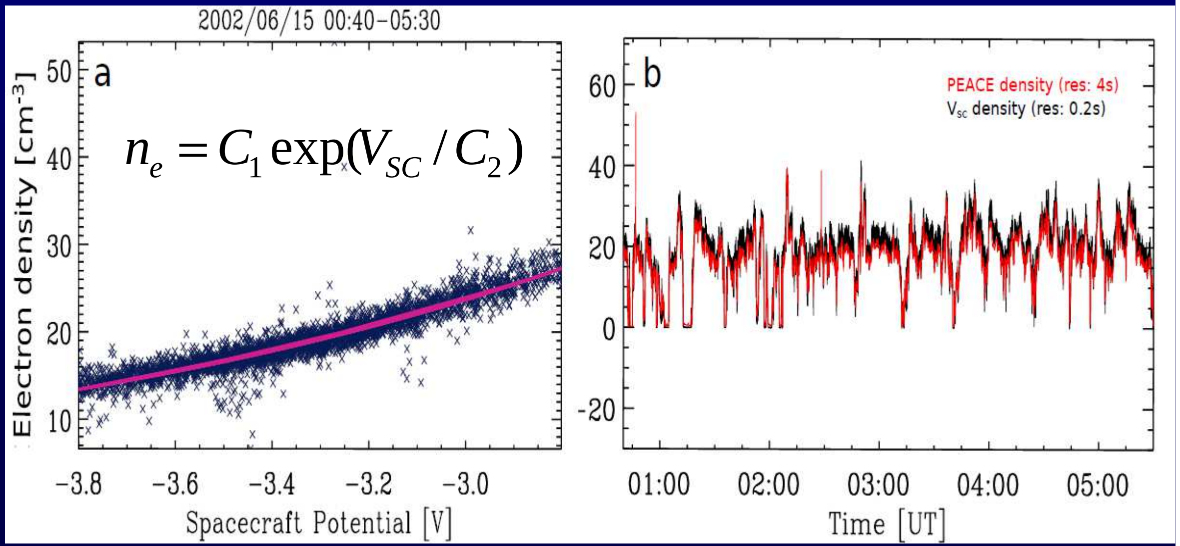

Hadid et al., 2016b

Instruments overview: fields (4)

Onboard wave analyzers

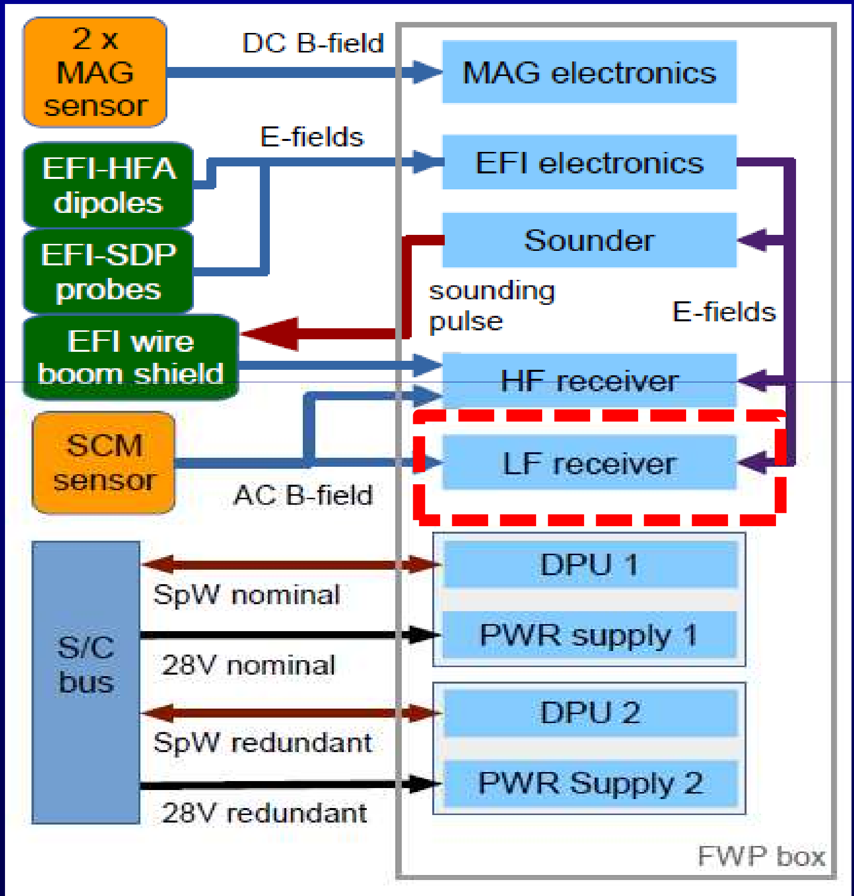

THOR/FWP (Field and Wave Processing Unit –Courtesy THOR proposal)

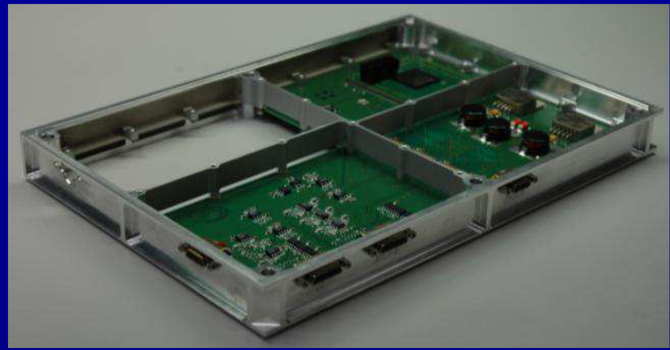

Solar Orbiter/LF analyzer

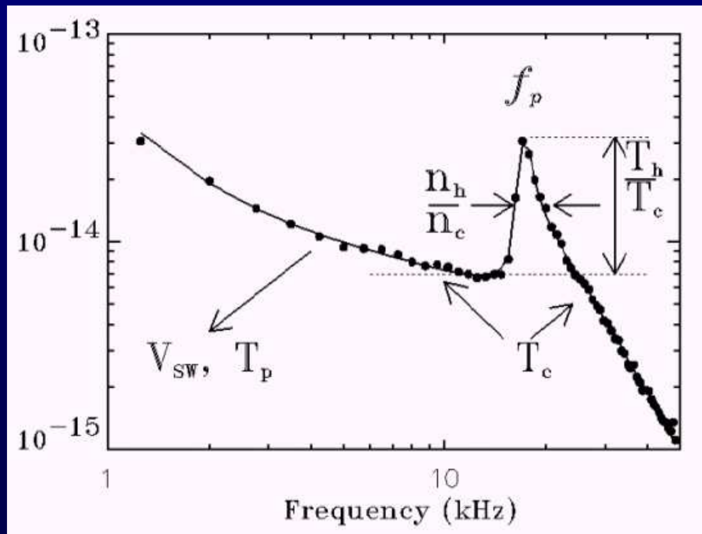

TNR/HFR → High time resolution measurement of N_e and T_e

Instruments overview: particles (1)

MSA
BepiColombo

(Ion and electron) mass spectrometers

Energy selection

Angle selection

LEF

MCP LEF

Carbon foil

-15 kV

Departure of the Time Of Flight analysis

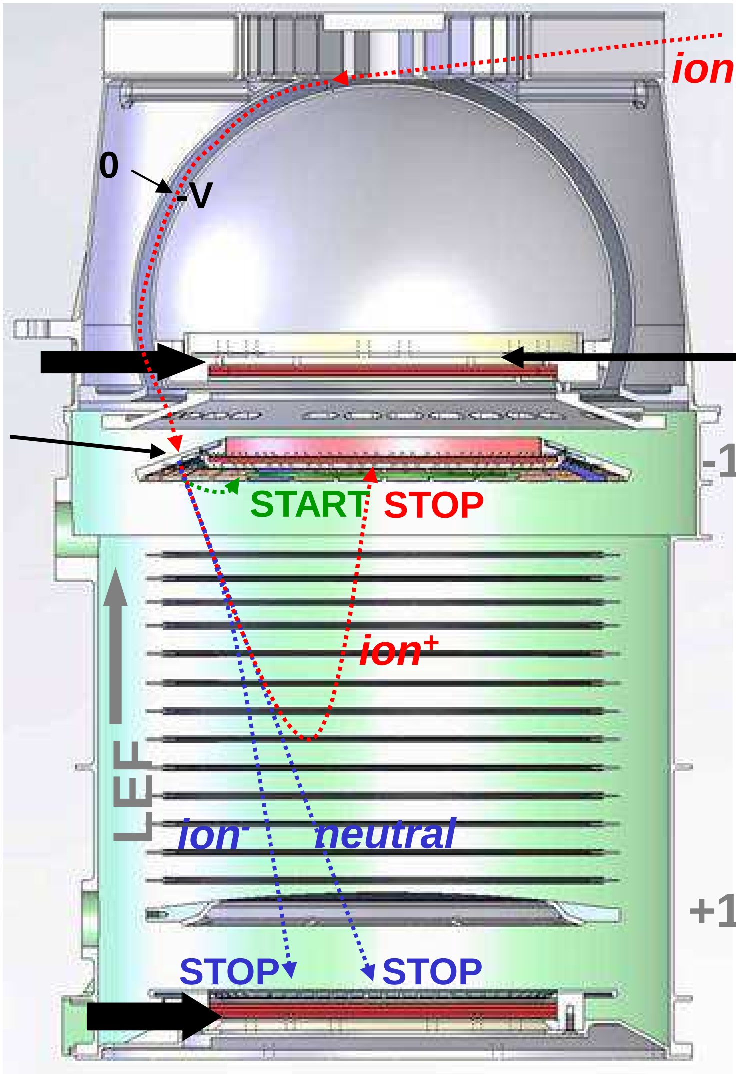

End of the flight : TOF gives the m/q ratio

+15 kV

ST

MCP ST

Output measurements :

- The nature of the particles (m/q)
- Their direction and energy/velocity
- Velocity distribution function (VDF)
- Moments of the VDF :

density, velocity, temperature

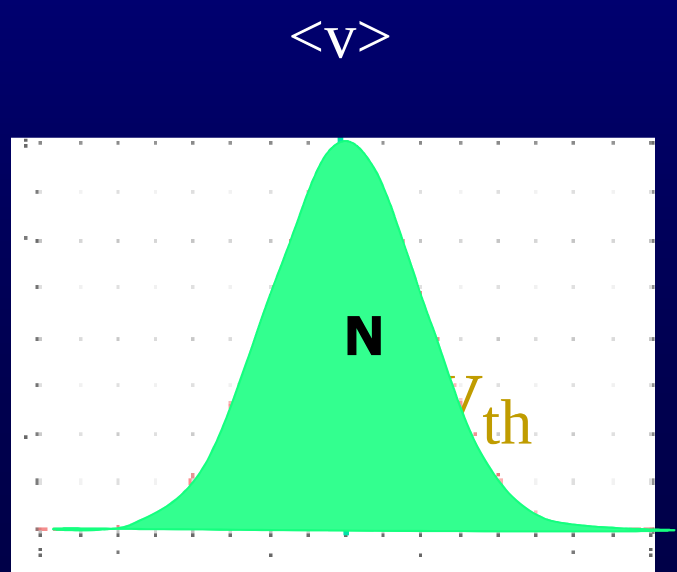

Instruments overview: particles (2)

Particle Processing Unit (PPU)

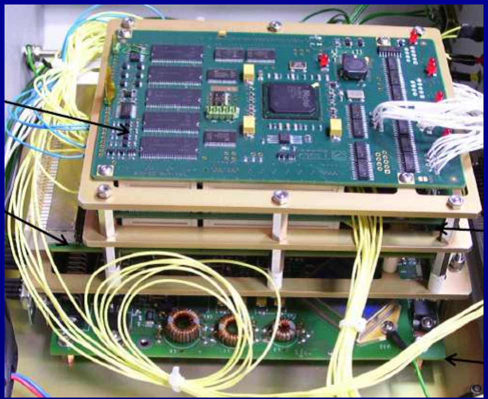

Solar Orbiter/PPU (Courtesy of TSD/RTI --from THOR proposal).

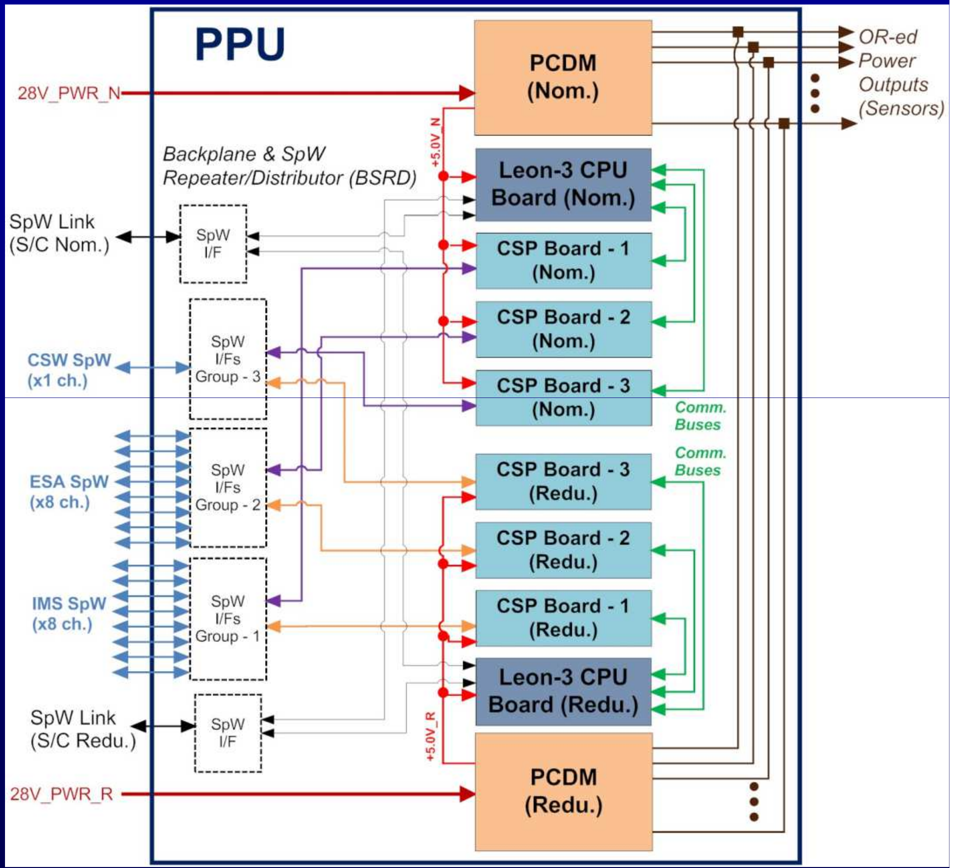

THOR/PPU (Courtesy of TSD/RTI and THOR proposal).

+Energetic particles + ASPOC + active sounder + …

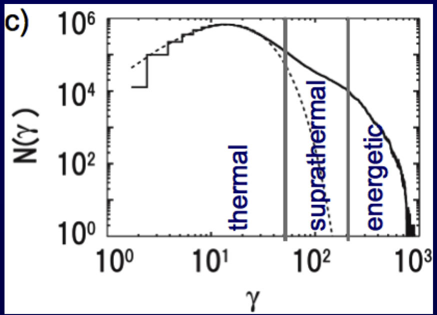

Back to turbulence: phenomenology

NS equation:

$$\partial_t \mathbf{V} + \mathbf{F}_{\mathbf{i}} = -\mathbf{V}.\nabla\mathbf{V} - \nabla P + \nu\nabla^2\mathbf{V}$$

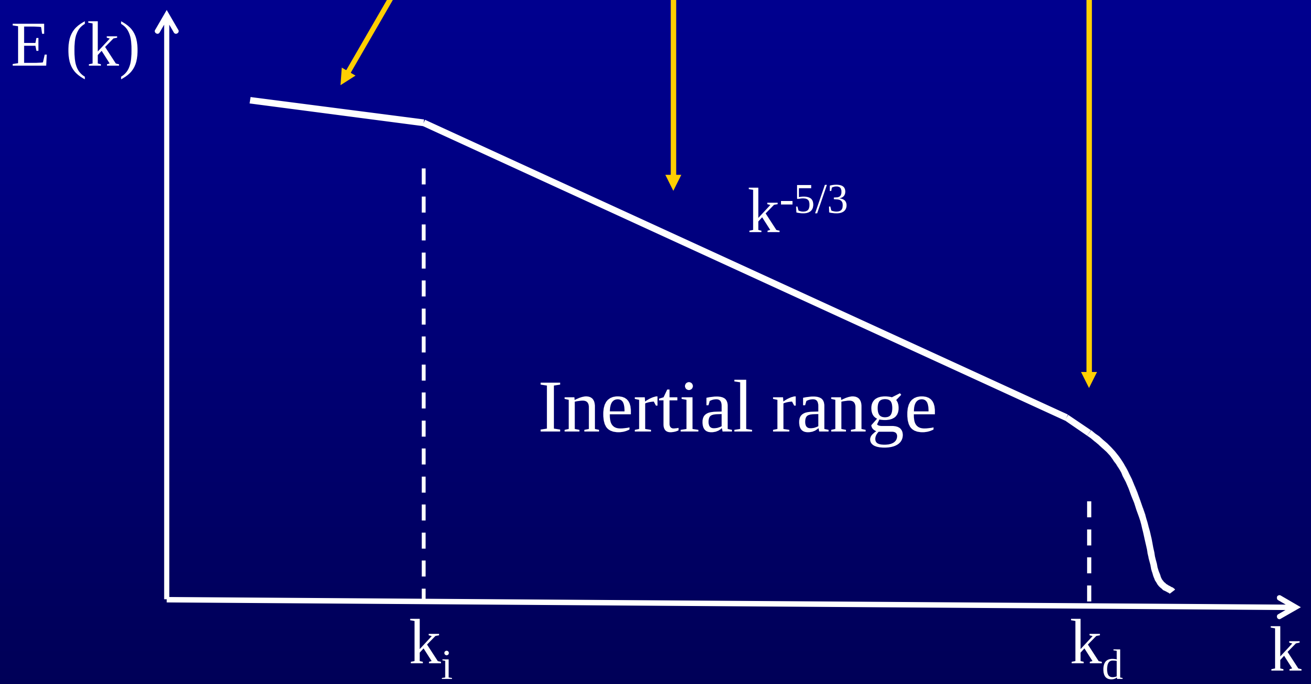

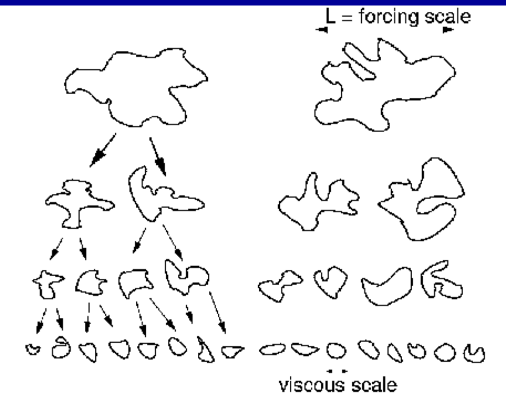

" Big whorls have little whorls
That feed on their velocity,
And little whorls have lesser whorls
And so on to viscosity"

Lewis Fry Richardson (1920)

Courtesy of A. Celani

- Hydro: Scale invariance down to the dissipation scale $1/k_d$
- Collisionless Plasmas: - Breaking of the scale invariance at $\rho_{i,e}$ $d_{i,e}$

  - Absence of the viscous dissipation scale $1/k_d$

Solar wind turbulence

Typical power spectrum of magnetic energy at 1 AU

Does the energy cascade or dissipate below the ion scale ρ_i?

Matthaeus & Goldstein, 82

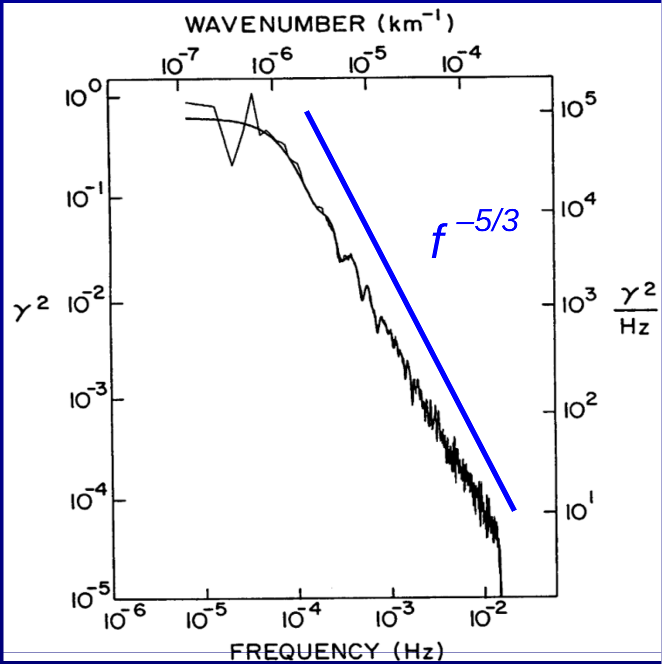

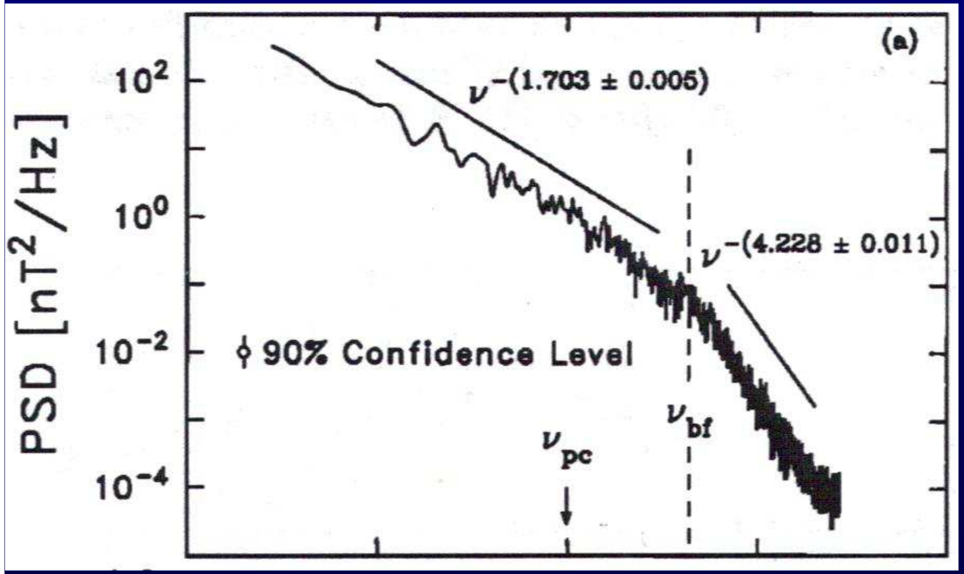

Leamon *et al.* 98; Goldstein *et al.* JGR, 94

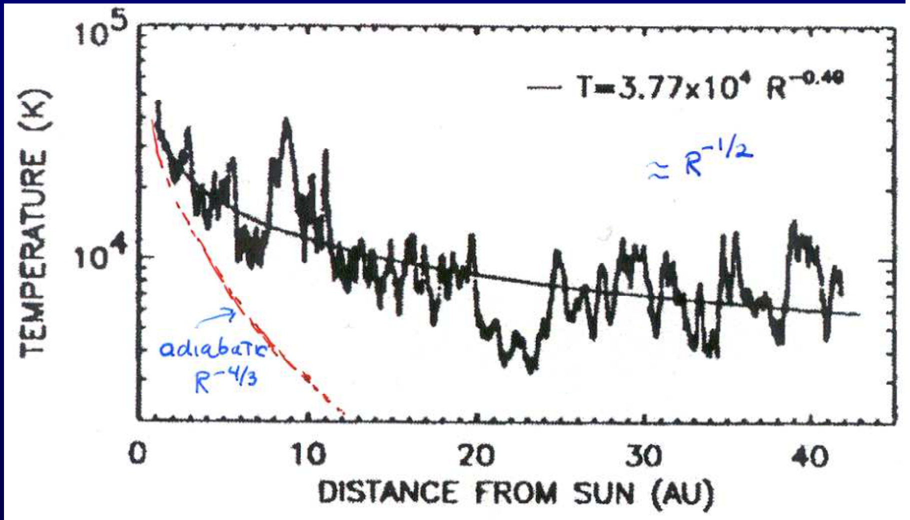

Richardson & Paularena, GRL, 1995 (Voyager data)

How to analyse space turbulence ?

Turbulence theories generally predict spatial spectra: K41 ($k^{-5/3}$); IK ($k^{-3/2}$), Anisotropic MHD turbulence ($k_{\perp}^{-5/3}$),Whistler turbulence ($k^{-7/3}$), ...

Example of measured spectra in the SW

But measurements provide only temporal spectra (generally with different power laws at differe)

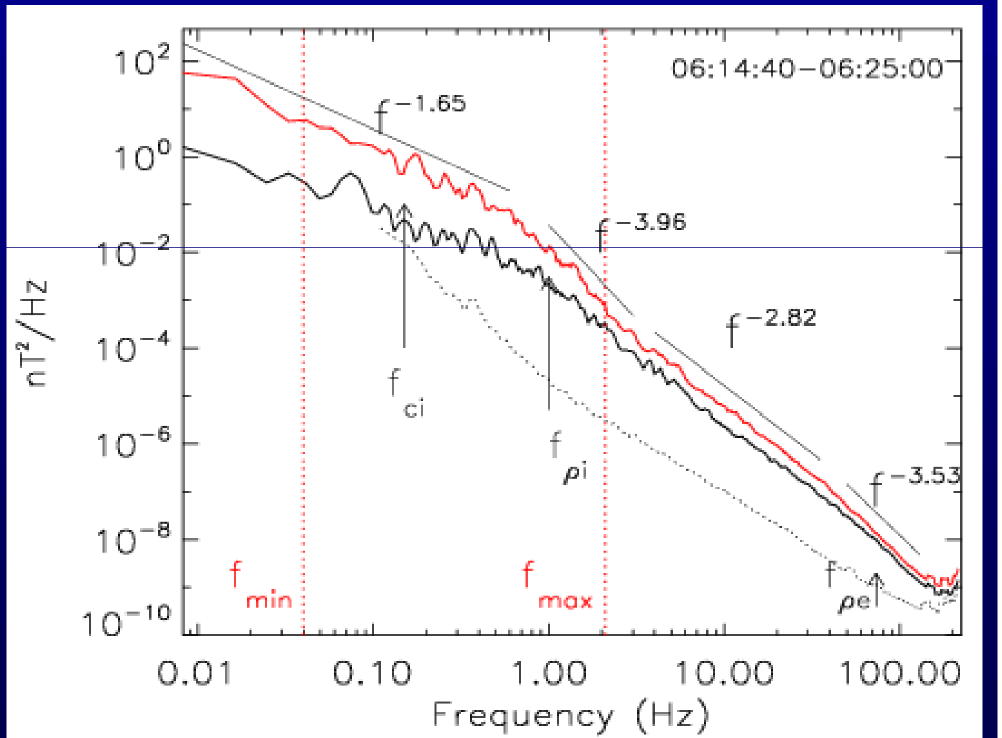

How to infer *spatial spectra* from *temporal* ones measured in the spacecraft frame? $B^2 \sim \omega_{sc}^{-\alpha} \Rightarrow B^2 \sim k_{//}^{-\beta} k_{\perp}^{-\gamma}$?

The spatio-temporal ambiguity (1)

Spacecraft measurements show highly variable phenomena.
With 1 point measurement one cannot distinguish space effects from temporal effects

Monochromatic wave

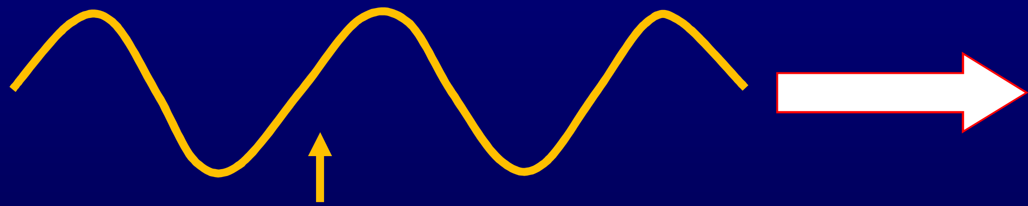

Single Observer
crossing the wave

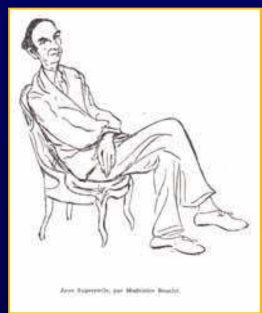

The spatio-temporal ambiguity (2)

A minimum of 4 spacecraft is needed to sample the 3 directions of space (e.g., ESA/Cluster and NASA/MMS missions)

Monochromatic wave

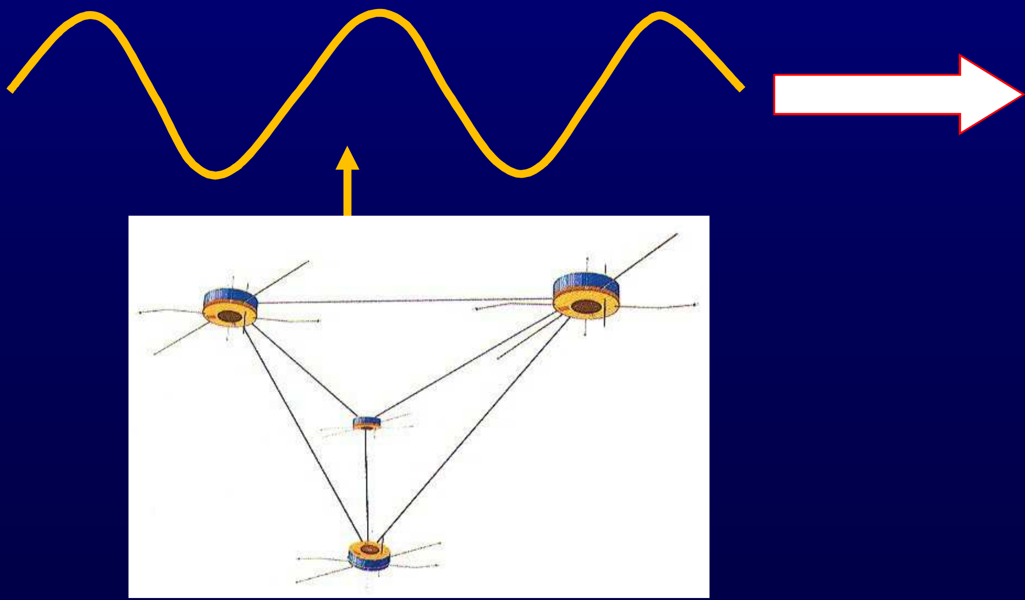

Multipoint measurements

The Taylor frozen-in flow assumption

In the solar wind (SW) the Taylor's hypothesis can be valid *at MHD scales*

High SW speeds: V ~600km/s >> V_{φ}~V_A~50km/s ⇒

$$\omega_{spacecraft} = \omega_{plasma} + \mathbf{k.V} \approx \mathbf{k.V} = k_V V$$

⇒Inferring the *k*-spectrum is possible with one spacecraft

But only along one single direction

1. At MHD scales, even if the Taylor assumption is valid, inferring 3D *k*-spectra from an *ω*-spectrum is impossible

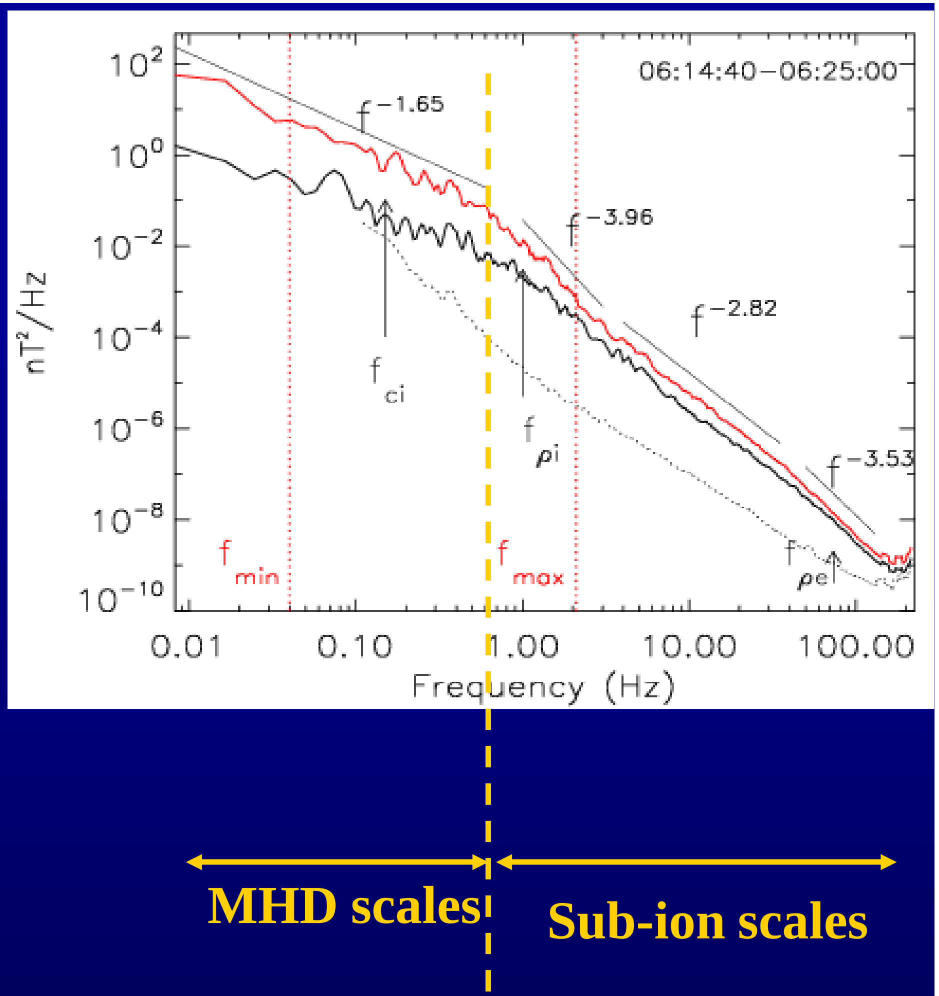

2. At sub-ion and electron scales scales Vφ can be larger than V_{sw} ⇒ The Taylor's hypothesis is invalid

1 & 2 ⇒ Need to use multi-spacecraft measurements and appropriate methods to infer 3D k-spectra

The k-filtering technique (1)

Goal: estimation of the spectral energy density $P(\omega,\mathbf{k})$ **f**rom the multipoint measurements of a turbulent field

Method: it uses a filter bank approach*:* the filter bank is constructed to absorb all signals, except those corresponding to plane waves with a specified frequency and wave vector, which pass unaffected.

By going through all frequencies and wave vectors, one gets an estimate of the wave-field energy distribution $P(\omega,\mathbf{k})$

[Pinçon & Lefeuvre, 1991; Sahraoui et al., 2003, 2004, 2006; 2010; Narita et al., 2010; Grison et al., 2005; Tjulin et al., 2005; Roberts et al., 2012]

The k-filtering technique (2)

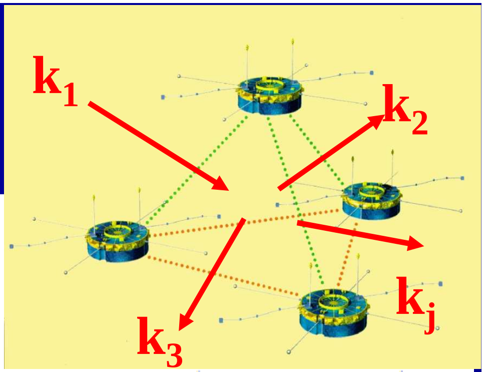

k-filtering – notations

The wave field consists of *L* real quantities:

$$A(r,t)=\begin{pmatrix} A_1(\boldsymbol{r},t) \\ A_2(\boldsymbol{r},t) \\ \vdots \\ A_L(\boldsymbol{r},t) \end{pmatrix}$$

The Fourier transformed measurements from *N* spacecraft are put into one vector:

$$\boldsymbol{A}(\omega)=\begin{pmatrix} \boldsymbol{A}(\boldsymbol{r}_1,\omega) \\ \boldsymbol{A}(\boldsymbol{r}_2,\omega) \\ \vdots \\ \boldsymbol{A}(\boldsymbol{r}_N,\omega) \end{pmatrix}$$

A spatial correlation matrix is defined:

$$\boldsymbol{M}(\omega)=\langle \boldsymbol{A}(\omega)\boldsymbol{A}^{T*}(\omega)\rangle$$

The k-filtering technique (3)

The *k*-filtering equation

Wave-field energy density distribution

$$M(\omega)=\langle A(\omega)A^{T*}(\omega)\rangle$$

$$A(\omega)=\begin{pmatrix} A(r_1,\omega) \\ A(r_2,\omega) \\ \vdots \\ A(r_N,\omega) \end{pmatrix} \qquad A(r,t)=\begin{pmatrix} A_1(r,t) \\ A_2(r,t) \\ \vdots \\ A_L(r,t) \end{pmatrix}$$

Spatial correlation matrix

Data from *N* different spacecraft

Wave-field of *L* real quantities

$$P(\omega,k)=\mathrm{Tr}\left\{C(\omega,k)\left(C^{T*}(\omega,k)H^{T*}(k)M^{-1}(\omega)H(k)C(\omega,k)\right)^{-1}C^{T*}(\omega,k)\right\}$$

Constraining matrix

Matrix to keep track of the spacecraft positions

$$\mathbf{k}.\mathbf{B}=0$$

$$\omega\mathbf{B}=\mathbf{k}\times\mathbf{E}$$

$$H(k)=\begin{pmatrix} I_L e^{ik\cdot r_1} \\ I_L e^{ik\cdot r_2} \\ \vdots \\ I_L e^{ik\cdot r_N} \end{pmatrix}$$

$L\times L$ unit matrix

The k-filtering technique (4)

Simple 1D example

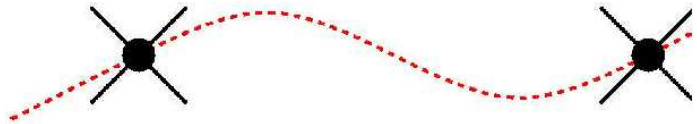

Two satellites (at x_1 and x_2) measuring one field quantity $\Phi(x,t)$.

The wave field is given by:

$$\phi(x,\omega)=\phi_0(\omega)\mathrm{e}^{ik_0 x}$$

The spatial correlation matrix is then:

$$M(\omega)=\left|\phi_0(\omega)\right|^2\begin{pmatrix} 1 & \mathrm{e}^{ik_0(x_1-x_2)} \\ \mathrm{e}^{-ik_0(x_1-x_2)} & 1 \end{pmatrix}$$

This is not invertible, we must thus add some incoherent noise:

$$M(\omega)=\left|\phi_0(\omega)\right|^2\begin{pmatrix} 1+\varepsilon & \mathrm{e}^{ik(x_1-x_2)} \\ \mathrm{e}^{-ik(x_1-x_2)} & 1+\varepsilon \end{pmatrix}$$

The ***H***-matrix in this case is:

$$H(k)=\begin{pmatrix} \mathrm{e}^{ikx_1} \\ \mathrm{e}^{ikx_2} \end{pmatrix}$$

The k-filtering technique (5)

[Tjulin et al., 2005]

Simple 1D example

This gives (after some managable algebra):

$$P(\omega, k) = \left|\phi_0(\omega)\right|^2 \frac{\varepsilon(2+\varepsilon)}{2\left(1+\varepsilon-\cos\left[\left(k-k_0\right)\left(x_1-x_2\right)\right]\right)}$$

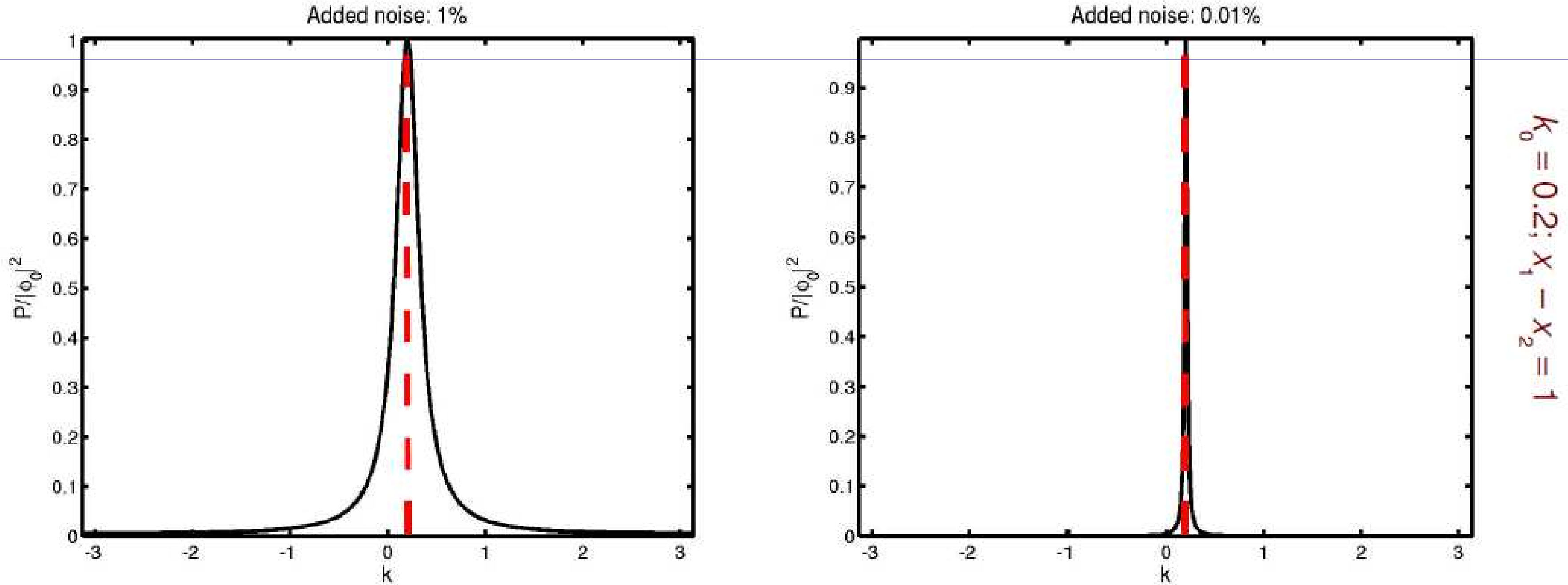

Note that the result is periodic in *k*!

The k-filtering technique (6)

Spatial Aliasing effect: Two satellites cannot distinguish between $\mathbf{k_1}$ and $\mathbf{k_2}$ if : $\Delta\mathbf{k}.\mathbf{r}_{12} = 2\pi n$ $(n=1,2, \ldots)$

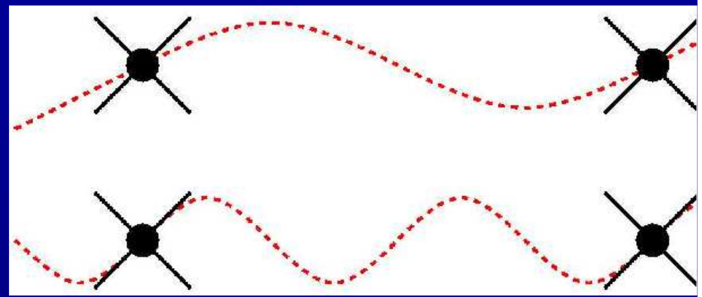

For Cluster: $\Delta\mathbf{k} = n_1\,\Delta\mathbf{k_1} + n_2\,\Delta\mathbf{k_2} + n_3\,\Delta\mathbf{k_3}$

with: $\Delta\mathbf{k_1} = (\mathbf{r}_{31}\times\mathbf{r}_{21})2\pi/V$,

$\Delta\mathbf{k_2} = (\mathbf{r}_{41}\times\mathbf{r}_{21})2\pi/V$,

$\Delta\mathbf{k_3} = (\mathbf{r}_{41}\times\mathbf{r}_{31})2\pi/V$

$V = \mathbf{r}_{41}.(\mathbf{r}_{31}\times\mathbf{r}_{21})$ [Neubaur & Glassmeir, 1]

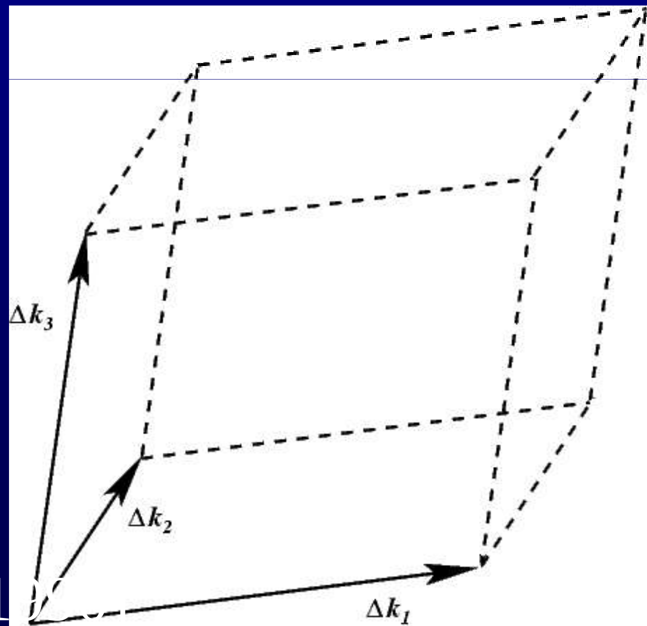

END of Part I

PART II: MHD scale turbulence

1. Theoretical models: HD, incompressible and compressible MHD
2. Turbulence at MHD scales in the solar wind
    - *Energy cascade rate: incompressible vs compressible models*
    - *Spatial anisotropy and scaling properties*
3. Comparisons with magnetosheath turbulence

Incompressible HD turbulence

$$\partial_t u + (u \cdot \nabla) u = -\nabla p + \nu \Delta u$$

Kolmogorov's phenomenological theory

Andrei N. Kolmogorov (1941a)

The local structure of turbulence in incompressible viscous fluid for very large Reynolds numbers†

By A. N. Kolmogorov

The first hypothesis of similarity. *For the locally isotropic turbulence the distributions F_n are uniquely determined by the quantities ν and $\bar{\epsilon}$.*

The second hypothesis of similarity.† *If the moduli of the vectors $y^{(k)}$ and of their differences $y^{(k)} - y^{(k')}$ (where $k \neq k'$) are large in comparison with λ, then the distribution laws F_n are uniquely determined by the quantity $\bar{\epsilon}$ and do not depend on ν.*

$$B_{dd}(r) \sim C\bar{\epsilon}^{\frac{2}{3}} r^{\frac{2}{3}}.$$

$$S_L(r) = \langle \{[\boldsymbol{u}(\boldsymbol{x}+\boldsymbol{r}) - \boldsymbol{u}(\boldsymbol{x})] \cdot \hat{\boldsymbol{r}}\}^2 \rangle \sim C \epsilon^{\frac{2}{3}} r^{\frac{2}{3}}$$

$$E(k) = C' \epsilon^{\frac{2}{3}} k^{-\frac{5}{3}}$$

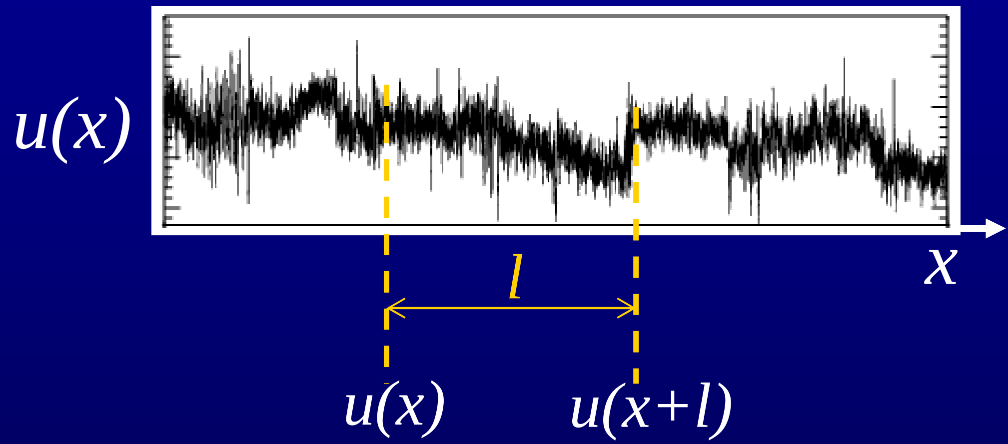

$$S_3(l) = \langle \delta u_l^{\,3} \rangle = \langle [u(x+l) - u(x)]^3 \rangle = -\frac{4}{5}\varepsilon l$$

ε is the energy cascade (dissipation) rate

$$E(k) = u_k^2 \sim k^{-5/3}$$

Incompressible MHD turbulence: equations and phenomenolgy (1)

Incompressible MHD equations

$$\frac{\partial \mathbf{v}}{\partial t} + \mathbf{v}.\nabla\mathbf{v} = -\nabla\left(p + \frac{B^2}{8\pi}\right) + \frac{\mathbf{B}.\nabla\mathbf{B}}{4\pi}$$

$$\nabla.\mathbf{B} = 0$$

$$\nabla.\mathbf{v} = 0$$

$$\frac{\partial \mathbf{B}}{\partial t} = \nabla\times(\mathbf{v}\times\mathbf{B})$$

Elsässer variables:

$$\mathbf{z}^{\pm} = \mathbf{v} \pm \frac{\mathbf{B}}{\sqrt{4\pi\rho_0}} = \mathbf{v} \pm \mathbf{v}_A$$

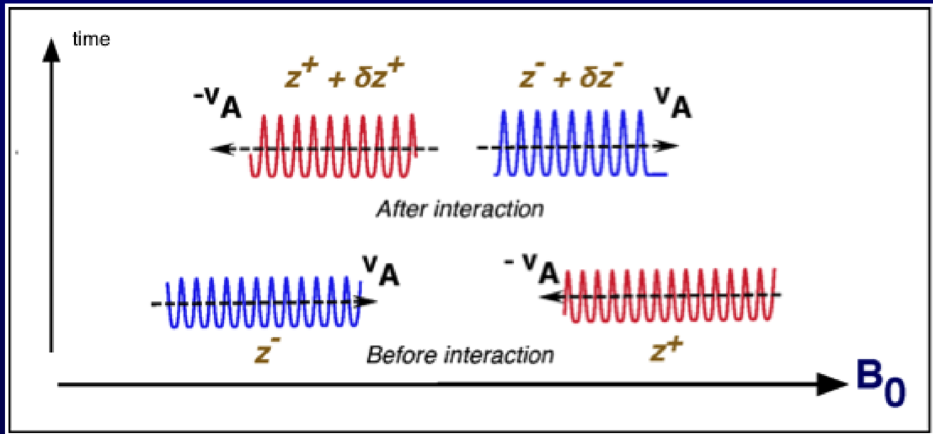

Incompressible MHD turbulence: third order law and energy casade rate (2)

$$\partial_t \mathbf{z}^{\pm} \mp \mathbf{v}_{\mathbf{A}}.\nabla \mathbf{z}^{\pm} + \mathbf{z}^{\mp}.\nabla \mathbf{z}^{\pm} = -\nabla p$$

Linear term: $k_{||} v_A z^+$

Nonlinear term: $k_{\perp} v_{\perp} z^+$

Ratio of nonlinear to linear terms $\chi = \frac{k_{\perp} v_{\perp}}{k_{//} v_A}$

χ~1 → Critically Balanced turbulence

Third order law

[Politano & Pouquet, PRE, 1998]

$$\left\langle (\delta \mathbf{z}^{\pm})^2 \delta z_l^{\mp} \right\rangle = \frac{4}{3} \varepsilon^{\pm} l$$

$$\mathbf{z}^{\pm} = \mathbf{v} \pm \frac{\mathbf{B}}{\sqrt{4\pi\rho_0}}$$

$\varepsilon^{\pm}$ is the cascade rate of the pseudo-energies

$$E^{\pm} = \frac{1}{2} z^{\pm} z^{\mp}$$

Compressible isothermal MHD turbulence: Equations

Compressible MHD equations

$$\rho\left(\frac{\partial \mathbf{v}}{\partial t}+\mathbf{v}.\nabla\mathbf{v}\right)=-\nabla\left(p+\frac{B^2}{8\pi}\right)+\frac{\mathbf{B}.\nabla\mathbf{B}}{4\pi}$$

$$\frac{\partial \mathbf{B}}{\partial t}=\nabla\times(\mathbf{v}\times\mathbf{B})$$

$$\nabla.\mathbf{B}=0$$

$$P=C_S{}^2\rho$$

Isothermal closure

C_s sound speed (constant)

Compressible MHD turbulence: linear solutions

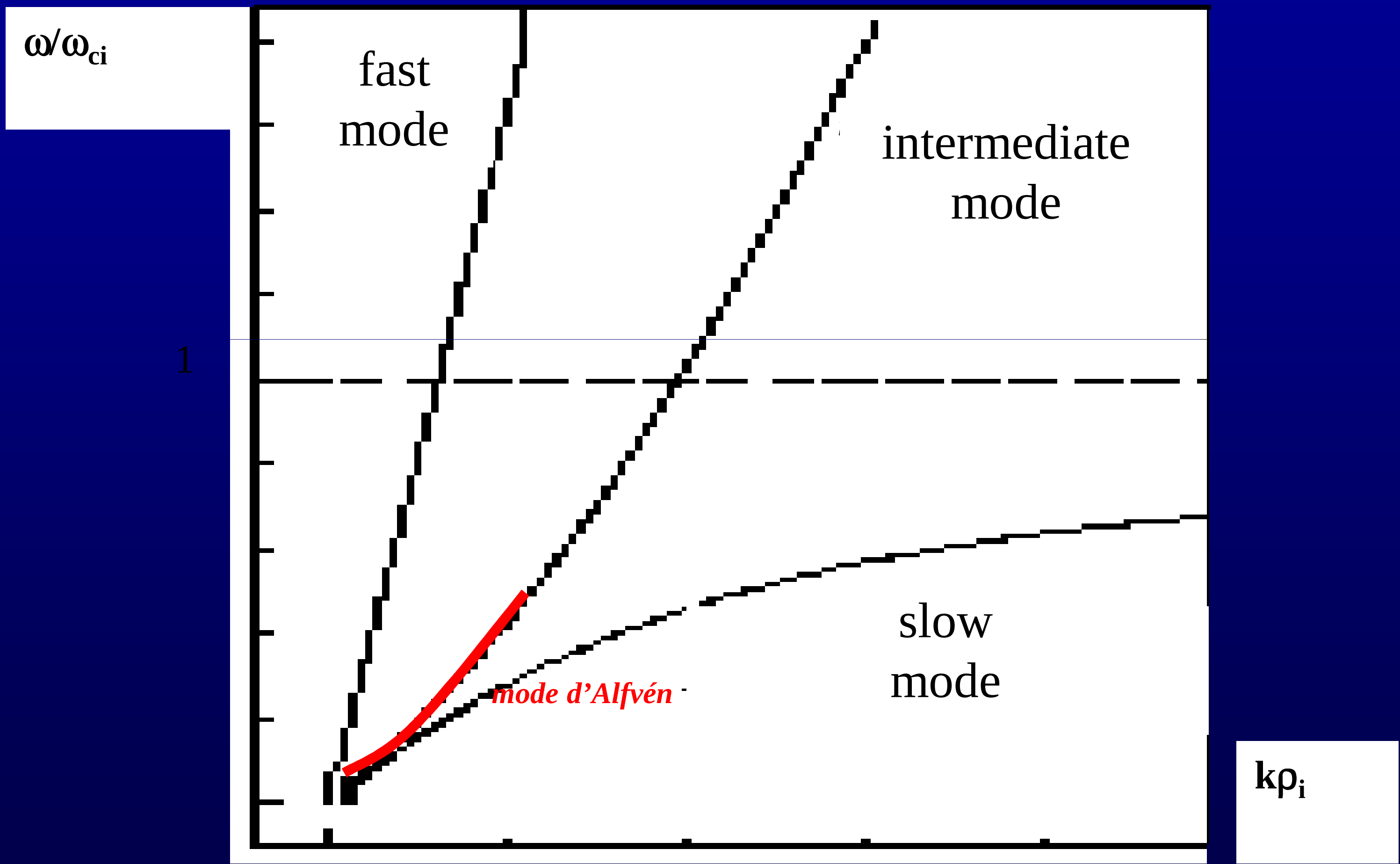

Compressible isothermal MHD turbulence: 3rd order law and energy casade rate (3)

In the inertial zone we obtain (Banerjee & Galtier, PRE, 2013)

$$-2\varepsilon = \tfrac{1}{2}\nabla_{\mathbf{r}} \cdot \overbrace{\left\langle \left[\frac{1}{2}\delta(\rho\mathbf{z}^-)\cdot\delta\mathbf{z}^- + \delta\rho\delta e\right]\delta\mathbf{z}^+ + \left[\frac{1}{2}\delta(\rho\mathbf{z}^+)\cdot\delta\mathbf{z}^+ + \delta\rho\delta e\right]\delta\mathbf{z}^- + \bar{\delta}(e + \frac{v_A^2}{2})\delta(\rho\mathbf{z}^- + \rho\mathbf{z}^+)\right\rangle}^{\text{Usual flux term}}$$

$$\underbrace{-\frac{1}{4}\left\langle \frac{1}{\beta'}\nabla'\cdot(\rho\mathbf{z}^+ e') + \frac{1}{\beta}\nabla\cdot(\rho'\mathbf{z}'^+ e) + \frac{1}{\beta'}\nabla'\cdot(\rho\mathbf{z}^- e') + \frac{1}{\beta}\nabla\cdot(\rho'\mathbf{z}'^- e)\right\rangle}_{\text{New type of flux term}}$$

$$+\left\langle(\nabla\cdot\mathbf{v})\left[R'_E - E' - \tfrac{\bar{\delta}\rho}{2}(\mathbf{v_A}'\cdot\mathbf{v_A}) - \tfrac{P'}{2} + \tfrac{P'_M}{2}\right]\right\rangle + \left\langle(\nabla'\cdot\mathbf{v}')\left[R_E - E - \tfrac{\bar{\delta}\rho}{2}(\mathbf{v_A}\cdot\mathbf{v_A}') - \tfrac{P}{2} + \tfrac{P_M}{2}\right]\right\rangle$$

$$+\left\langle(\nabla\cdot\mathbf{v_A})\left[R_H - R'_H + H' - \bar{\delta}\rho(\mathbf{v}'\cdot\mathbf{v_A})\right]\right\rangle + \left\langle(\nabla'\cdot\mathbf{v_A}')\left[R'_H - R_H + H - \bar{\delta}\rho(\mathbf{v}\cdot\mathbf{v_A}')\right]\right\rangle$$

where

$$E = \rho(\mathbf{v}\cdot\mathbf{v} + \mathbf{v}_A\cdot\mathbf{v}_A)/2 + \rho e,\;\; E' = \rho'(\mathbf{v}'\cdot\mathbf{v}' + \mathbf{v}'_A\cdot\mathbf{v}'_A)/2 + \rho' e';$$

$$R_E = \rho(\mathbf{v}\cdot\mathbf{v}' + \mathbf{v}_A\cdot\mathbf{v}'_A)/2 + \rho e',\;\; R'_E = (\rho'\mathbf{v}'\cdot\mathbf{v} + \mathbf{v}'_A\cdot\mathbf{v}_A)/2 + \rho' e;$$

$$R_H = \rho(\mathbf{v}\cdot\mathbf{v}'_A + \mathbf{v}'\cdot\mathbf{v}_A)/2,\;\; R'_H = \rho'(\mathbf{v}'\cdot\mathbf{v}_A + \mathbf{v}\cdot\mathbf{v}'_A)/2$$

$$H = \rho\mathbf{v}\cdot\mathbf{v}_A,\;\; H' = \rho'\mathbf{v}'\cdot\mathbf{v}'_A;\;\; \beta = 2C_S^2/v_A^2;\;\; \beta' = 2{C_S}'^2/{v_A}'^2$$

Additional assumptions:

- Neglect the source terms
- Isotropy
- Uniform β

$$\Phi = \frac{1}{\beta}\nabla_{\boldsymbol{\ell}} \cdot \langle \rho \mathbf{v} e' - \rho' \mathbf{v}' e \rangle = -\frac{2}{\beta}\nabla_{\boldsymbol{\ell}} \cdot \langle \overline{\delta} e \delta(\rho \mathbf{v}) \rangle$$

$$-\frac{4}{3}\varepsilon_C \ell = \mathcal{F}_{C+\Phi}(\ell)$$

$$\mathcal{F}_{C+\Phi}(\ell) = \mathcal{F}_1(\ell) + \mathcal{F}_2(\ell) + \mathcal{F}_3(\ell)$$

$$\begin{aligned}
\mathcal{F}_1(\ell) &= \left\langle \frac{1}{2}\left[\delta(\rho \mathbf{z}^-) \cdot \delta \mathbf{z}^-\right] \delta z_\ell^+ + \frac{1}{2}\left[\delta(\rho \mathbf{z}^+) \cdot \delta \mathbf{z}^+\right] \delta z_\ell^- \right\rangle , \\
\mathcal{F}_2(\ell) &= \langle 2\delta\rho\delta e \delta v_\ell \rangle , \\
\mathcal{F}_3(\ell) &= \left\langle 2\overline{\delta}\left[\left(1 + \frac{1}{\beta}\right) e + \frac{v_A^2}{2}\right] \delta(\rho_1 v_\ell) \right\rangle . \qquad (8)
\end{aligned}$$

The solar wind

The solar wind plasma is generally:

- Fully ionized (H^+, e^-)
- Non -relativistic (V_A<<c), V~350-800 km/s
- *Collisionless*

[Richardson & Paularena, 1995]

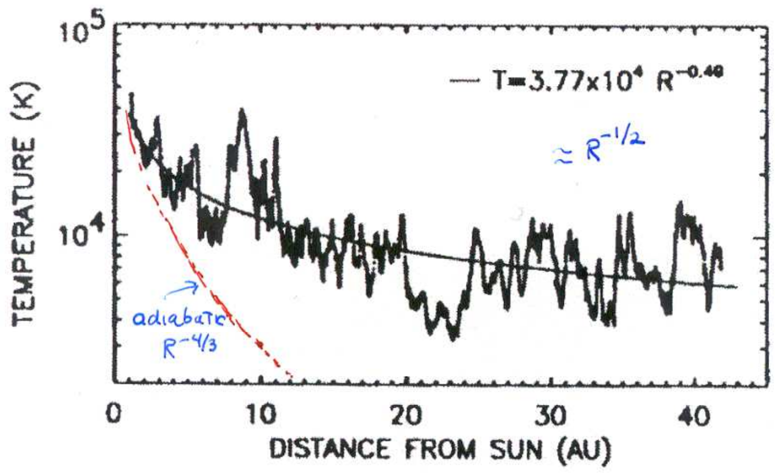

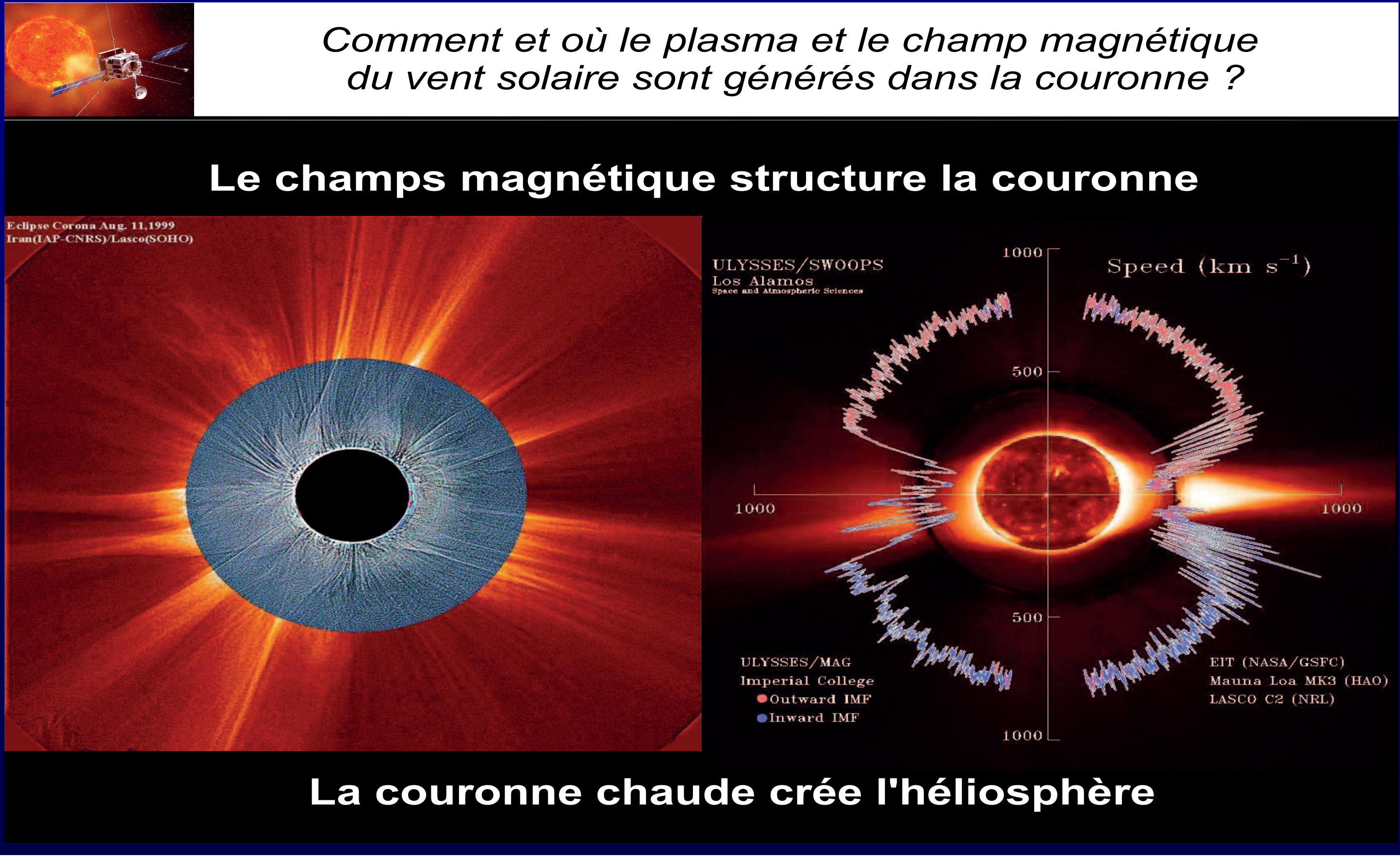

Typical magnetic power spectrum at 1AU

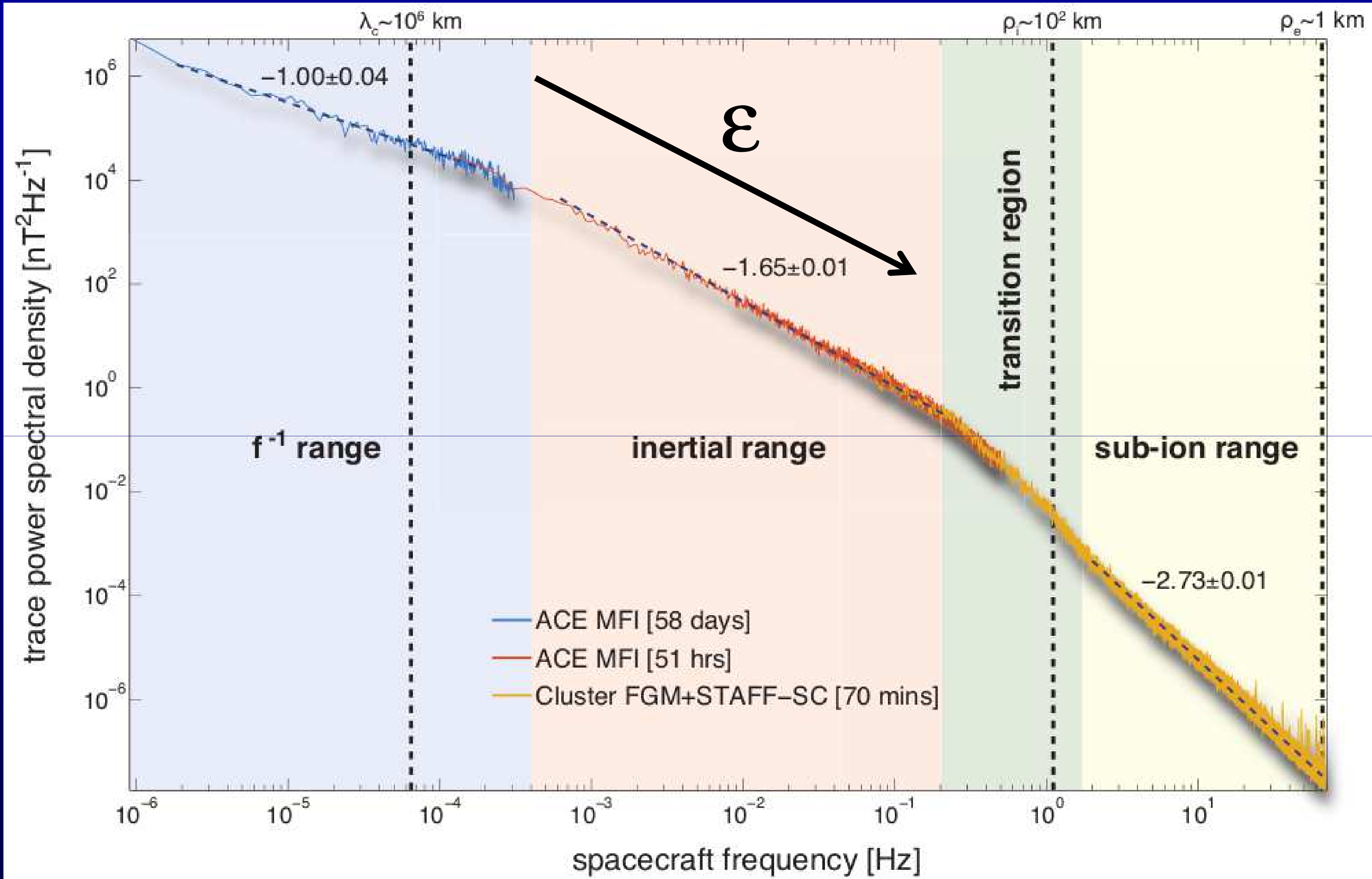

Kiyani et al., 2015

Estimation of the energy cascade rate : compressible vs incompressible MHD model (1)

$$\mathbf{z}^{\pm} = \mathbf{v} \pm \frac{\mathbf{B}}{\sqrt{4\pi\rho_0}}$$

$$\left\langle (\delta \mathbf{z}^{\pm})^2 \, \delta z_l^{\mp} \right\rangle = \frac{4}{3} \varepsilon^{\pm} l$$

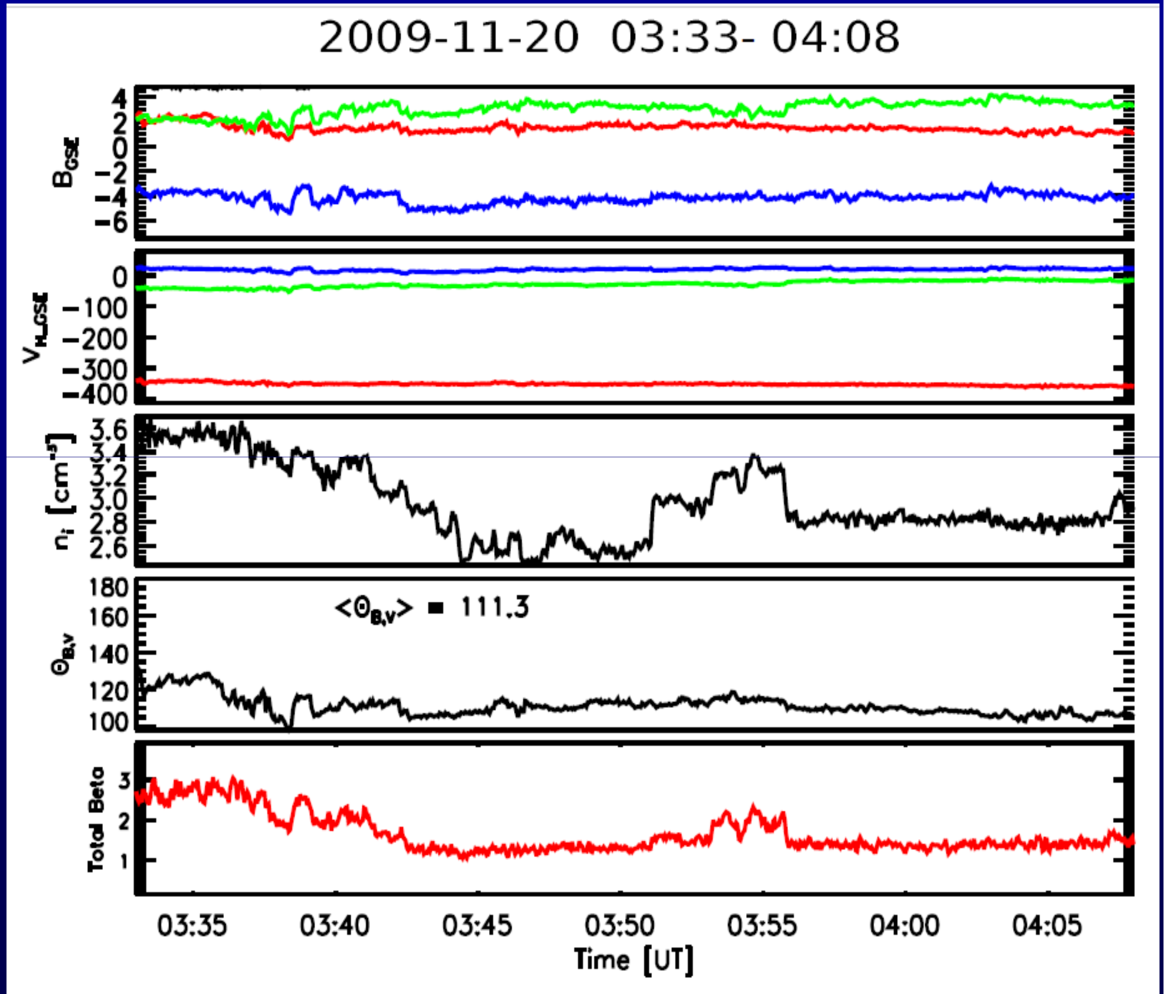

Estimation of the energy cascade rate : compressible vs incompressible MHD model (2)

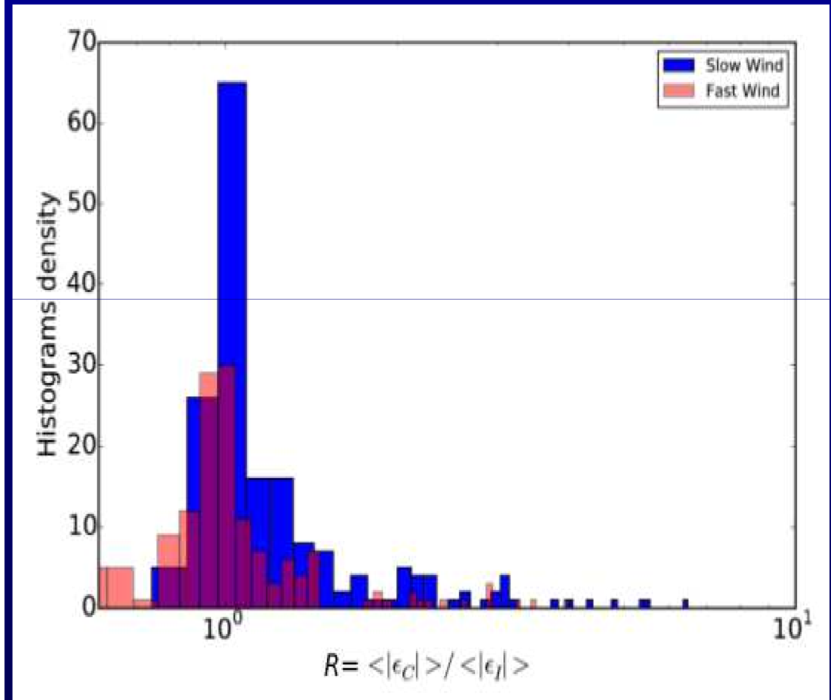

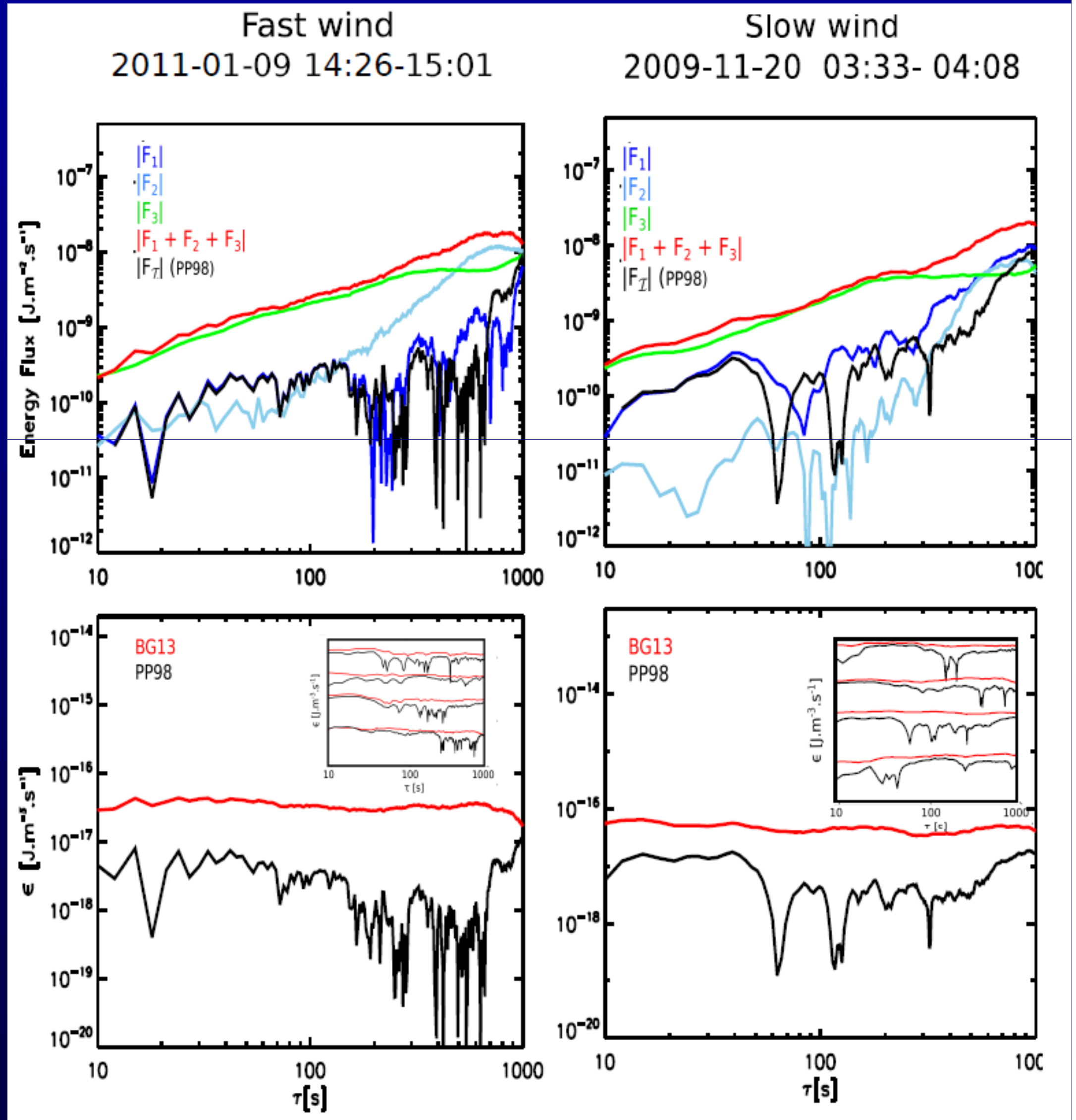

Hadid et al., ApJ, 2016

Estimation of the energy cascade rate : cross helicity and turbulent Mach number

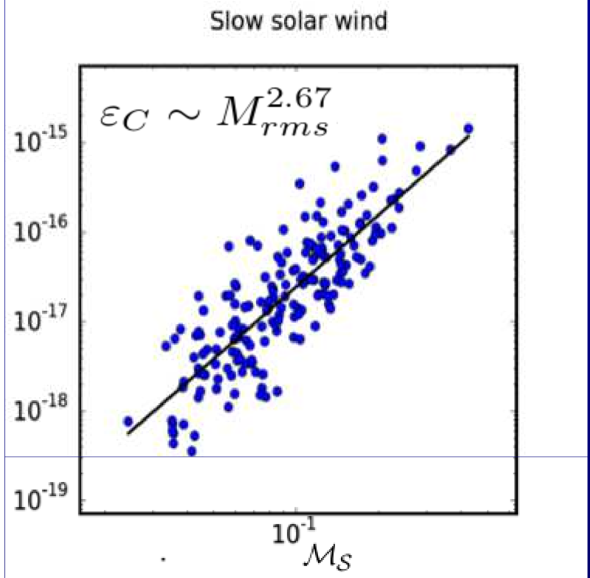

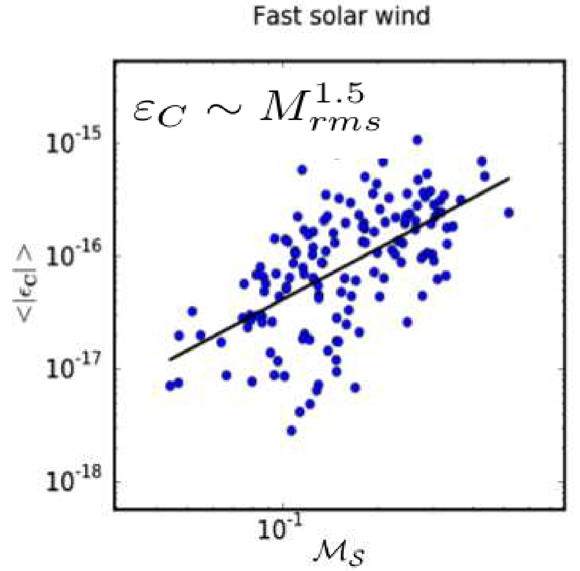

$$\sigma_c = \frac{H_c}{(1/2) < \delta \mathbf{v}^2 + \delta \mathbf{b}^2 >}$$

$$H_c = < \delta \mathbf{v} \cdot \delta \mathbf{b} >$$

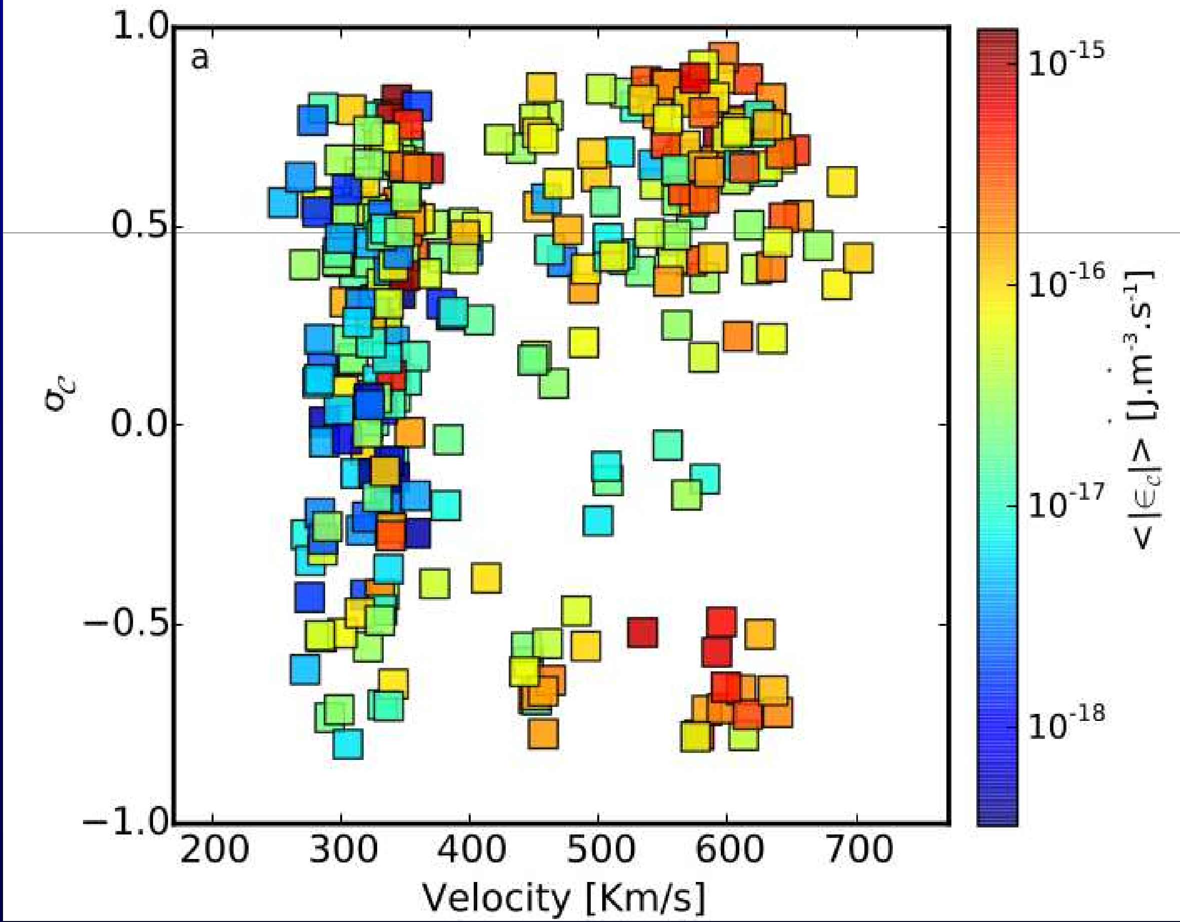

Spatial anisotropy

In MHD turbulence, the presence of a mean lagnetic field makes the turbulence anisotropic at small scales [Montgomery et al., 1983]

$l/L_0 \sim 1$ $l/L_0 \sim 1/10$ $l/L_0 \sim 1/100$

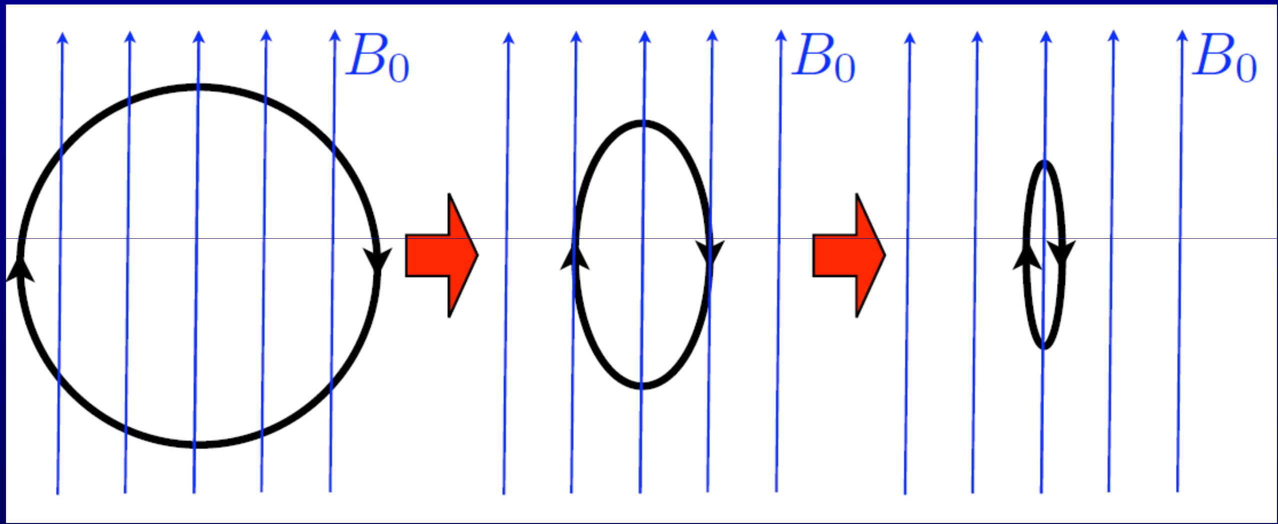

3D Electron -MHD simulations [Meyrand & Galtier, 2013]

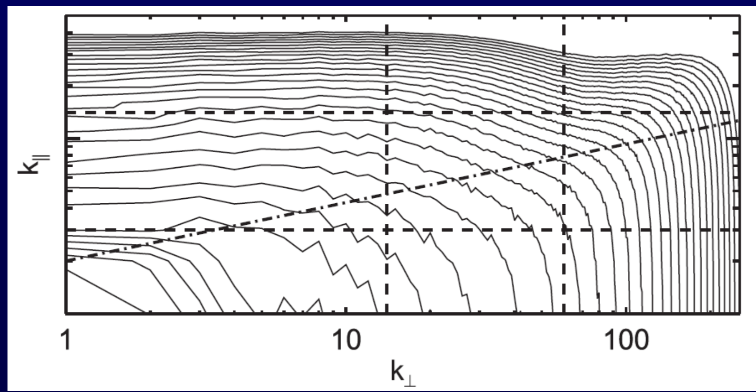

Anisotropy and the critical balance conjecture

The critical balance conjecture [Goldreich & Sridhar, 1995]:

Linear (Alfvén) time ~ nonlinear (turnover) time

$\Rightarrow \omega \sim k_{//} V_A \sim k_\perp u_\perp$

$\Rightarrow k_{//} \sim k_\perp^{2/3}$

See also [Boldyrev, ApJ, 2005] and [Galtier et al., Phys. Plasmas, 2005]

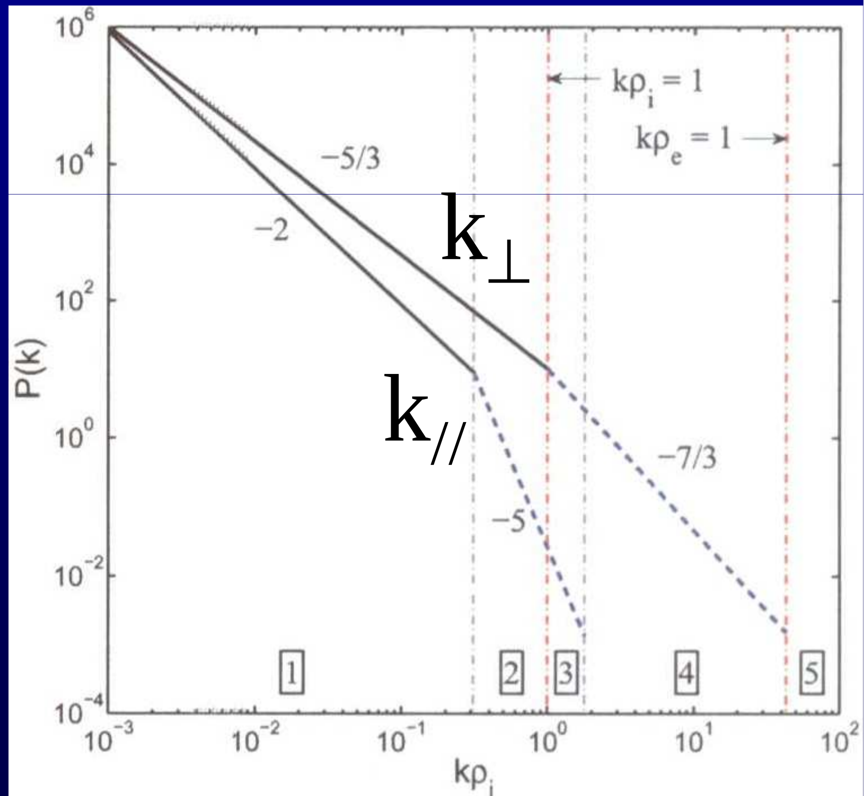

[Chen et al., ApJ, 2010]

Single satellite analysis → use of the Taylor assumption:

$\omega_{sc} \sim \mathbf{k.V}_{sw} \sim k_v V_{sw}$

V//B → $k_v = k_{//}$

V⊥B → $k_v = k_{\perp}$

Assumes axisymmetry around B

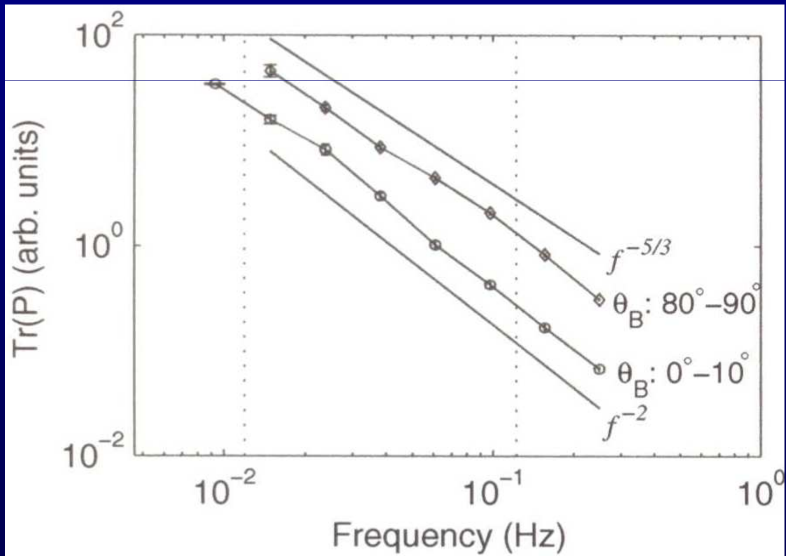

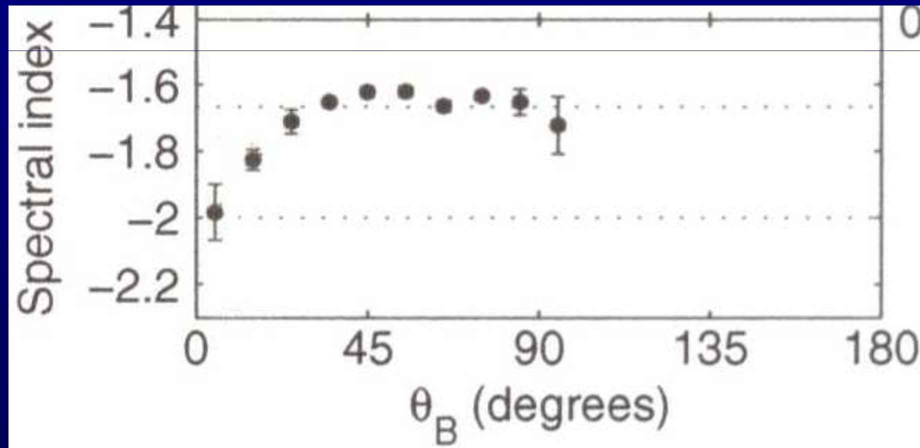

$\Theta_{BV} \rightarrow 0 \Rightarrow B^2 \sim k_{//}^{-2} \Rightarrow$ *Partial* evidence of the critical balance [Horbury et al., PRL, 2008]

Results confirmed by
Podesta, ApJ, 2009

See also Chen et al.,
PRL, 2010

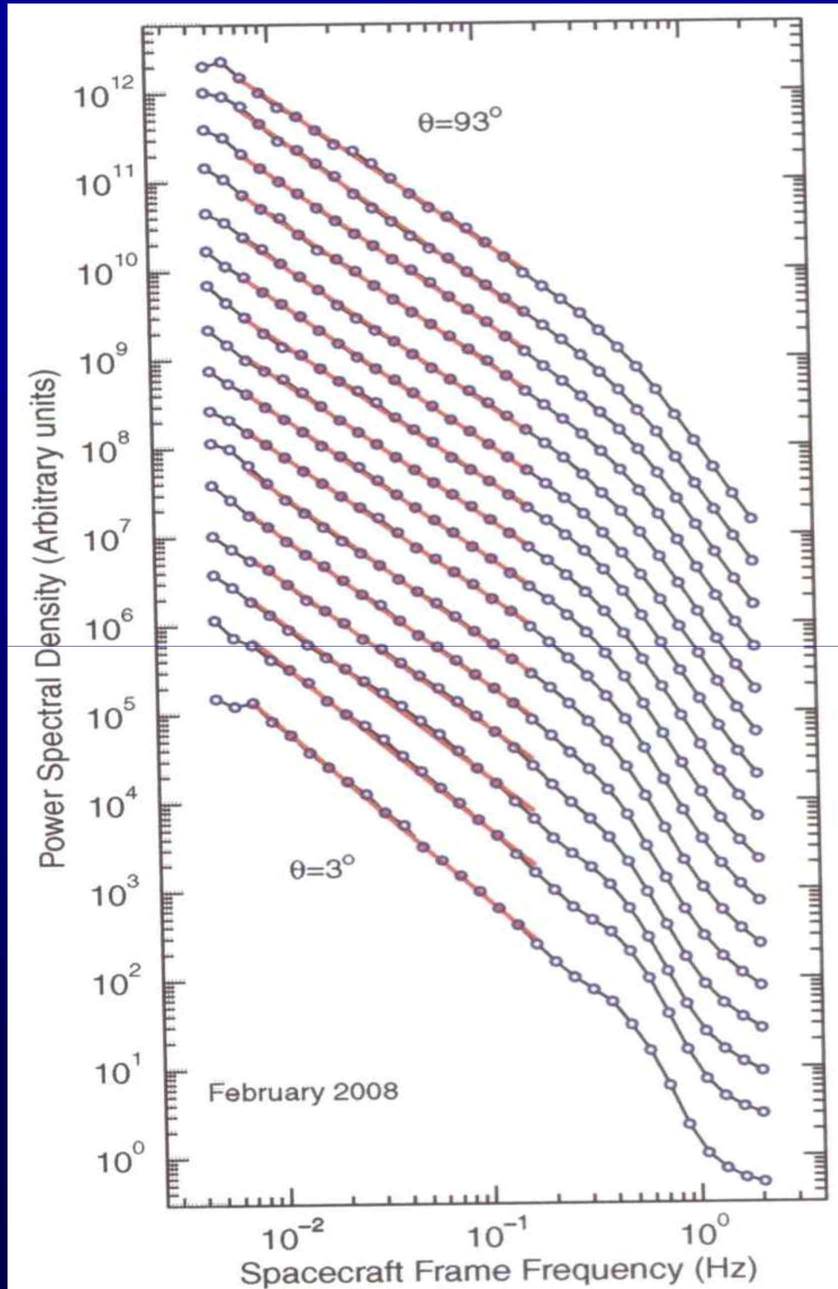

The ESA/Cluster mission

The first multispacecraft mission: 4 identical satellites

Objetives:

- **3D exploration** of the Earth magnetosphere boundaries (magnetopause, bow shock, magnetotail) & SW

- **Mesurements of 3D quantities:**
J=∇x**B**, …

- **Fundamental physics:**
turbulence, reconnection, particle acceleration, …

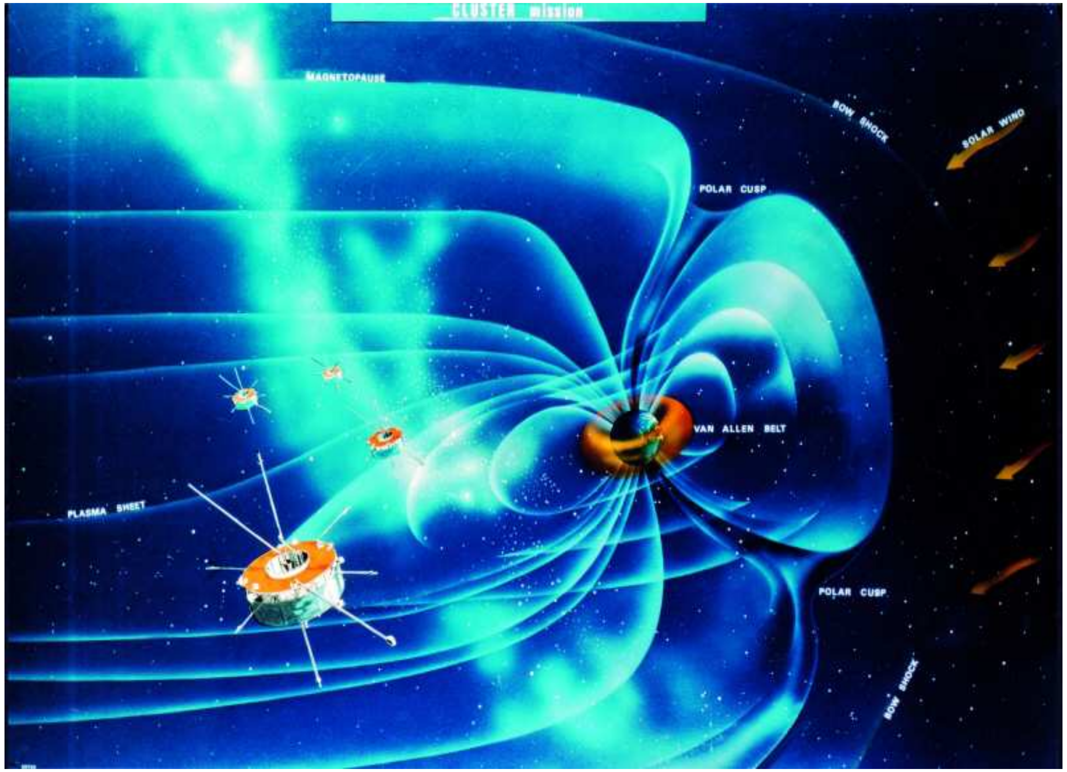

Different orbits and separations (10^2 to 10^4km) depending on the scientific goal

The 4 satellites before launch

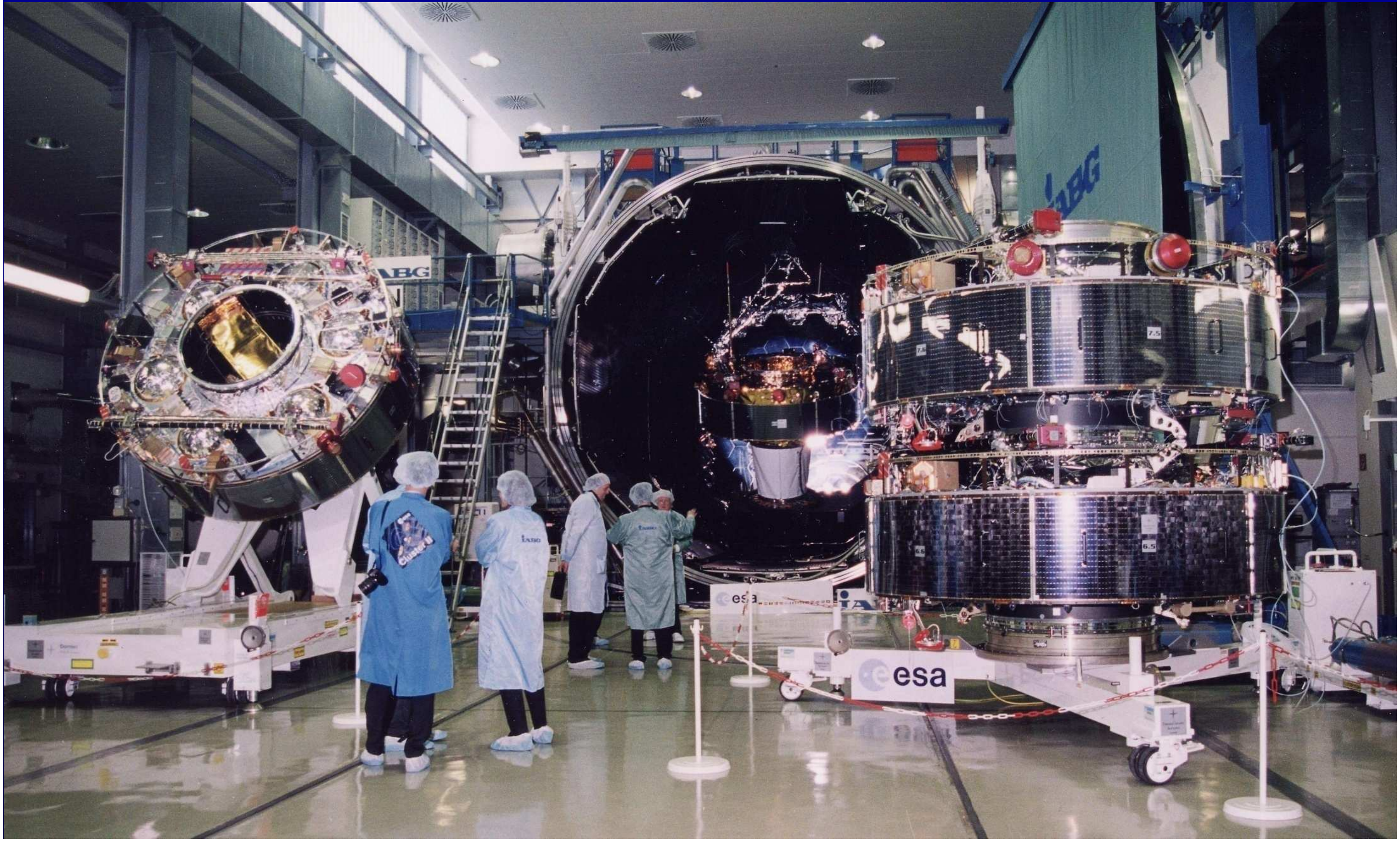

The *k*-filtering technique

Interferometric method: it provides, by using a NL filter bank approach, an optimum estimation of the 4D spectral energy density $P(\omega,\mathrm{k})$ from simultaneous multipoints measurements [Pinçon & Lefeuvre; Sahraoui et al., 03, 04, 06, 10; Narita et al., 03, 06,09]

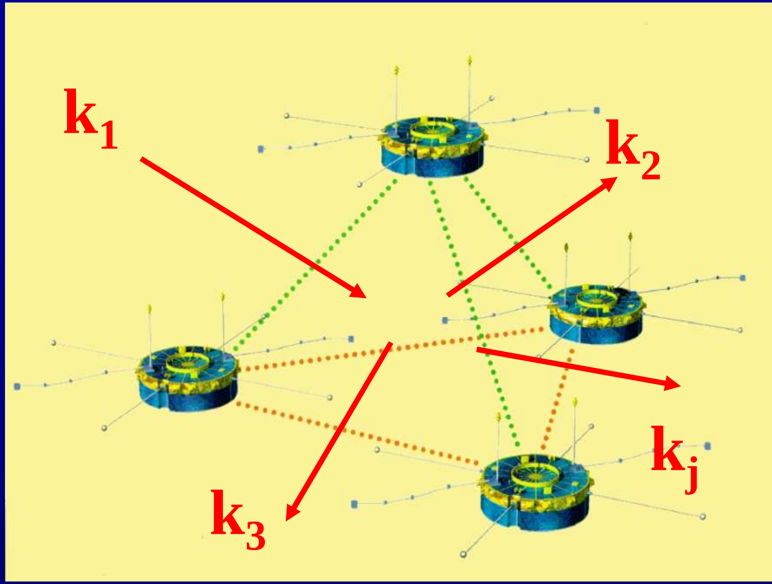

We use $P(\omega,\mathrm{k})$ to calculate

1. 3D ω-k spectra ⇒ plasma mode identification e.g. Alfvén, whistler
2. 3D *k*-spectra (anisotropies, scaling, …)

Measurable spatial scales

Given a spacecraft separation *d* only one decade of scales $2d < \lambda < 30d$ can be correctly determined

- $\lambda_{min} \simeq 2d$, otherwise *spatial* aliasing occurs.
- $\lambda_{max} \simeq 30d$, because larger scales are subject to higher uncertainties

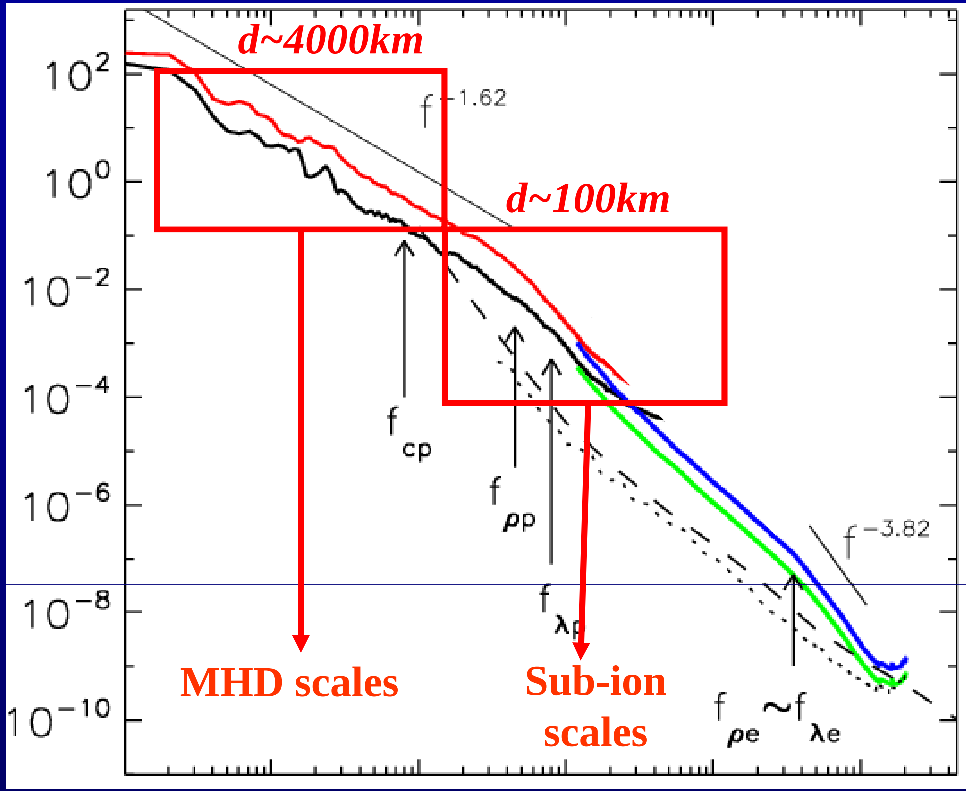

$\omega_{sat} \sim kV \Rightarrow f_{max} \sim k_{max} V/\lambda_{min}$ (V~500km/s)

- d~10^4 km ⇒ MHD scales
- d~10^2 km ⇒ Sub-ion scales
- d~1 km ⇒ Electron scales (*but not accessible with Cluster: d>100*)

1- MHD scale solar wind turbulence

Position of the Quartet on March 19, 2006

Position

time:

2006-03-19 20:30

Coordinate System:

GSE

Satellite	Color	X	Y	Z
Cluster-1	blue	15.038	-6.569	-9.299
Cluster-2	red	15.139	-7.034	-8.672
Cluster-3	green	13.979	-7.397	-10.41
Cluster-4	magenta	14.587	-7.292	-9.987

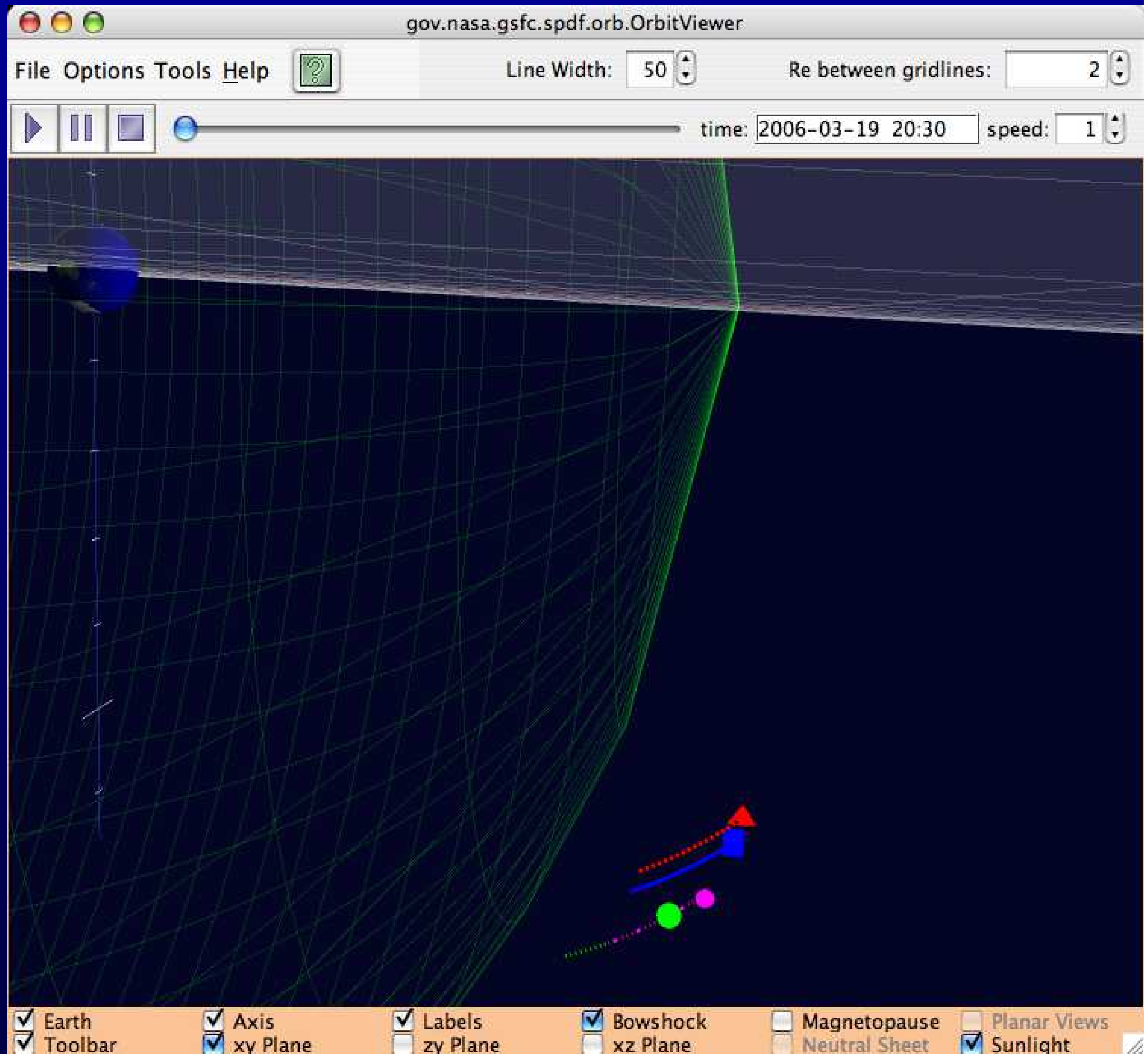

Data overview

FGM data (CAA, ESA)

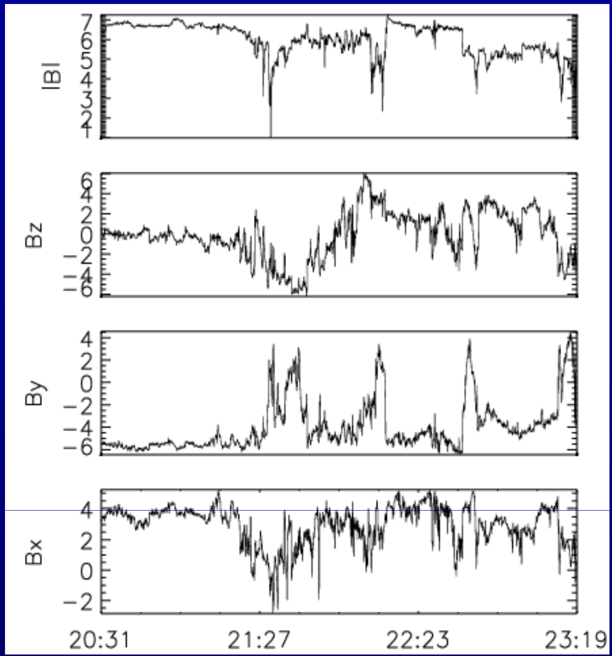

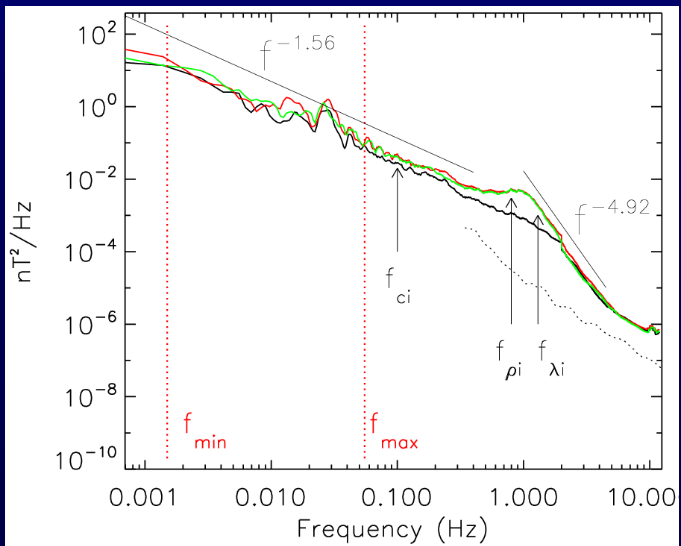

Ion plasma data from CIS (AMDA, CESR)

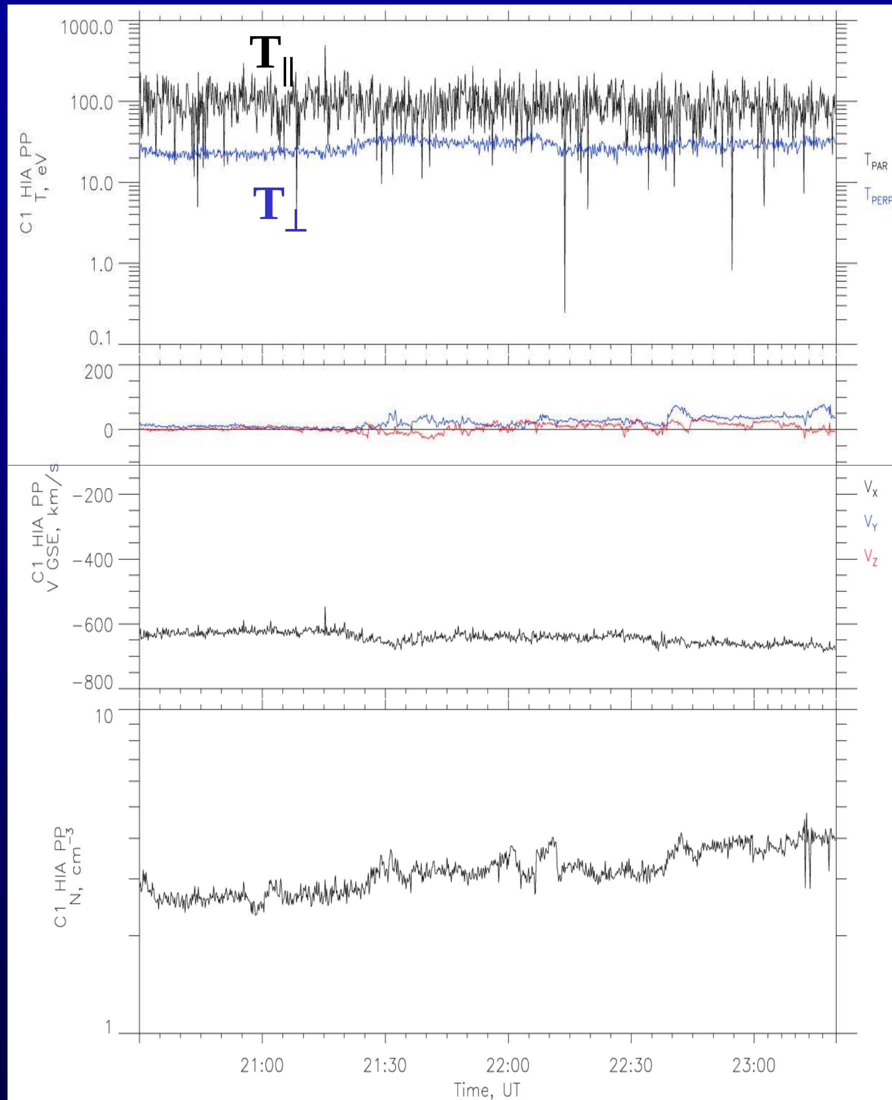

f_1=0.23Hz~2f_{ci}

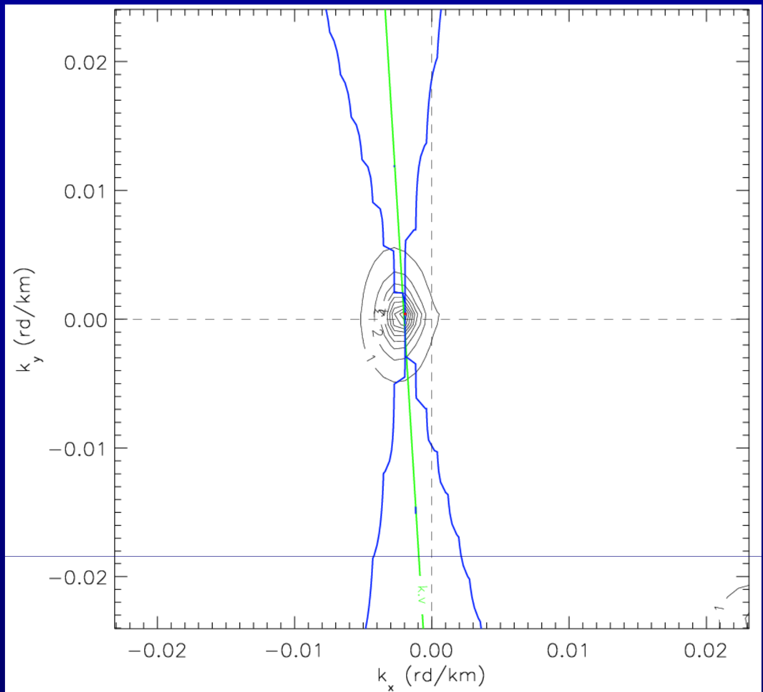

f_2=0.9Hz~6f_{ci}

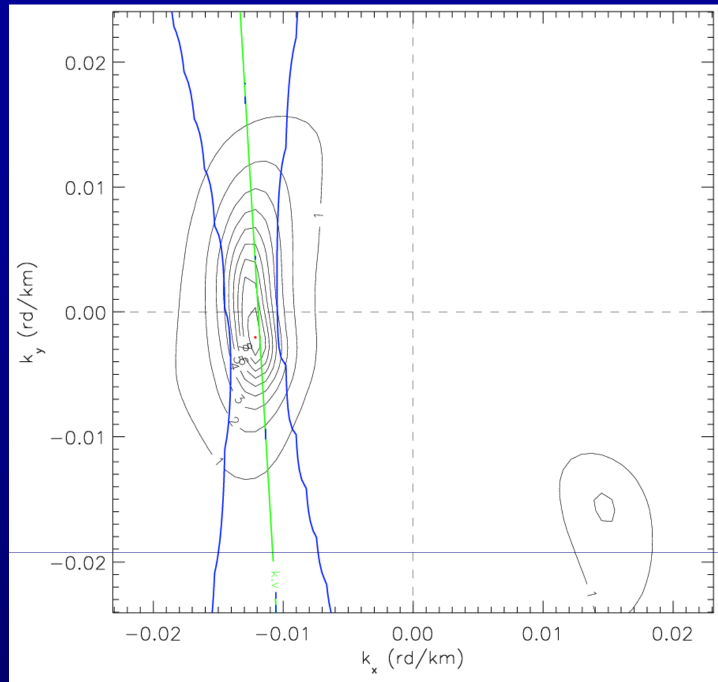

To compute reduced spectra we integrate over

1. all frequencies f_{sc}: $$\tilde{P}(\mathbf{k}) = \sum_{ky,k_z} P(f_{sc},\mathbf{k})$$

2. all $k_{i,j}$: $$\tilde{\tilde{P}}(k_x) = \sum_{ky,k_z} \tilde{P}(k_x,k_y,k_z)$$

Anisotropy of MHD turbulence along B_o and V_{sw}

[Narita et al. , PRL, 2010]

Turbulence is not axisymmetric (around B) [see also Sahraoui, PRL, 2006]

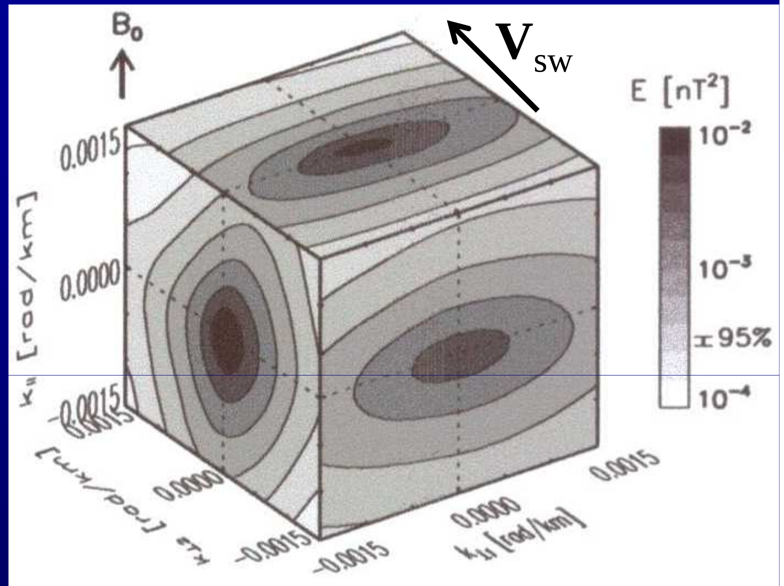

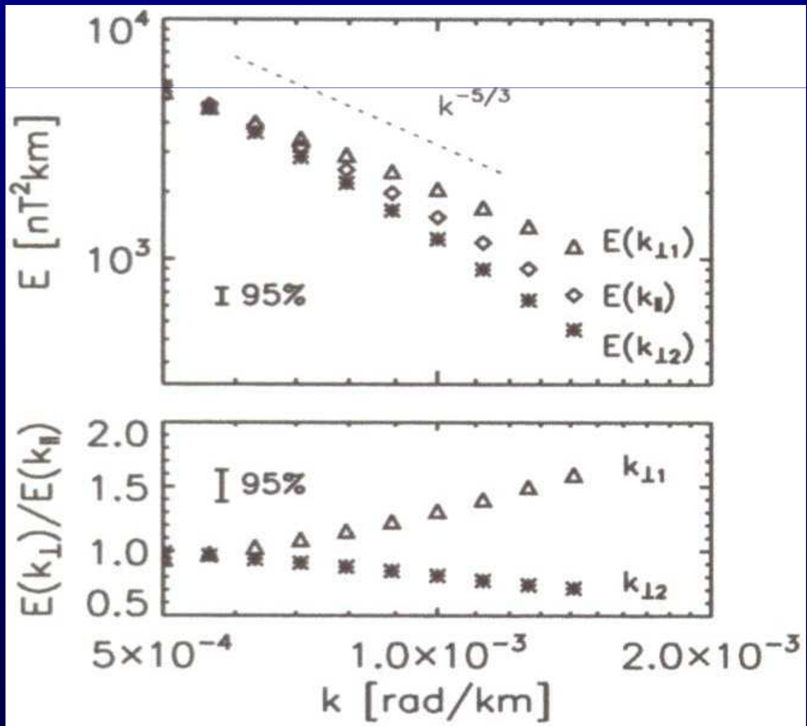

The anisotropy ($\perp$ B) is along $\mathbf{V}_{sw}$ → SW expansion effect ?[Saur & Bieber, JGR, 1999]

Mirror mode turbulence

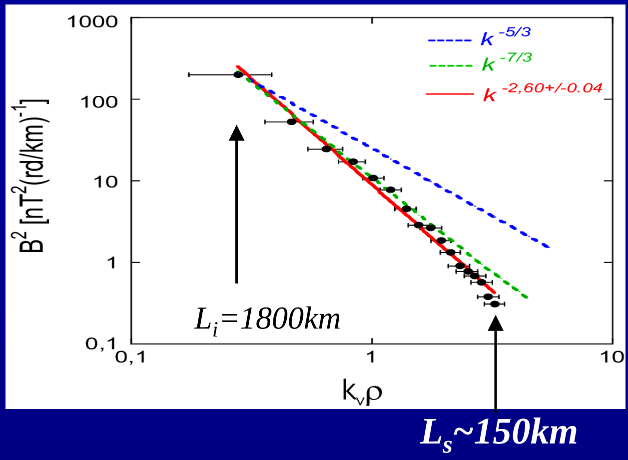

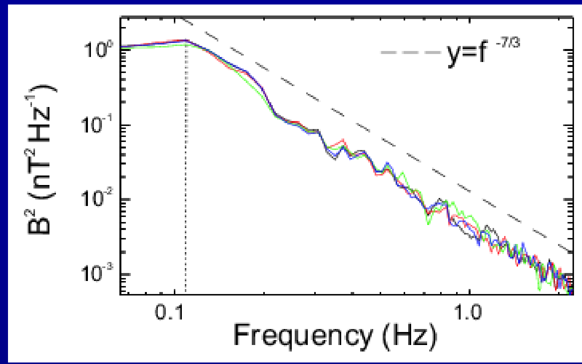

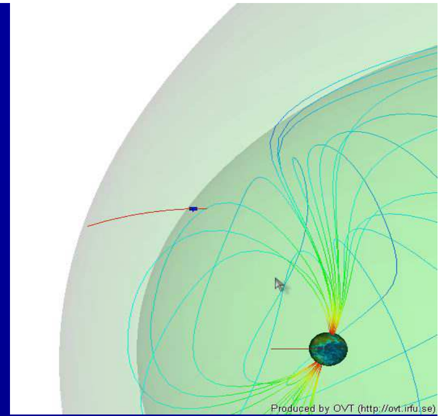

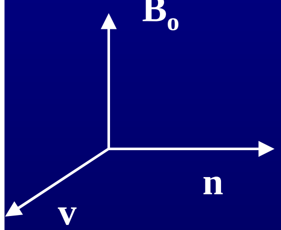

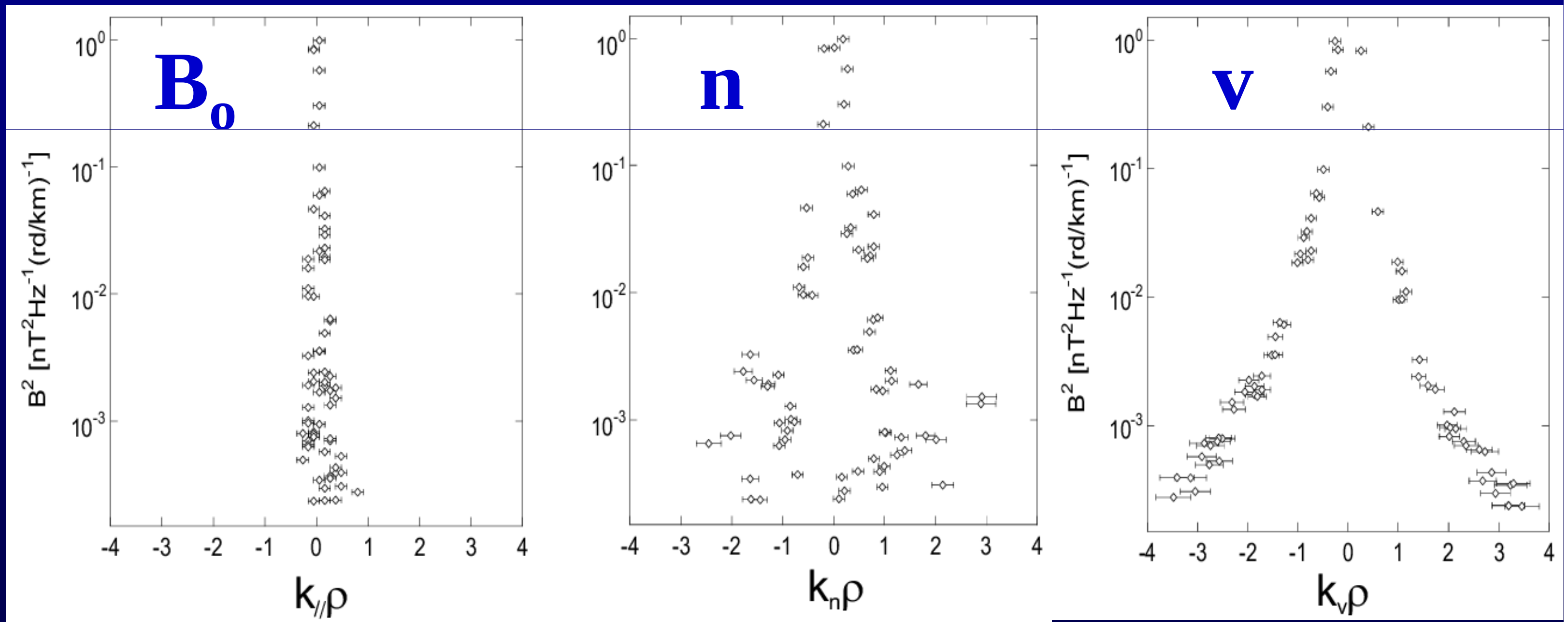

(v,n) ~ 104°
(v,B_o) ~ 110°
(n,B_o) ~ 81°

Compressible, anisotropic and non-axisymmetric turbulence (along **B_o**, the magnetopause normal **n**, and the flow **v**) [Sahraoui+, PRL,2006]

PART III:
Kinetic (sub-ion scale) turbulence

Kinetic turbulence

1. Kinetic scales in the SW: Some hotly debated question vs Cluster observations
   - *The nature of the cascade or dissipation below ρ_i: : KAW? whistler? Others?*
   - *The nature of the dissipation: wave-particle interactions? Current sheets/Reconnection?*
2. Conclusions & perspectives (turbulence & the future space missions)

I- Theoretical predictions on small scale turbulence

$$\mathbf{E} + \mathbf{V} \times \mathbf{B} = \frac{1}{en}\mathbf{J} \times \mathbf{B} - \frac{\nabla P_e}{en} + \ldots$$

1. Fluid models (Hall-MHD)

   - Whistler turbulence (E-MHD): (Biskamp *et al.*, 99, Galtier, 08)

   - Weak Turbulence of Hall-MHD (Galtier, 06; Sahraoui et al., 07)

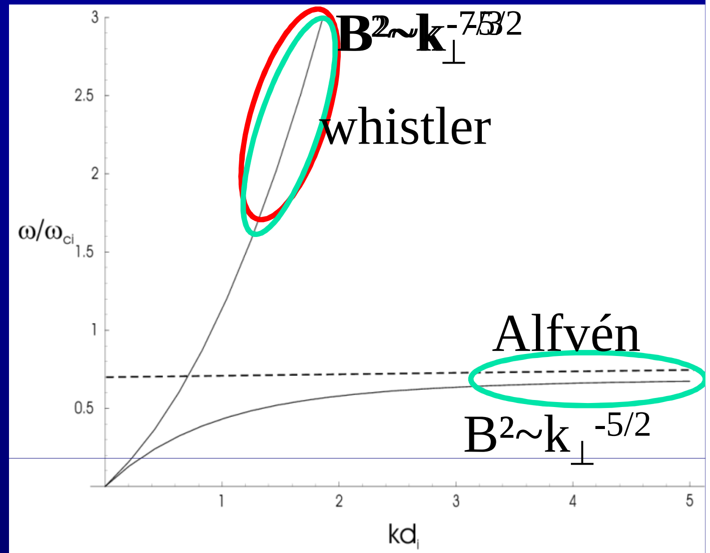

2. Gyrokinetic theory: $k_{//} \ll k_\perp$ and $\omega \ll \omega_{ci}$ (Schekochihin *et al.* 06; Howes *et al.*, 11)

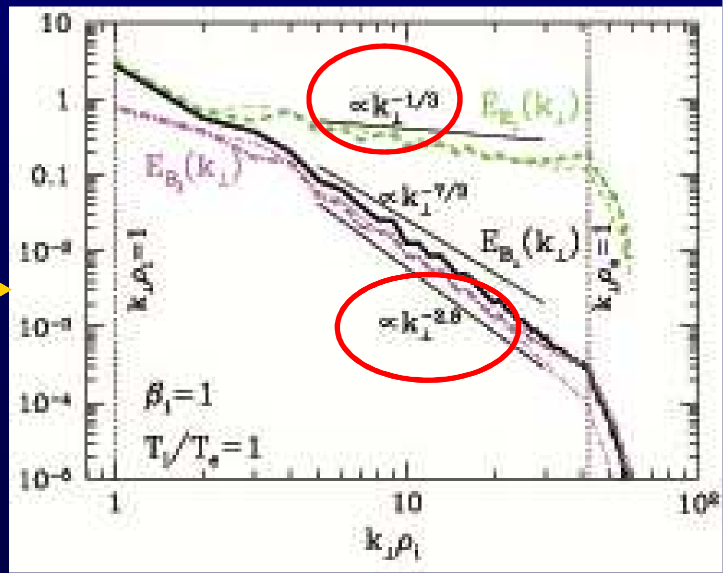

Other numerical predictions on electron scale turbulence

2D PIC simulations gave evidence of a power law dissipation range at $k\rho_e>1$

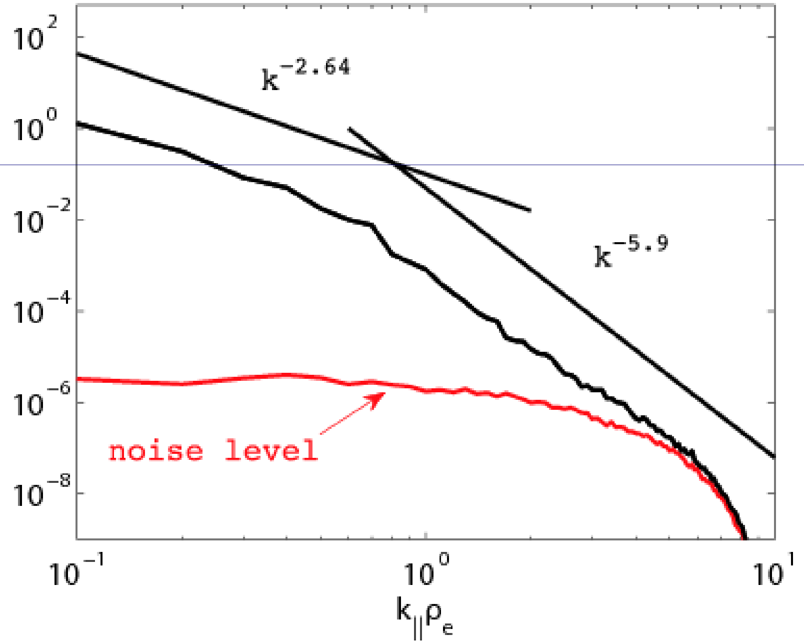

Figure 4. Spectrum of magnetic fluctuations $|\delta B|^2/|B_0|^2$ in the parallel direction $k\rho_{e\parallel}$. The noise level curve is in red. The power-law best fits are superimposed. (A color version of this figure is available in the online journal.)

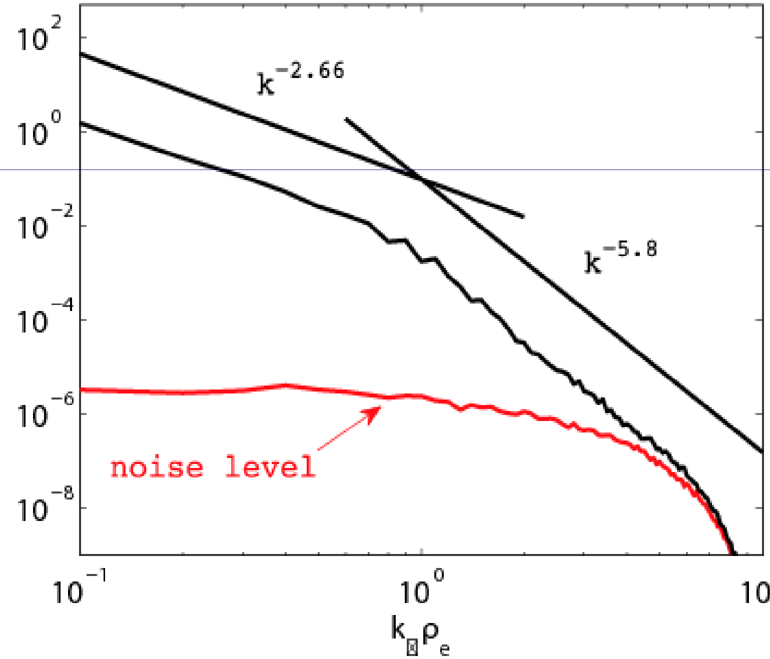

Figure 5. Spectrum of magnetic fluctuations $|\delta B|^2/|B_0|^2$ in the perpendicular direction $k\rho_{e\perp}$. The noise level curve is in red. The power-law best fits are superimposed.

[Camporeales & Burgess, ApJ, 2011]

3D PIC simulations of whistler turbulence : $k^{-4.3}$ at $kd_e>1$

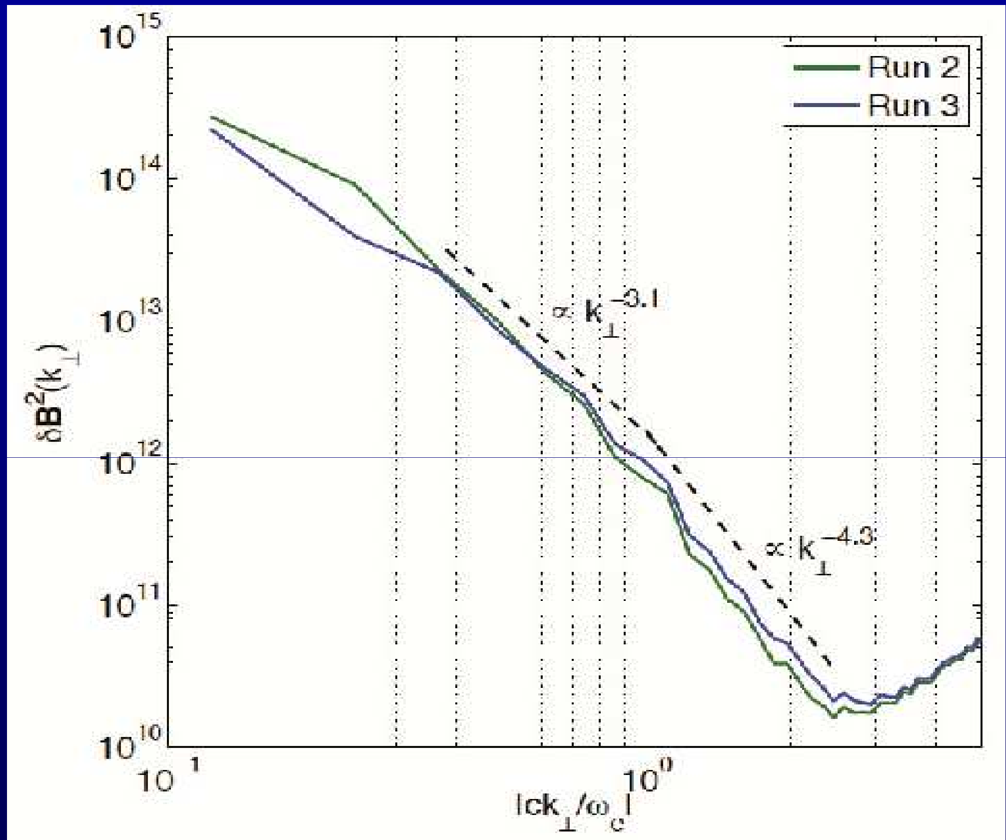

Chang & Gary, GRL 2011

First evidence of a cascade from MHD to electron scale in the SW

1. Two breakpoints corresponding to ρ_i and ρ_e are observed.
2. A clear evidence of a new inertial range ~ $f^{-2.5}$ below ρ_i
3. ***First evidence of a dissipation range ~ f^{-4} near the electron scale ρ_e***

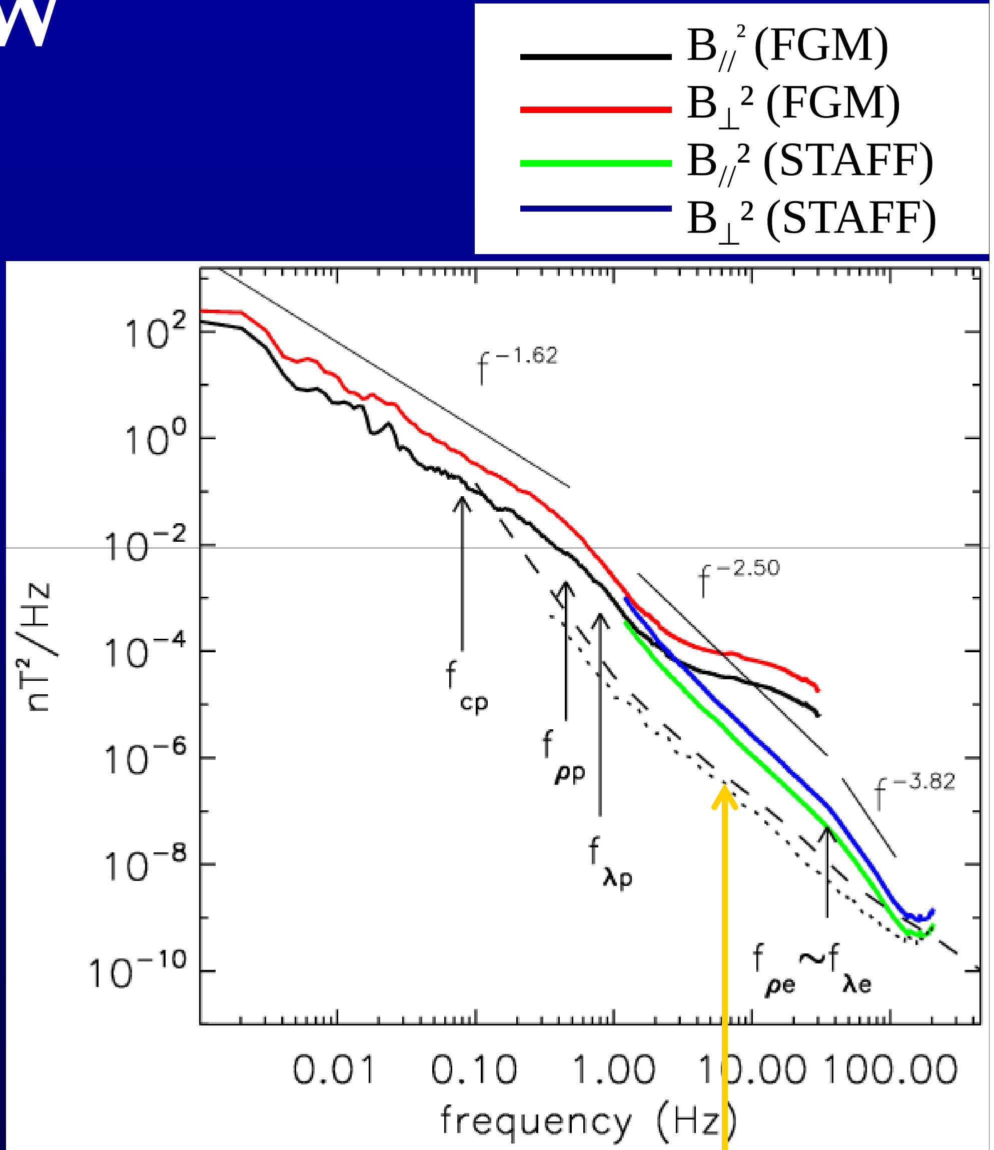

STAFF-SC sensitivity floor

Sahraoui et al., PRL, 2009

Whistler or KAW turbulence?

1. Large (MHD) scales ($L>\rho_i$): strong correlation of E_y and B_z in agreement with **E=-VxB**
2. Small scales ($L<\rho_i$): steepening of B² and enhancement of E² (however, strong noise in E_y for f>5Hz)

⇒ Good agreement with GK theory of Kinetic Alfvén Wave turbulence

FGM, STAFF-SC and EFW data

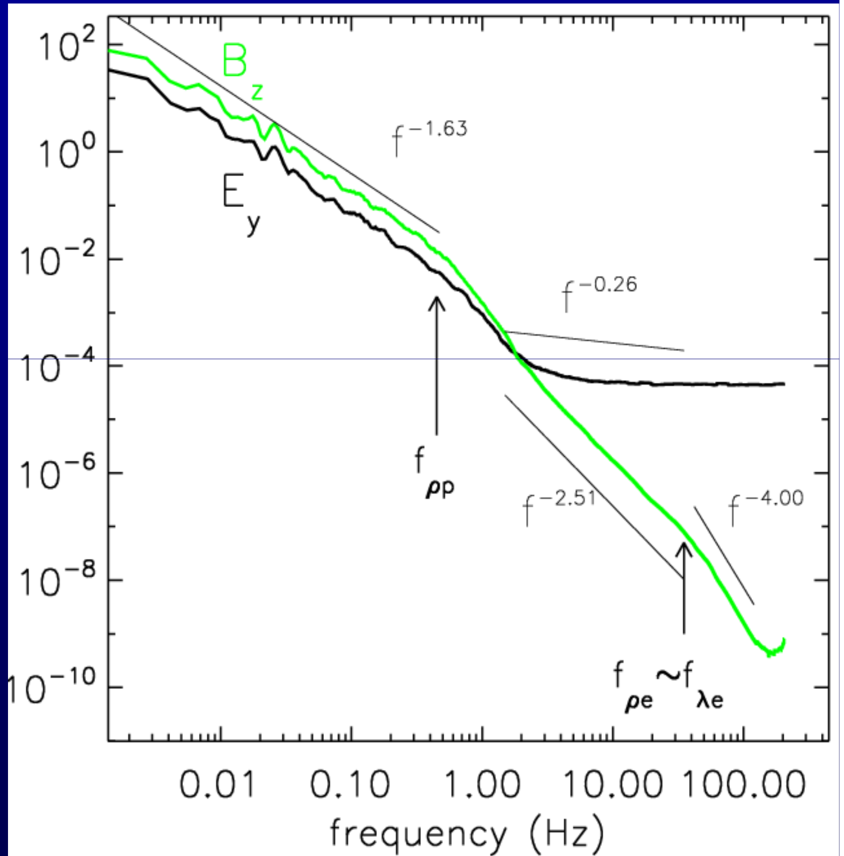

See also Bale et al., PRL, 2005

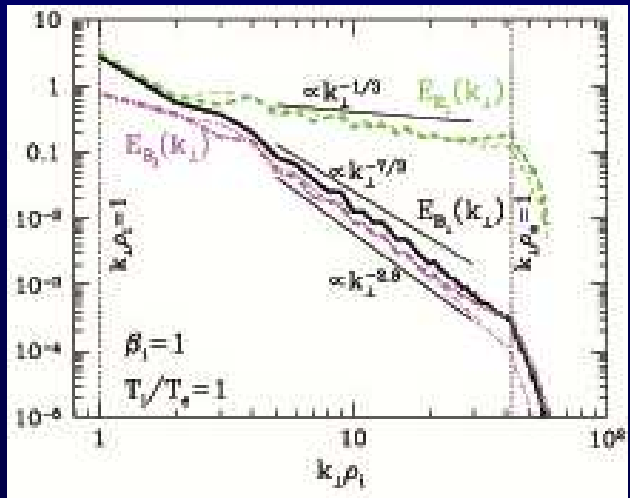

Howes *et al.* PRL, 11

Theoretical interpretation : KAW turbulence

Linear Maxwell-Vlasov solutions: Θ_{kB}~ 90°, β_i~2.5, T_i/T_e~4

The Kinetic Alfvén Wave solution extends **down to $k\rho_e$~1** with $\omega_r < \omega_{ci}$

[See also Podesta, ApJ, 2010]

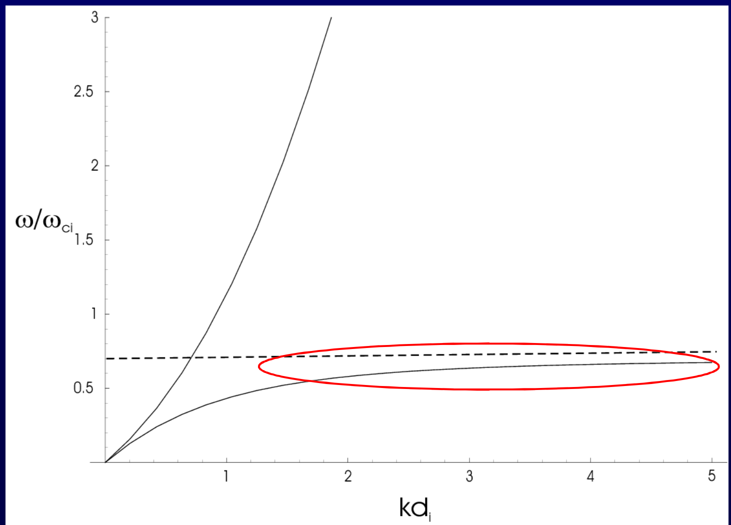

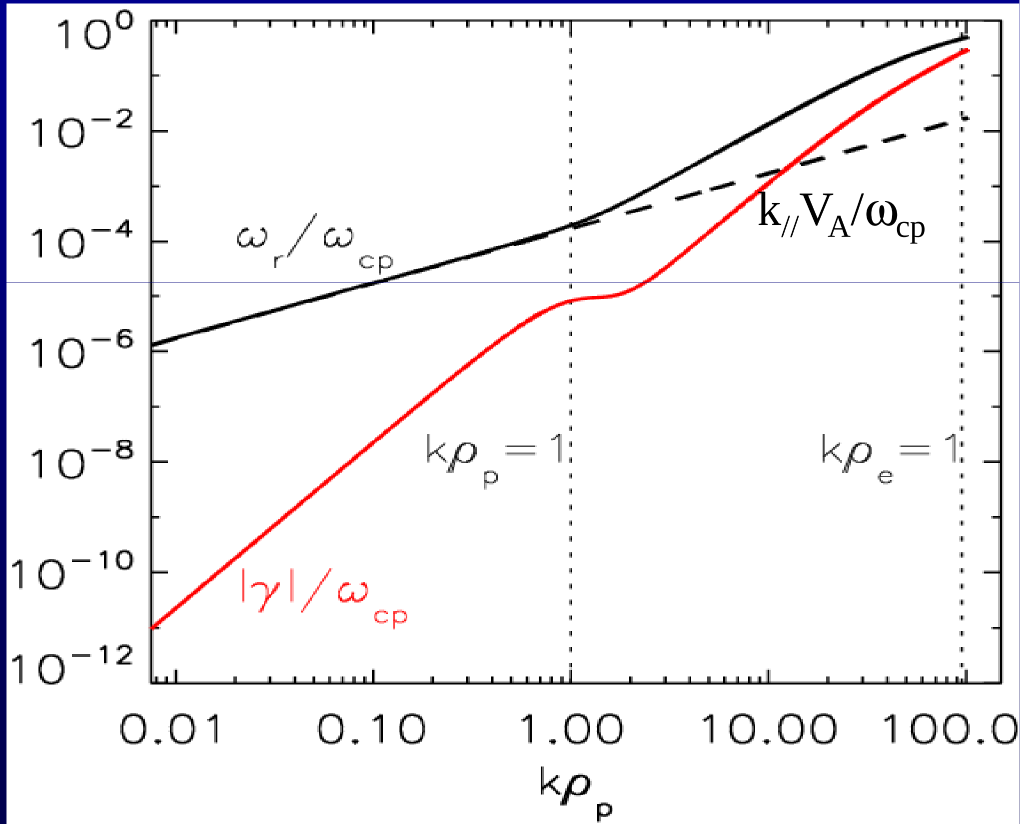

$$\omega_r = k_{//} V_A k_\perp \rho_i / \sqrt{\beta_i + 2/(1 + T_i / T_e)}$$

E/B : KAW theory vs observations

$$\omega_r = k_{//} V_A k_\perp \rho_i / \sqrt{\beta_i + 2/(1+T_i/T_e)}$$

- Lorentz transform: $\mathbf{E}_{sat} = \mathbf{E}_{plas} + \mathbf{V} \times \mathbf{B}$
- Taylor hypothesis to transform the spectra from f (Hz) to $k\rho_i$

1. Large scale ($k\rho_i<1$): $\delta E/\delta B \sim V_A$
2. Small scale ($k\rho_i>1$): $\delta E/\delta B \sim k^{1.1} \Rightarrow$ in agreement with GK theory of KAW turbulence $\delta E^2 \sim k_\perp^{-1/3}$ & $\delta B^2 \sim k_\perp^{-7/3} \Rightarrow \delta E/\delta B \sim k$
3. The departure from linear scaling ($k\rho_i$□10) is due to noise in Ey data

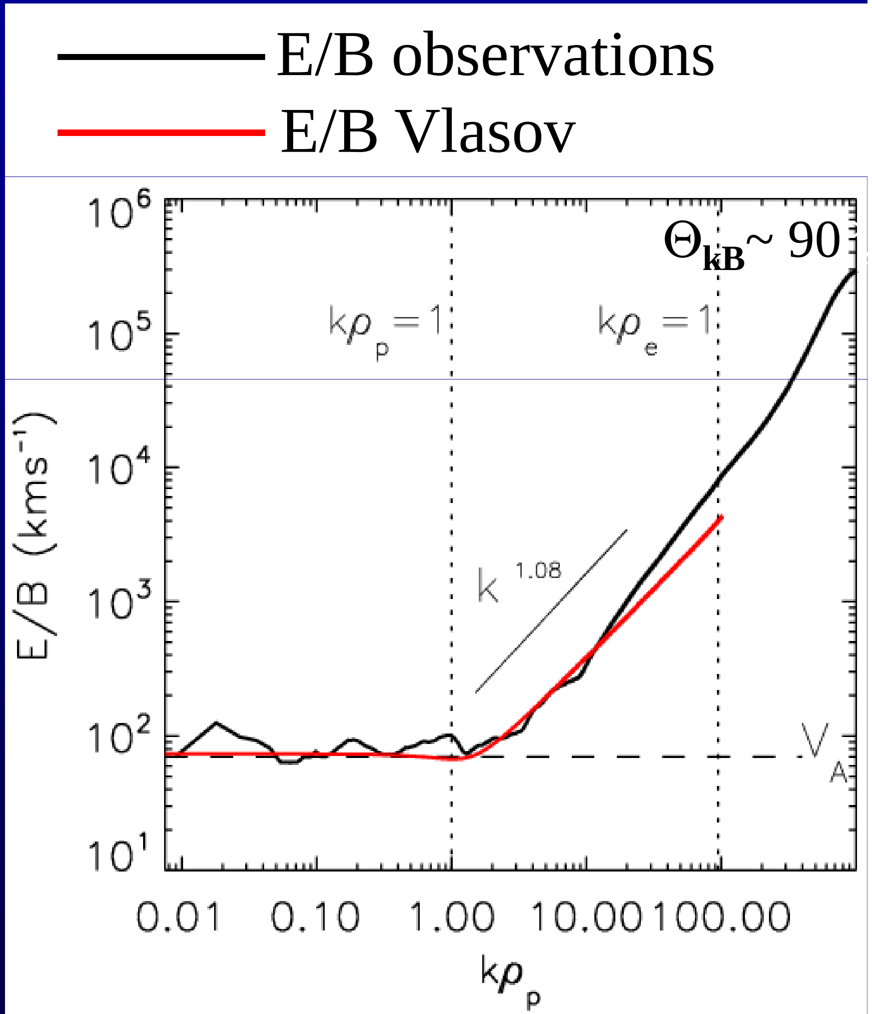

Sahraoui et al., PRL, 2009

Magnetic compressibility

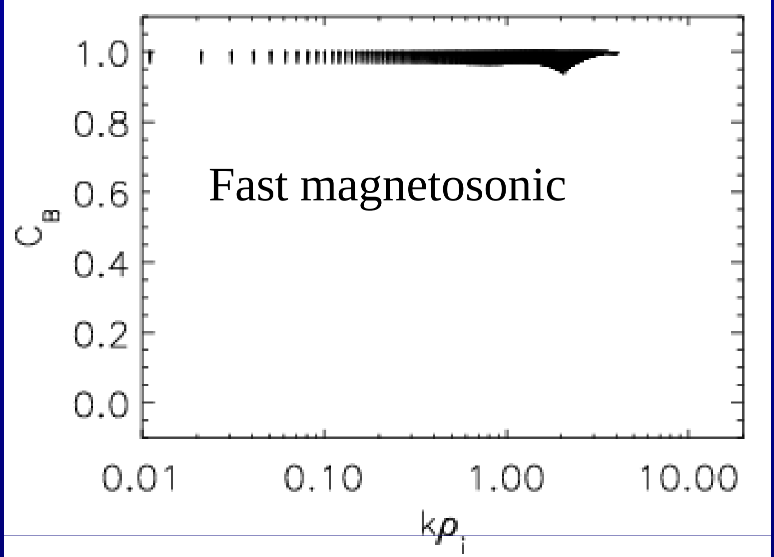

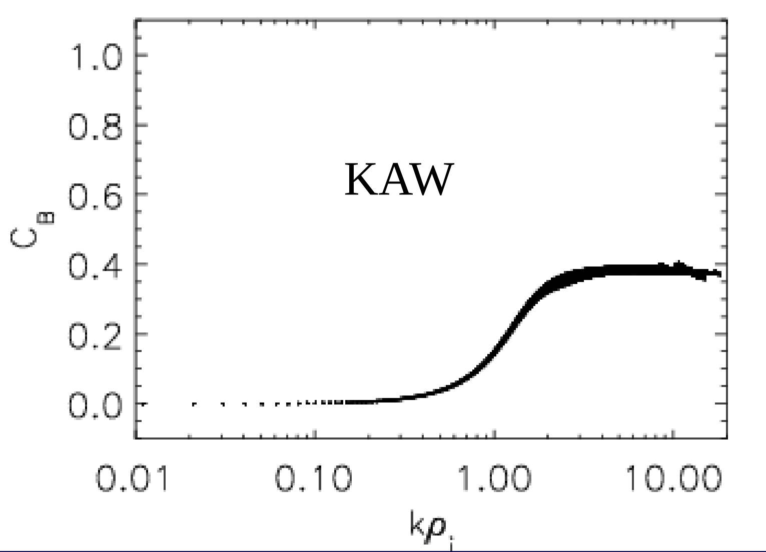

[Sahraoui+, ApJ, 2012]

Additional evidence of KAW at $k\rho_i > 1$

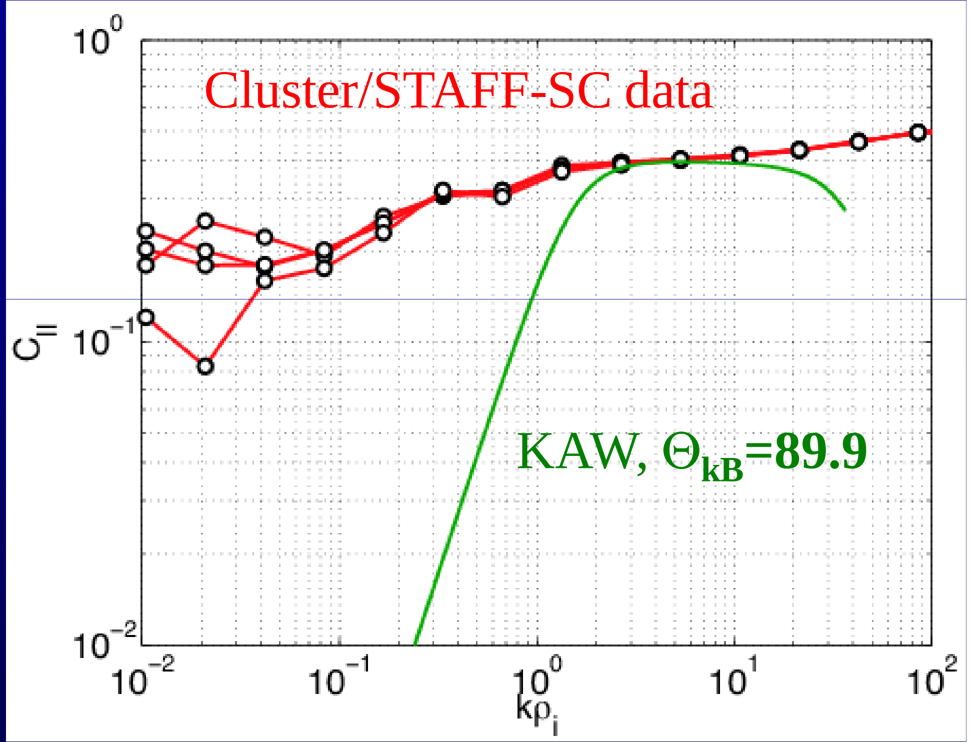

[Kiyani+, ApJ, 2012; Podesta+, 2012]

3D k-spectra at sub-proton scales of SW turbulence

Conditions required:

20040110, 06h05-06h55

1. Quiet SW: NO electron foreshock effects
2. Shorter Cluster separations (~100km) to analyze sub-proton scales
3. Regular tetrahedron to infer actual 3D *k*-spectra [Sahraoui et al., JGR, 2010]
4. High SNR of the STAFF data to analyse HF (>10Hz) SW turbulence.

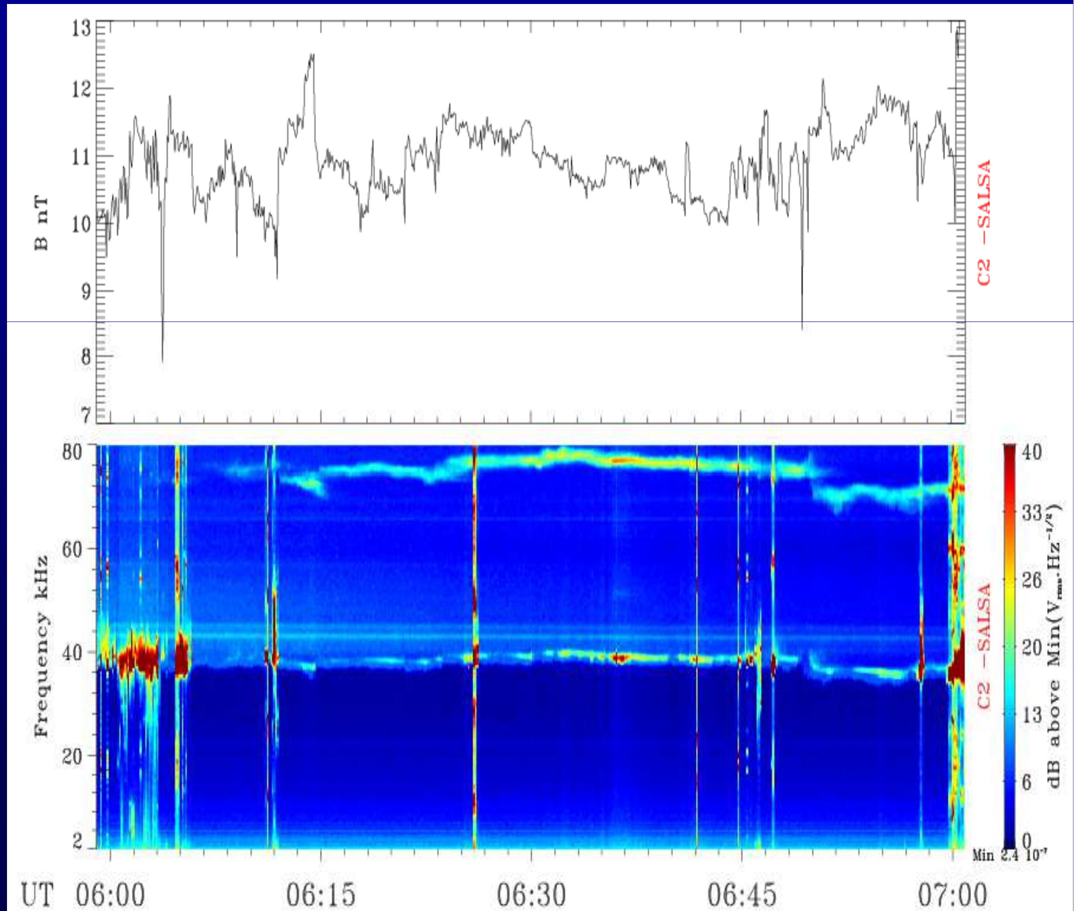

3D *k*-spectra at sub-proton scales

We use the *k*-filtering technique to estimate the 4D spectral energy density $P(\omega,\mathrm{k})$

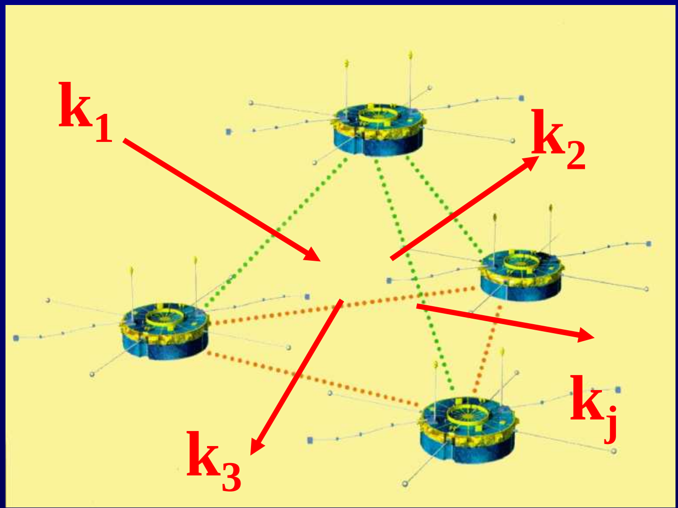

20040110 (d~200km)

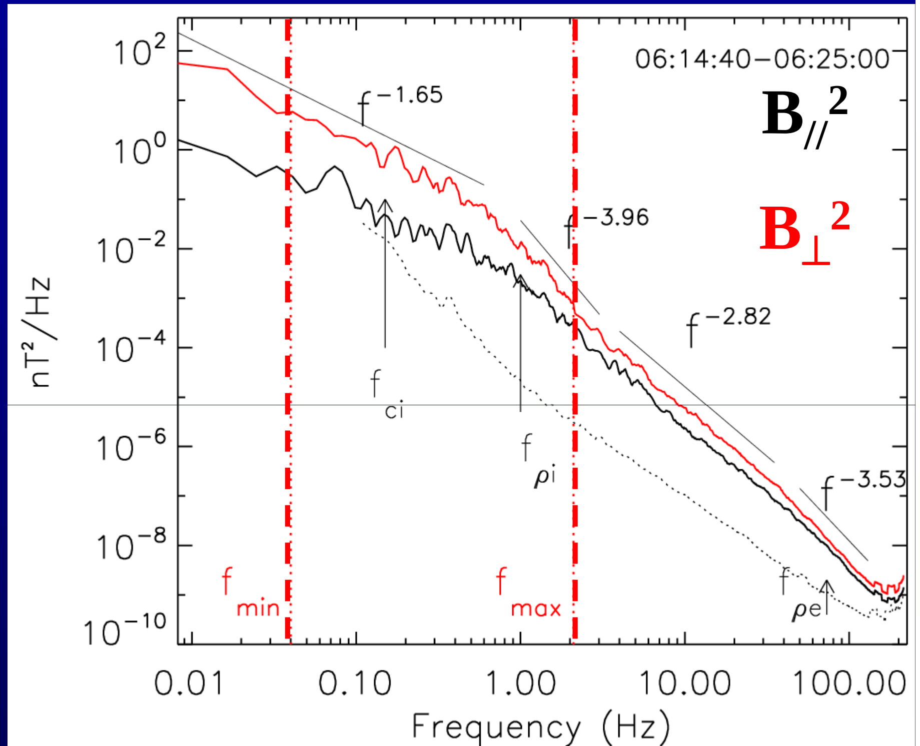

We use $P(\omega,\mathrm{k})$ to calculate

1. 3D ω-k spectra
2. 3D *k*-spectra (anisotropies, scaling, …)

Comparison with the Vlasov theory

Turbulence cascades following the Kinetic Alfvén mode (KAW) as proposed in Sahraoui et al., PRL, 2009

→ Rules out the cyclotron heating

→ Heating by p-Landau and e-Landau resonances

[Sahraoui et al., PRL, 2010]

$\beta_i \sim 2$ $T_i/T_e=3$ $85° < \Theta_{kB} < 89°$

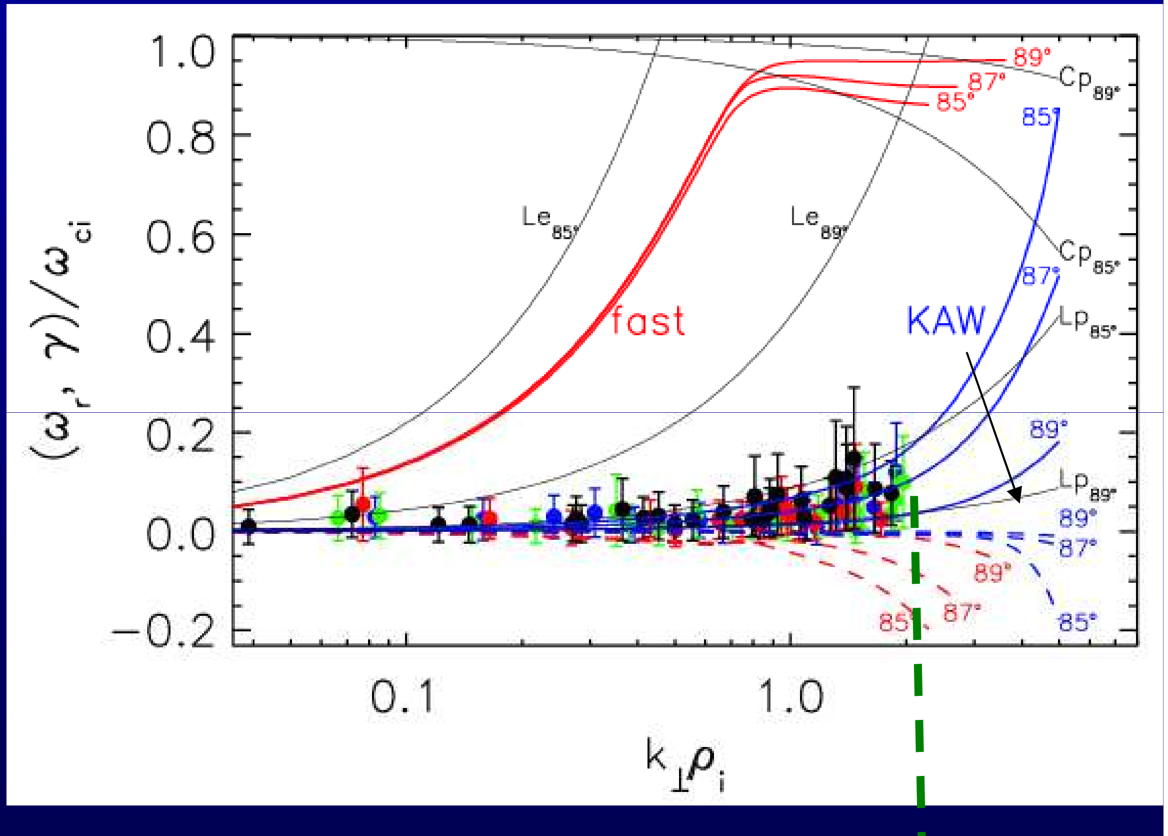

Limitation due to the Cluster separation (d~200km)

3D *k*-spectra at sub-ion scales

1. First *direct* evidence of the breakpoint near the proton gyroscale in *k*-space (***no additional assumption, e.g. Taylor hypothesis, is used***)
2. Strong steepening of the spectra below ρ_i → A ***Transition Range*** to dispersive/electron cascade

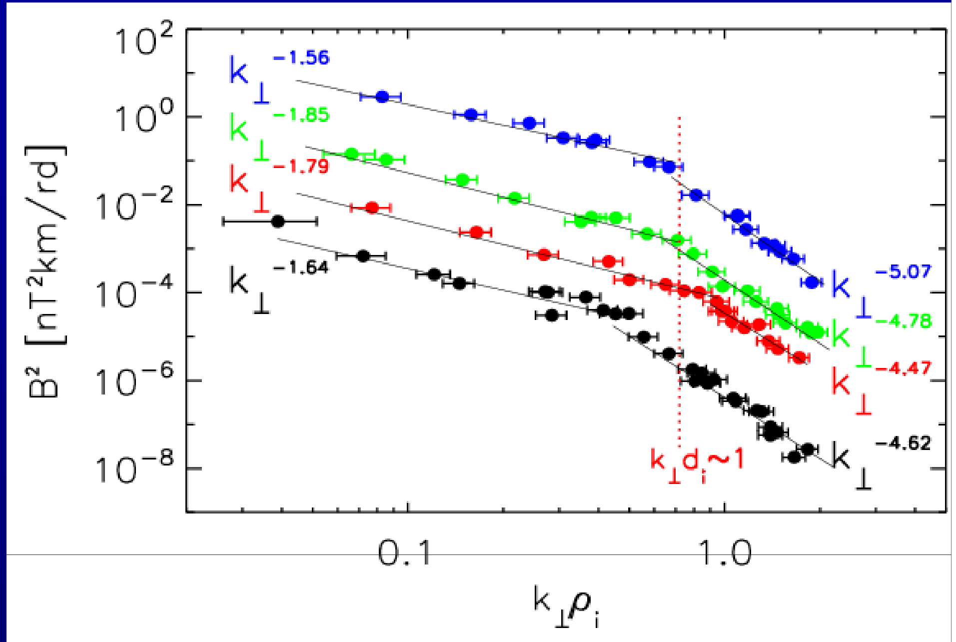

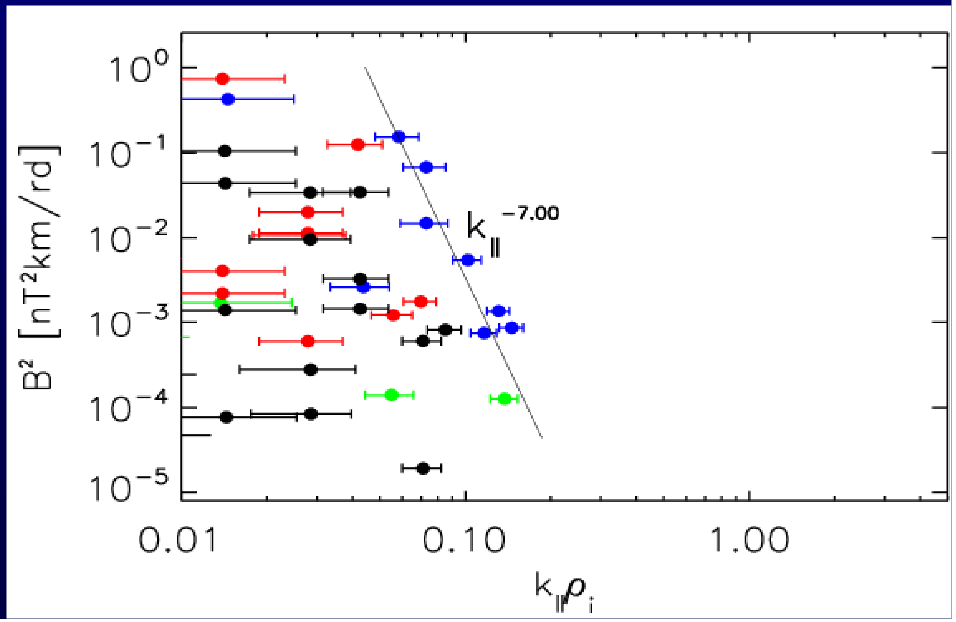

Journey of the energy cascade through scales

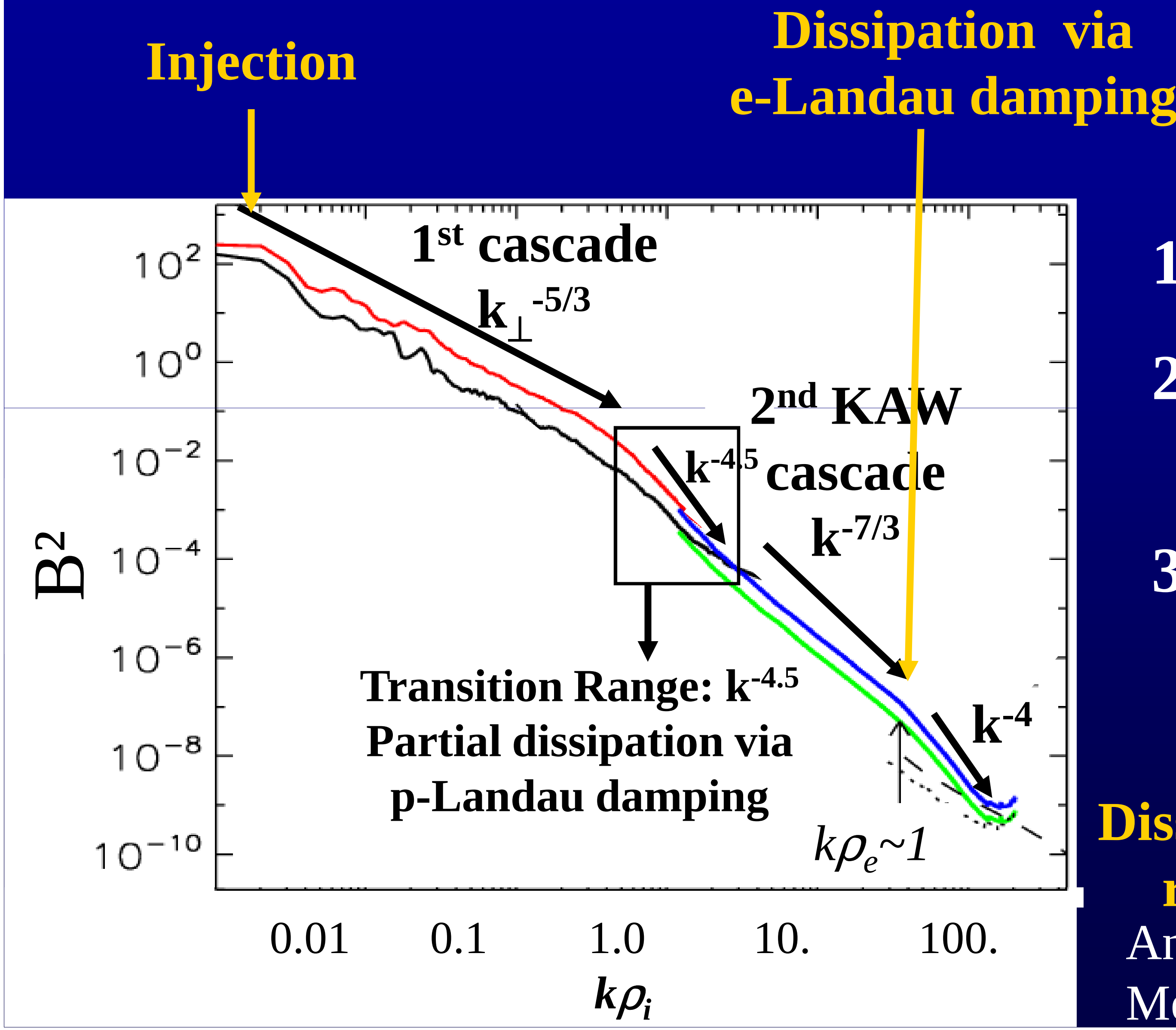

1. Turbulence
2. e-Acceleration & Heating
3. Reconnection

Dissipation range

Another interpretation in Meyrand & Galtier, 2010

Dissipation through reconnection/current sheets

Large scale laminar current sheet: reconnection can occur and the can be heated or accelerated (e..g. jets)

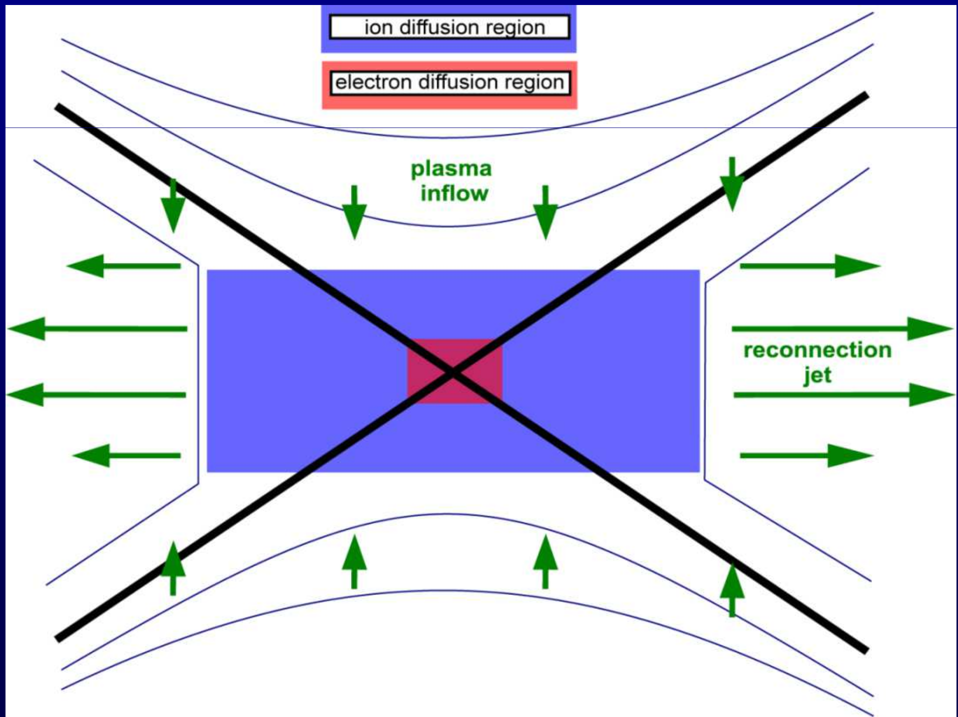

[Zhong+, Nature Physics, 2010]

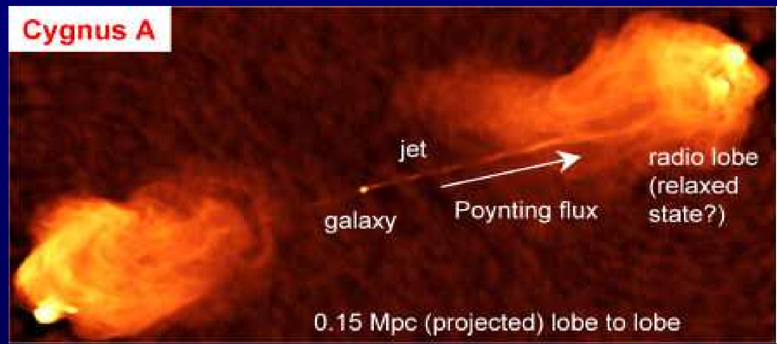

Turbulent current sheets

[Lazarian & Vishniac,1999]

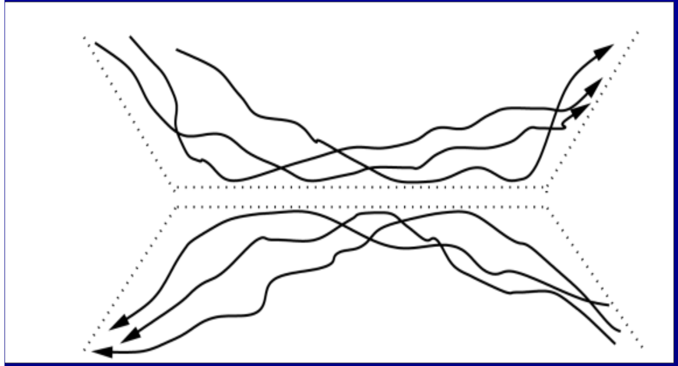

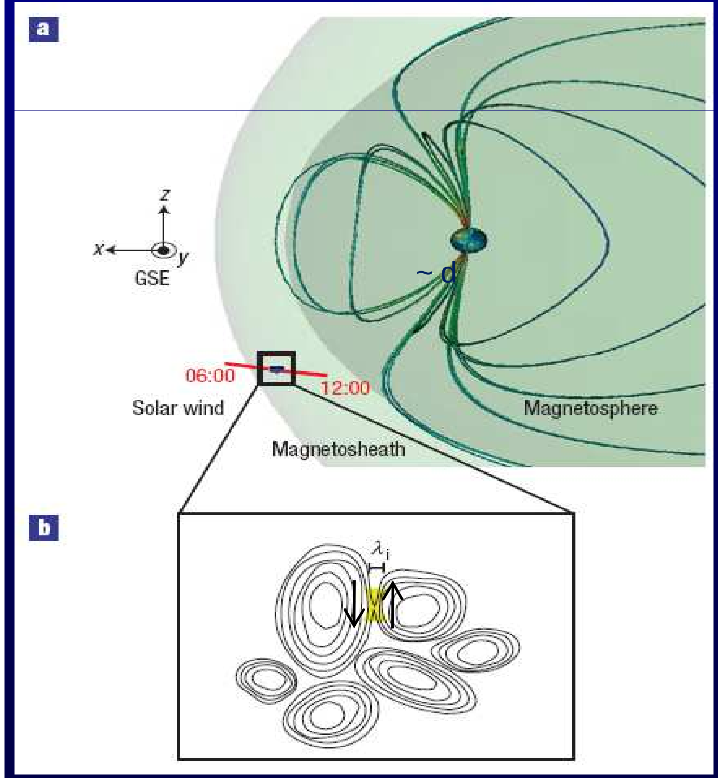

[e.g., Retinò+, Nature Physics, 2007]

2D Hall-MHD simulation of turbulence: evidence of a large number of reconnecting regions

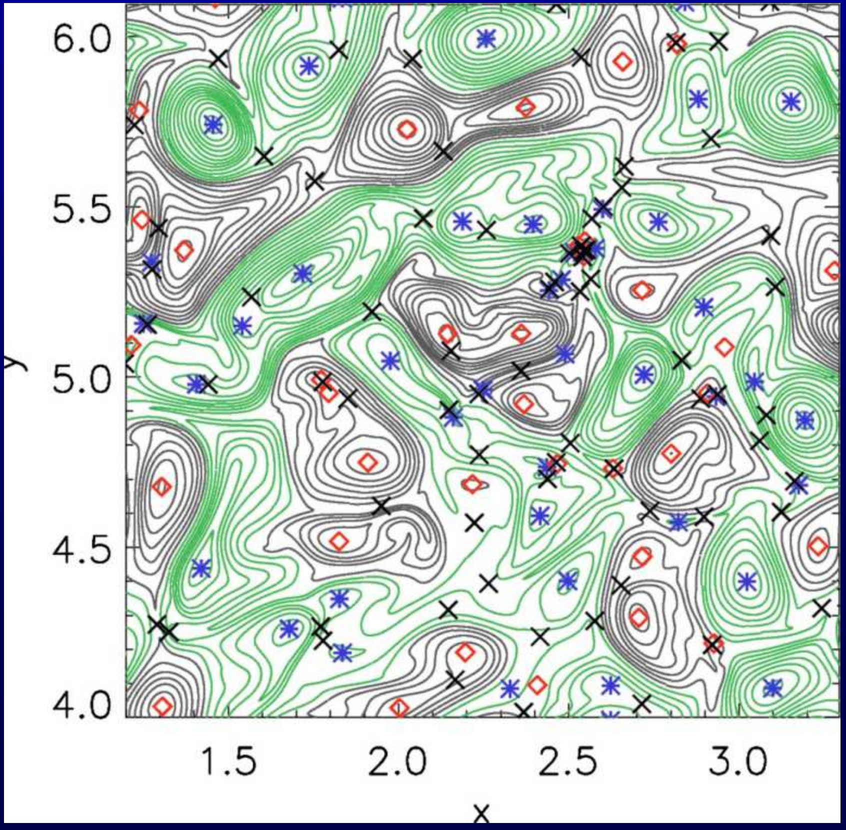

Dissipation by wave-particle interaction or via reconnection?

Good correlation between enhanced T_p and threshold of linear kinetic instabilities

Good correlation between enhanced high shear B angles and the threshold of linear instabilities !!

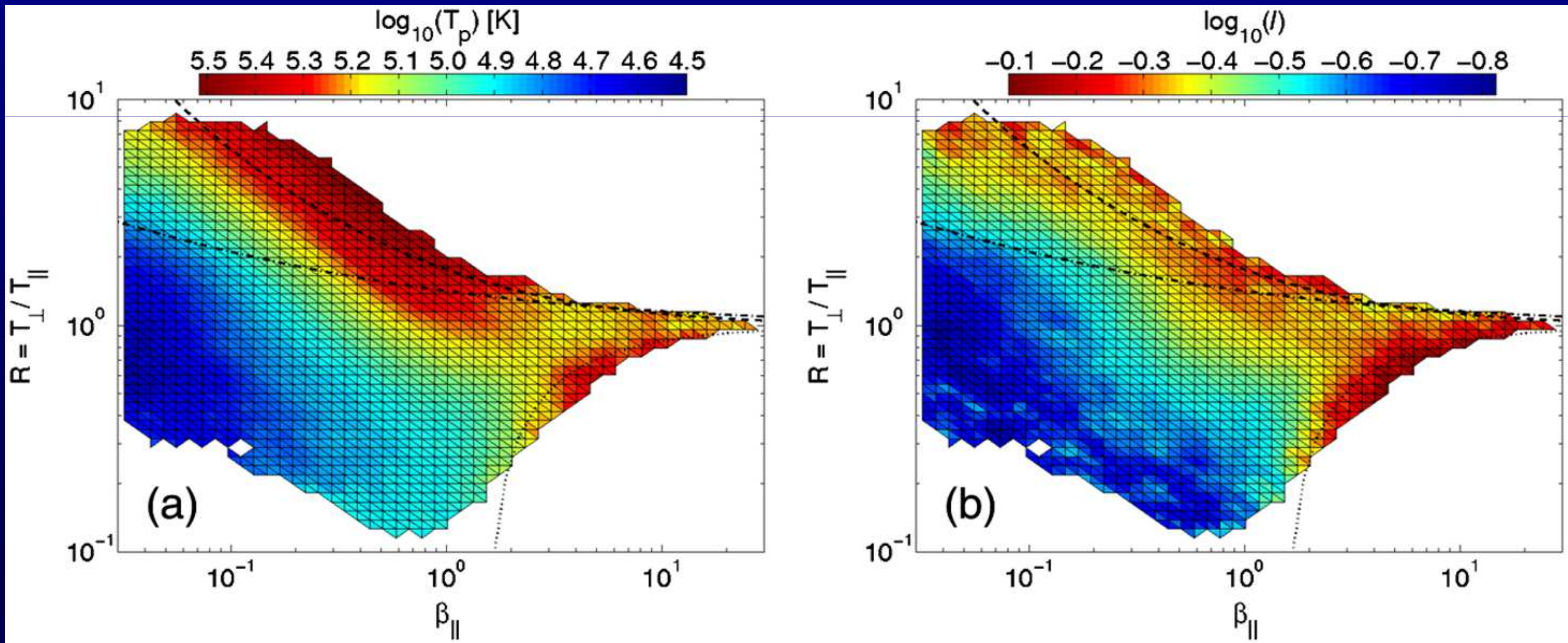

Osman et al., PRLs, 2012a,b

Higher order statistics and intermittency (1)

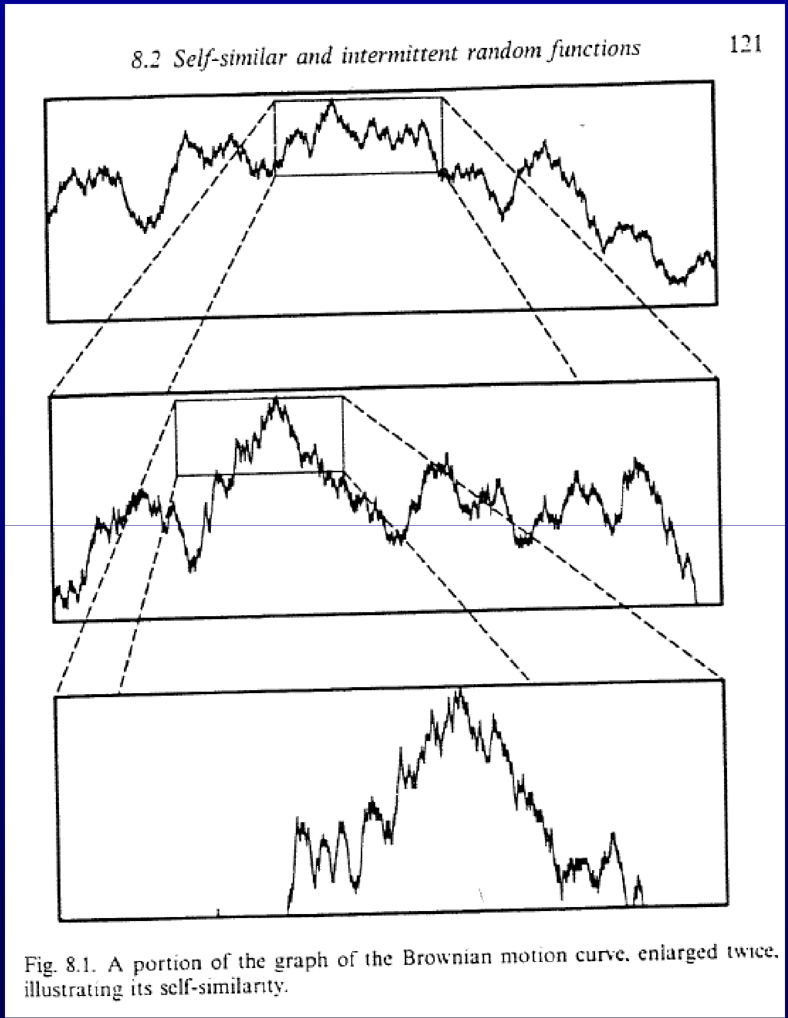

Self-similar signal

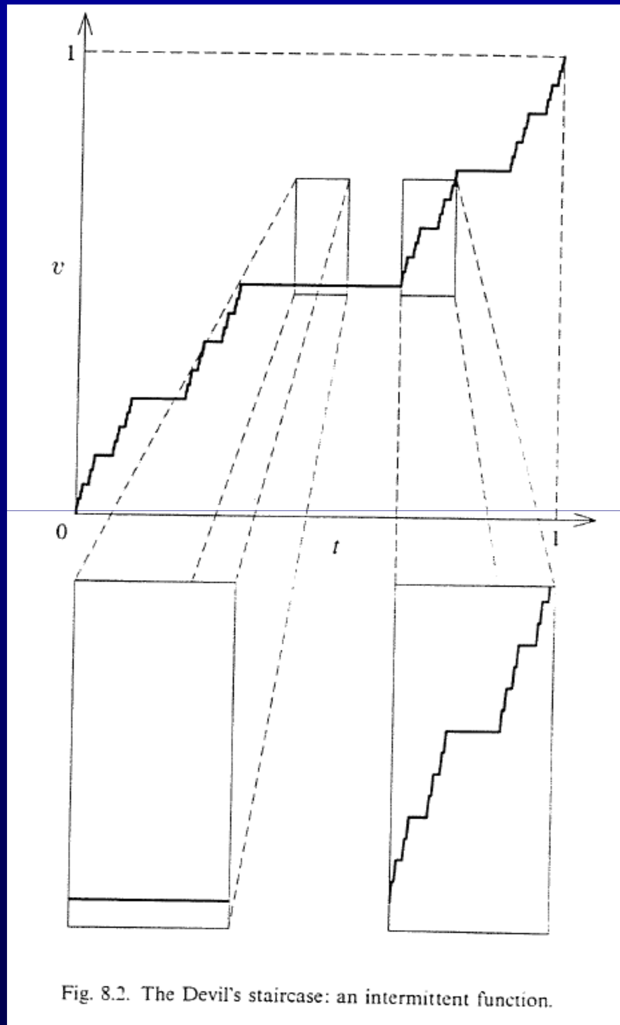

intermittent signal

[Frisch, 1995]

Higher order statistics and intermittency (2)

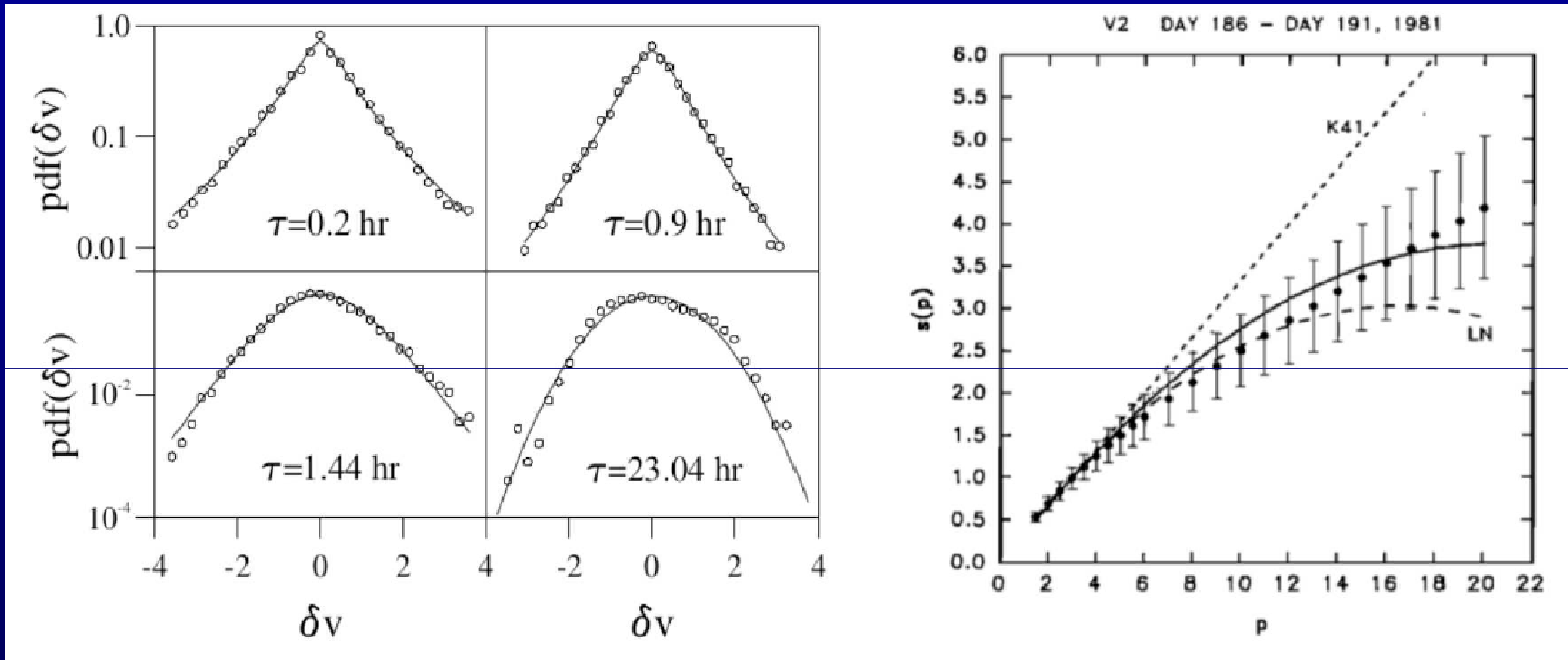

2. Monfractality *vs* multifractality in the dispersive range:

$n_e \sim 4$ cm^{-3} $\beta_i \sim 2$

$V_A \sim 50$ km s^{-1}

$T_i \sim 103$ eV $|B| \sim 4$ nT

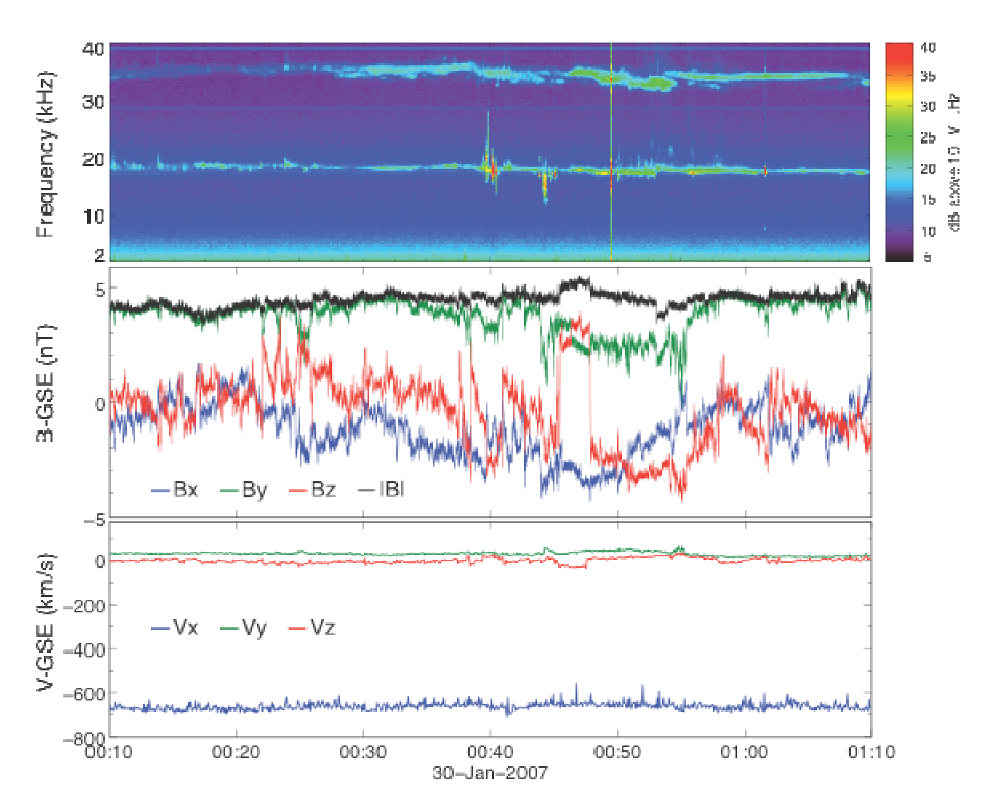

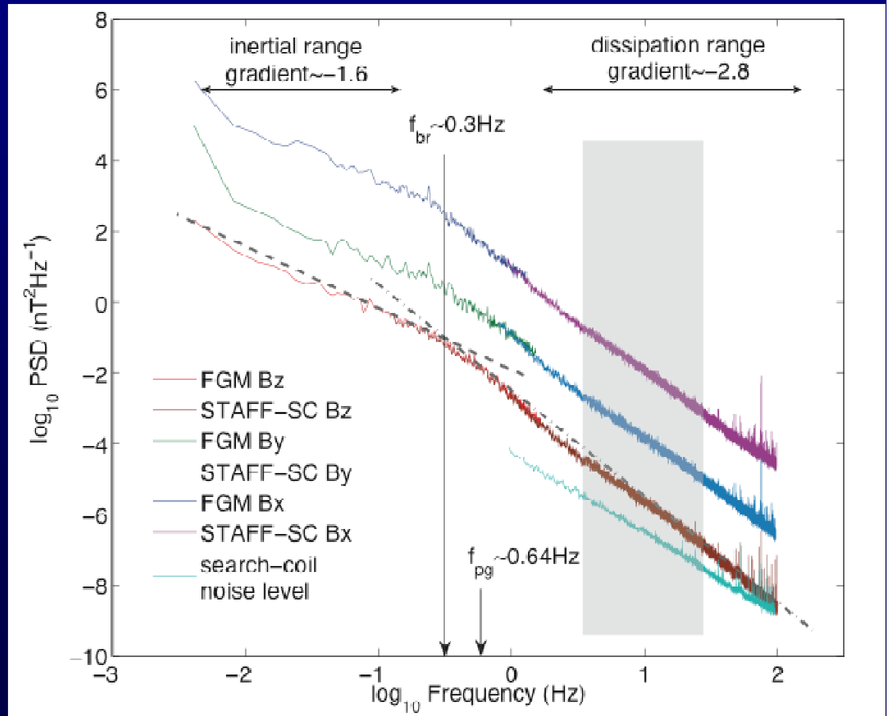

[Kiyani et al., PRL, 2009]

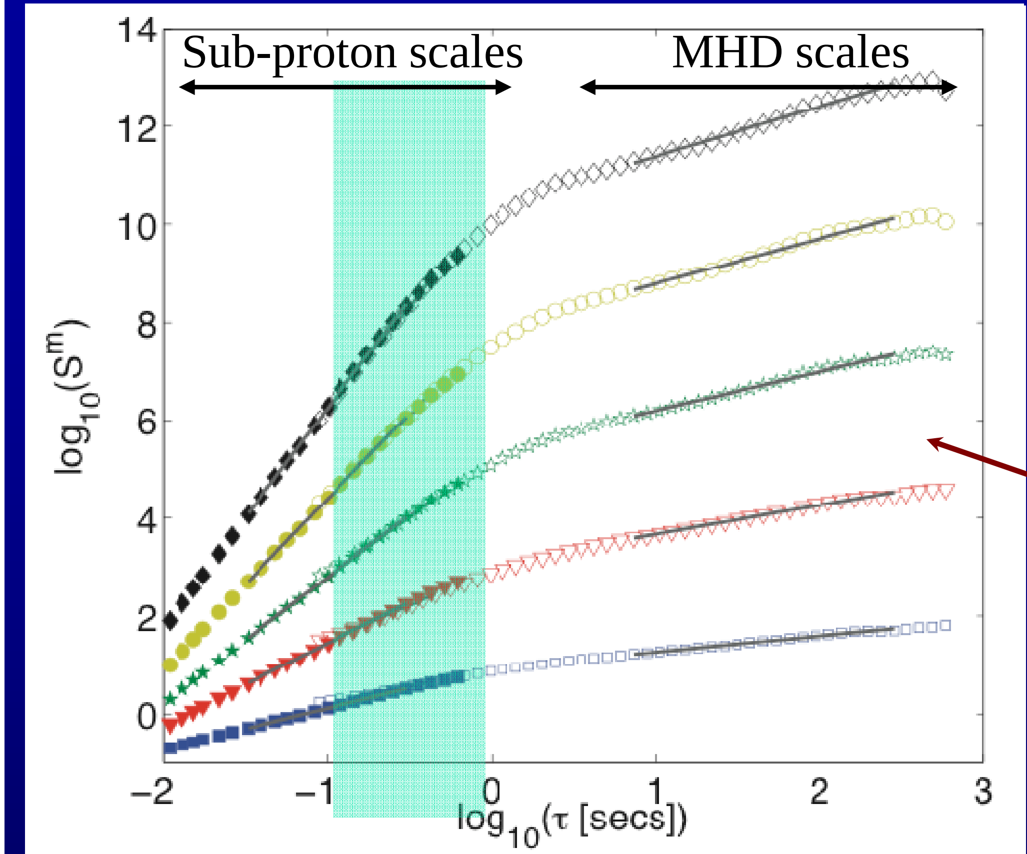

Stuctures functions:

$$S^m(\tau)=\sum_t \left|B(t+\tau)-B(t)\right|^m$$

Scaling:

$$S^m(\tau)=S^m(1)\tau^{\zeta(m)}$$

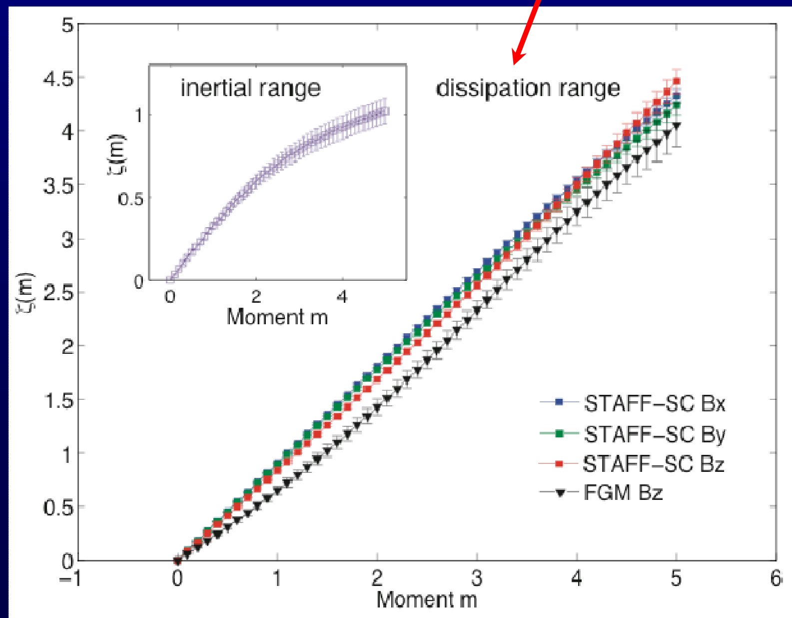

Evidence of monofractality (self-similarity) at sub-proton scales, while MHD-scales are multifractal (intermittent)

[See also Alexandrova et al., ApJ, 2008]

Conclusions

The Cluster data helps understanding crucial problems of astrophysical turbulence:

- Its nature and anisotropies in *k*-space at MHD and sub-ion scales
- Its cascade and dissipation down to the electron gyroscale $\rho_e \Rightarrow$ *electron heating and/or acceleration by turbulence*
- Strong evidences of KAW turbulence ($\omega \ll \omega_{ci}$, $k_{//} \ll k_{\perp}$)$\Rightarrow$ Heating by e-p-Landau dampings (no cyclotron heating)
- Importance of kinetic physics in SW turbulence
- Turbulence & dissipation are at the heart of the future space missions: ESA/Solar Orbiter (2018), NASA/Solar Probe Plus (2018), THOR (2026 ?)

Turbulence and the future space missions

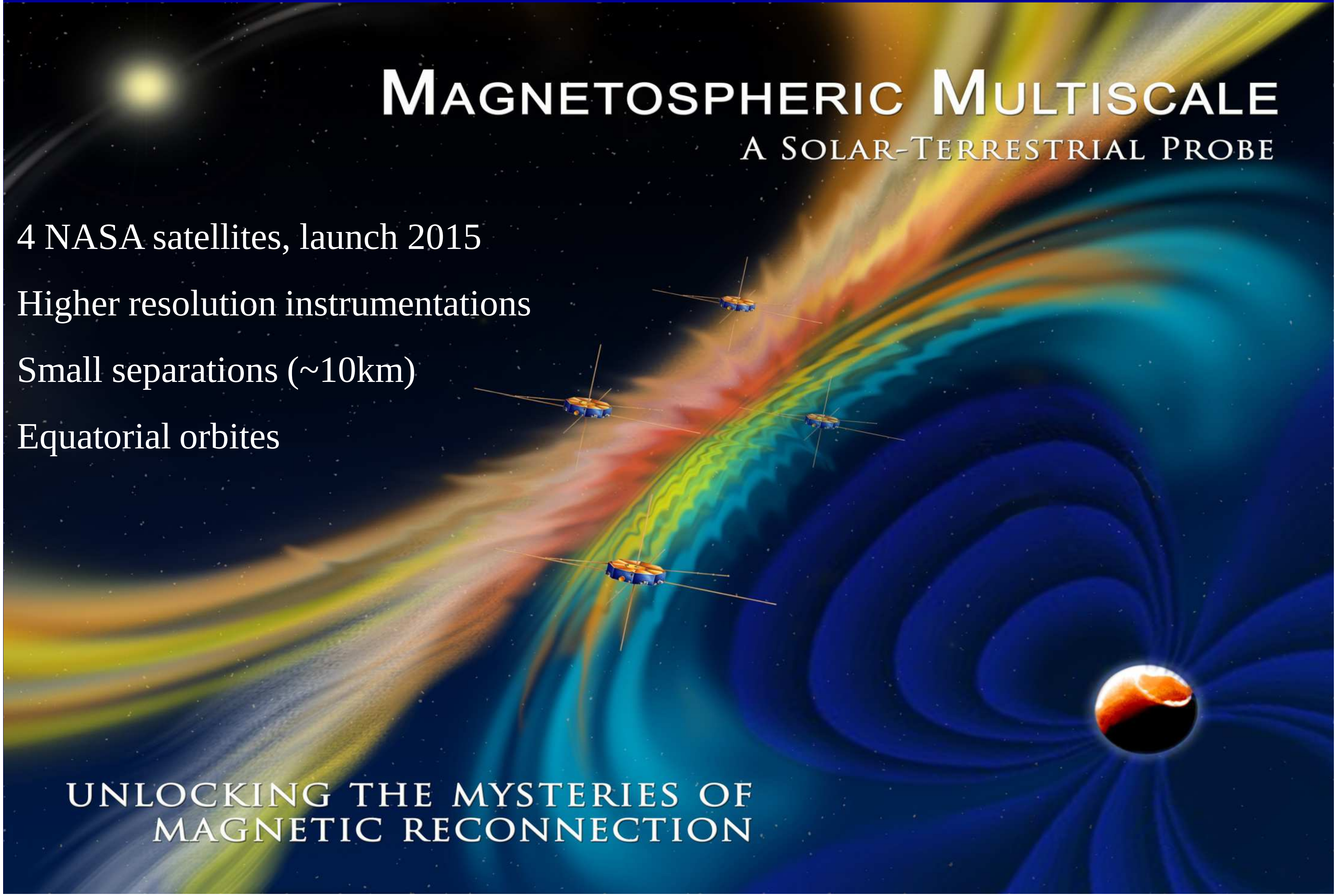

4 NASA satellites, launch 2015

Higher resolution instrumentations

Small separations (~10km)

Equatorial orbites

⇒ Need of multi-scale measurements ***with appropriate spacecraft separations***

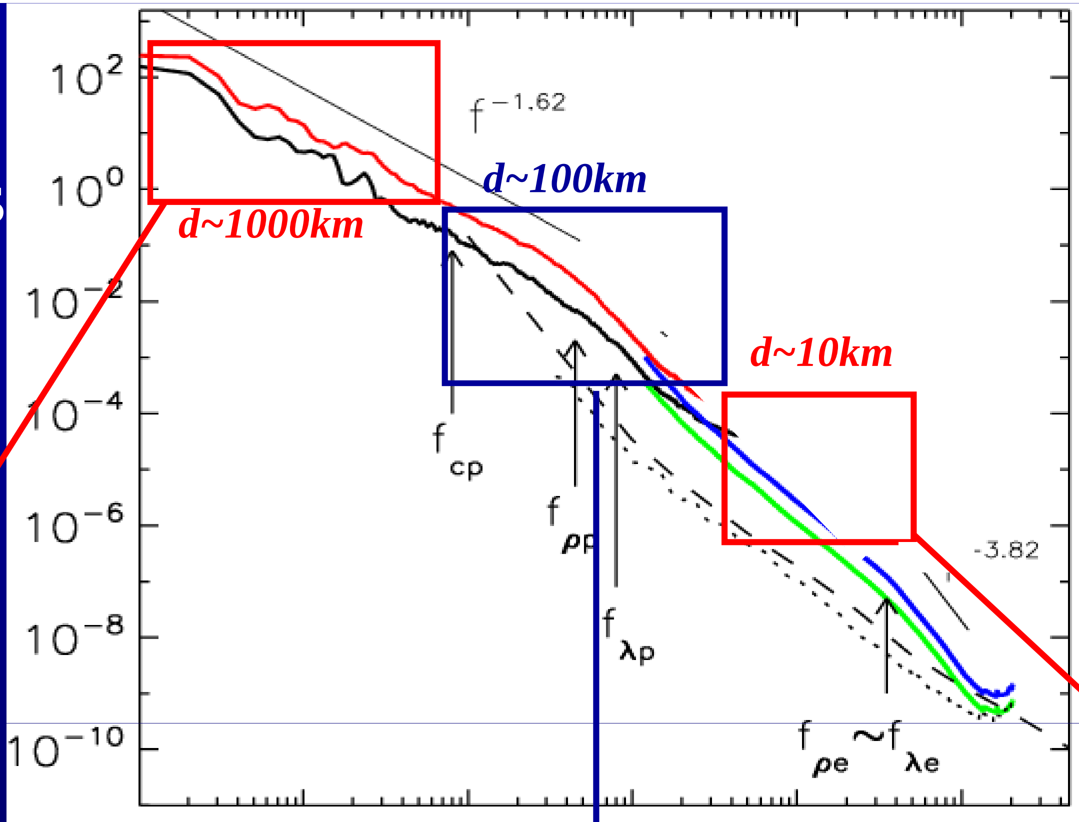

Narita *et al.* PRL, 2010

MMS

2015

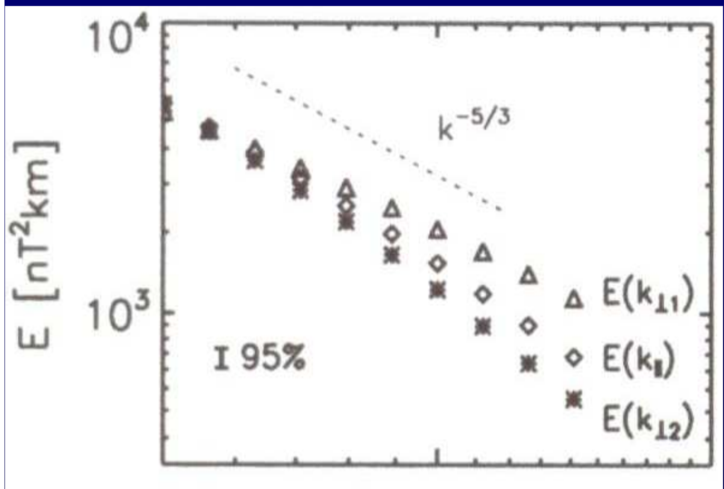

Sahraoui *et al.* PRL, 2010

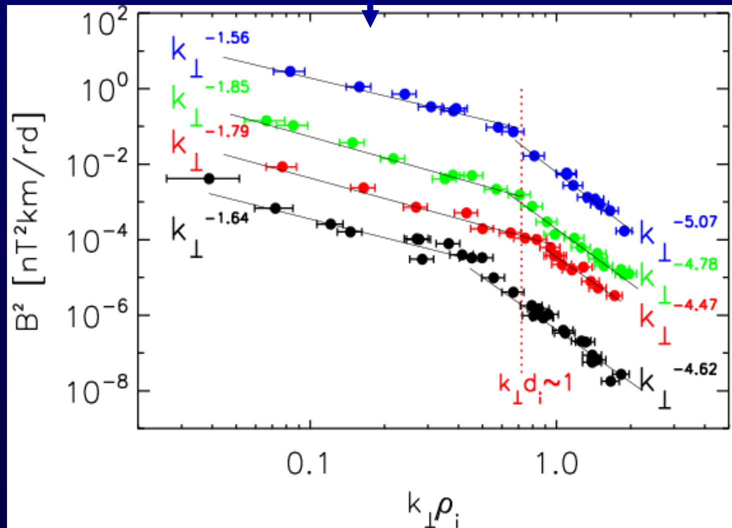


esa
Solar Orbiter
Exploring the Sun-Heliosphere Connection
Launch 2017
Distance : 0.28 AU
In-situ measurements & remote sensing


Launch 2019
Distance : ~0.03 AU
In-situ measurements & remote sensing
Solar Probe Plus
National Aeronautics and Space Administration
Goddard Space Flight Center
Greenbelt, Maryland 20771

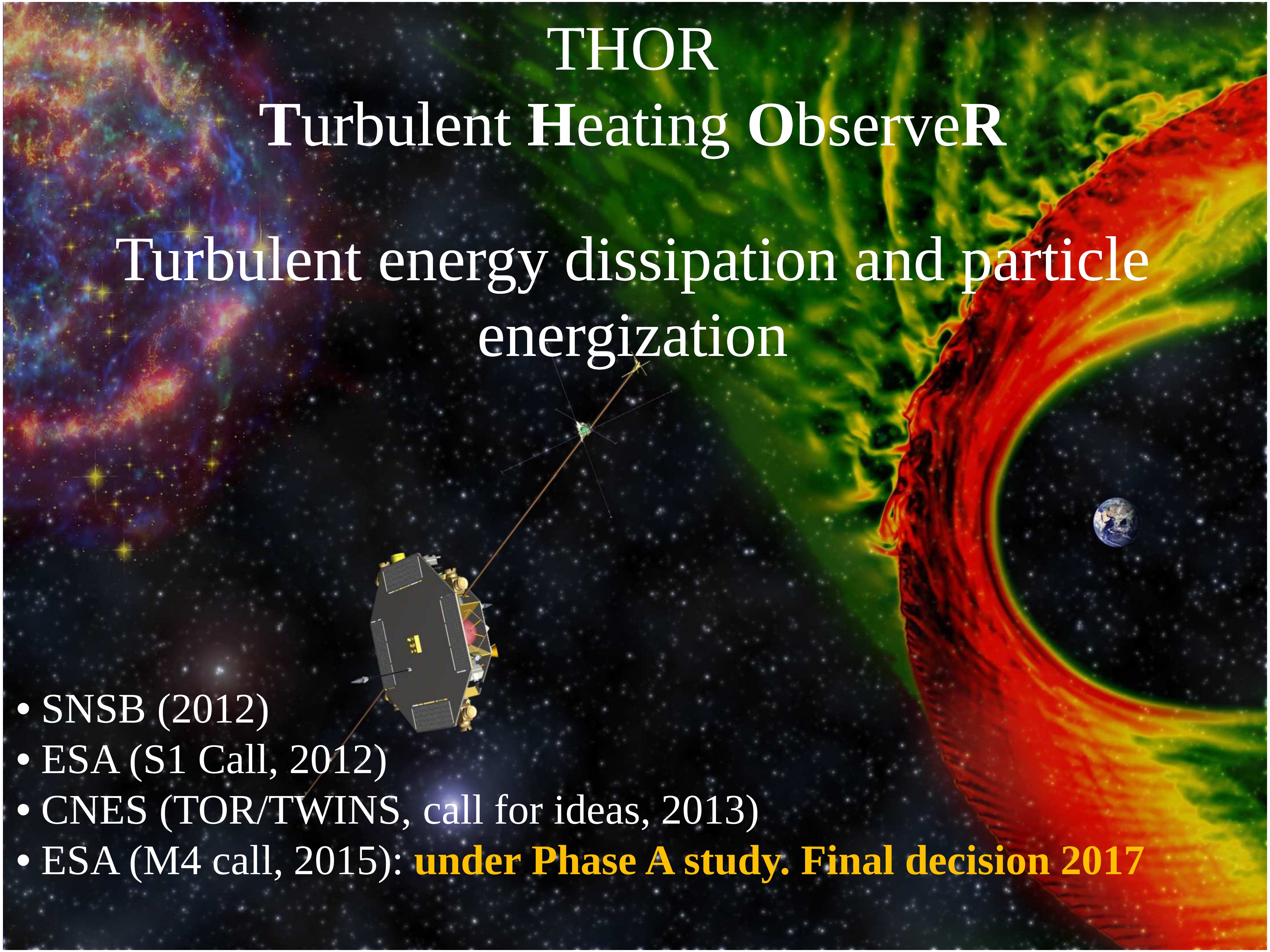
THOR
Turbulent **H**eating **O**bserve**R**
Turbulent energy dissipation and particle energization
• SNSB (2012)
• ESA (S1 Call, 2012)
• CNES (TOR/TWINS, call for ideas, 2013)
• ESA (M4 call, 2015): **under Phase A study. Final decision 2017**